NIH summer MRI course 2015

What we can and can not do with Diffusion MRI

Carlo Pierpaoli
NICHD

Conventional MRI

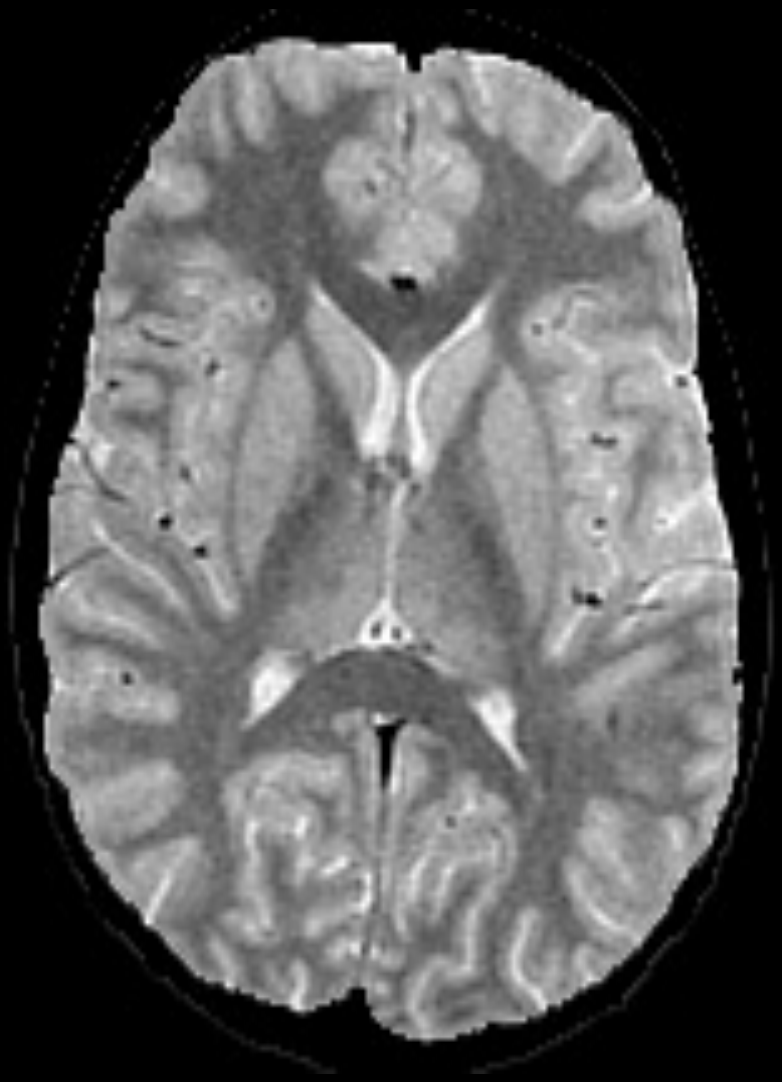

Tissue discrimination based on:

- Relaxation properties
- Water concentration

T2 weighted image of the adult human brain

Weaknesses of Conventional MRI

Weaknesses of Conventional MRI

Poor sensitivity to global changes

Weaknesses of Conventional MRI

Poor sensitivity to global changes

Lack of specificity (e.g., iron deposition vs. myelination vs. water content)

Weaknesses of Conventional MRI

Poor sensitivity to global changes

Lack of specificity (e.g., iron deposition vs. myelination vs. water content)

Not informative in the diagnosis of several common disorders (e.g., only 5% of subjects with mental retardation have MRI abnormalities).

Weaknesses of Conventional MRI

Poor sensitivity to global changes

Lack of specificity (e.g., iron deposition vs. myelination vs. water content)

Not informative in the diagnosis of several common disorders (e.g., only 5% of subjects with mental retardation have MRI abnormalities)

Problematic for longitudinal and multi-site studies

Weaknesses of Conventional MRI

Poor sensitivity to global changes

Lack of specificity (e.g., iron deposition vs. myelination vs. water content)

Not informative in the diagnosis of several common disorders (e.g., only 5% of subjects with mental retardation have MRI abnormalities).

Problematic for longitudinal and multi-site studies

Interpretation operator dependent

Rationale for Quantitative MRI*

Increased sensitivity to global changes

Ideally suited for longitudinal and multi-site studies

Potentially improved biological specificity

* Values that refer to meaningful physical quantities and are measured on an absolute scale

Diffusion MRI

IVIM (Intravoxel Incoherent Motion)

DTI (Diffusion Tensor Imaging)

HARDI (High Angular Resolution Diffusion Imaging)

Diffusion is a transport process in which molecules change their position by random thermal collisions.

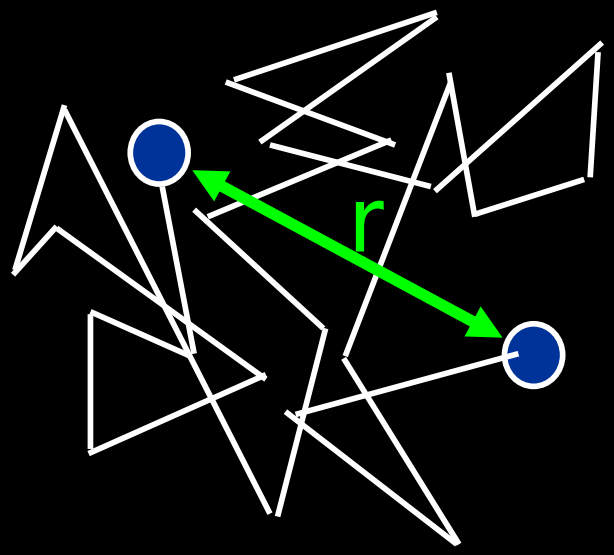

$$< r^2 > = 6\ D\ t$$

$< r^2 >$: mean-square displacement.

t : diffusion time.

Spin-echo Diffusion Preparation

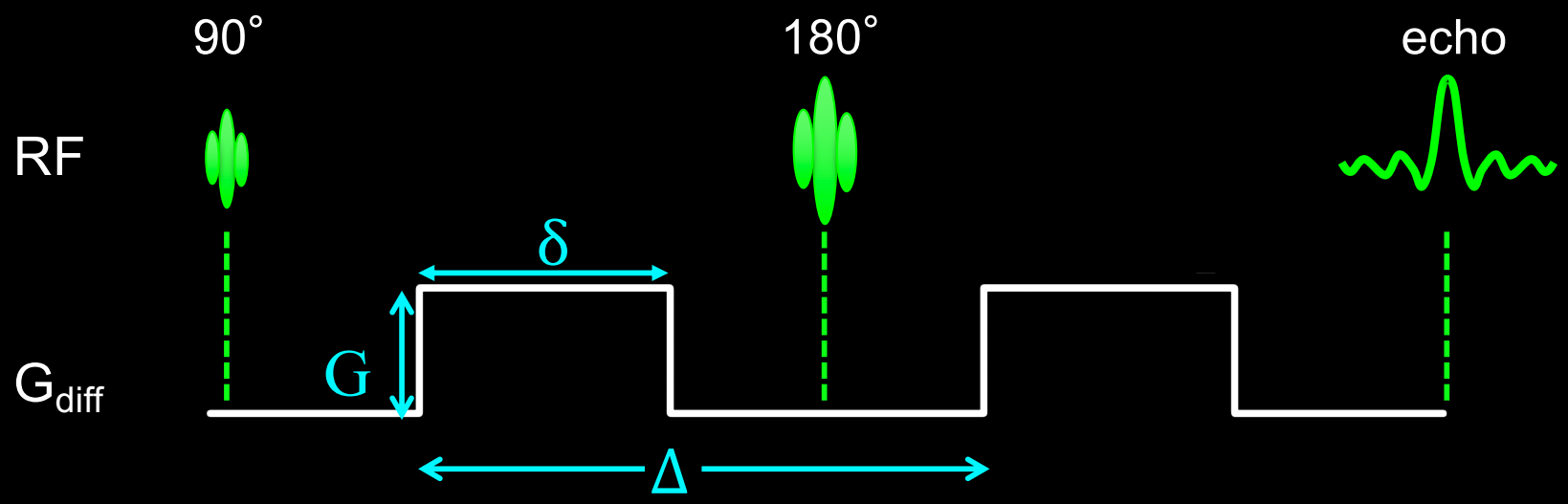

$$b = (\gamma G \delta)^2 \left(\Delta - \frac{\delta}{3} \right)$$

Stejskal, EO and Tanner, JE. J Chem Phys (1965) 42 : 288-292

DWI

$$S = S_0 e^{-bD}$$

Non-diffusion-weighted signal intensity

B-value
sec/mm^2

Diffusion Coefficient
mm^2/sec

Spin Diffusion Measurements: Spin Echoes in the Presence of a Time-Dependent Field Gradient*

E. O. STEJSKAL† AND J. E. TANNER
Department of Chemistry, University of Wisconsin, Madison, Wisconsin

(Received 20 July 1964)

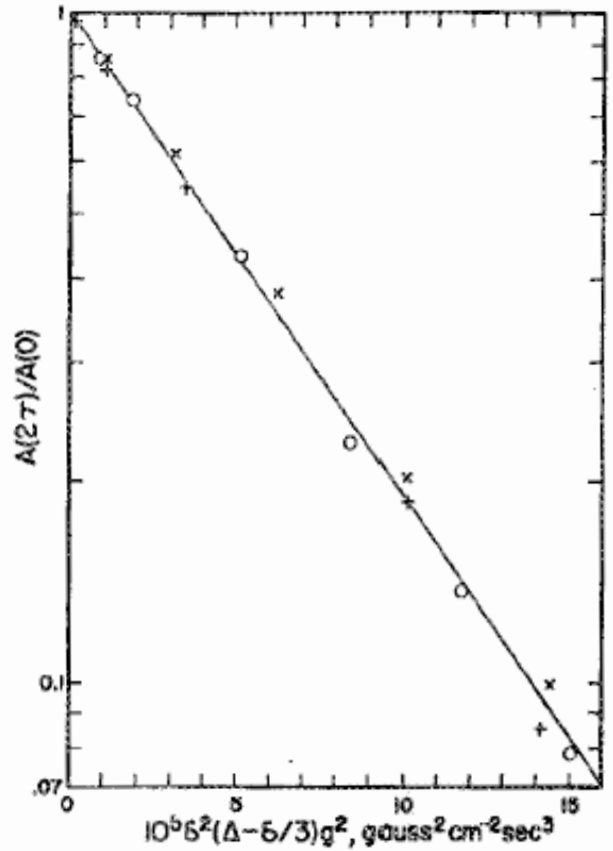

FIG. 1. Effect of the pulsed gradient on the echo amplitude, as observed in several aqueous $CuSO_4$ solutions at 25.5°±0.5°C. (See Table I for an identification of the symbols used.)

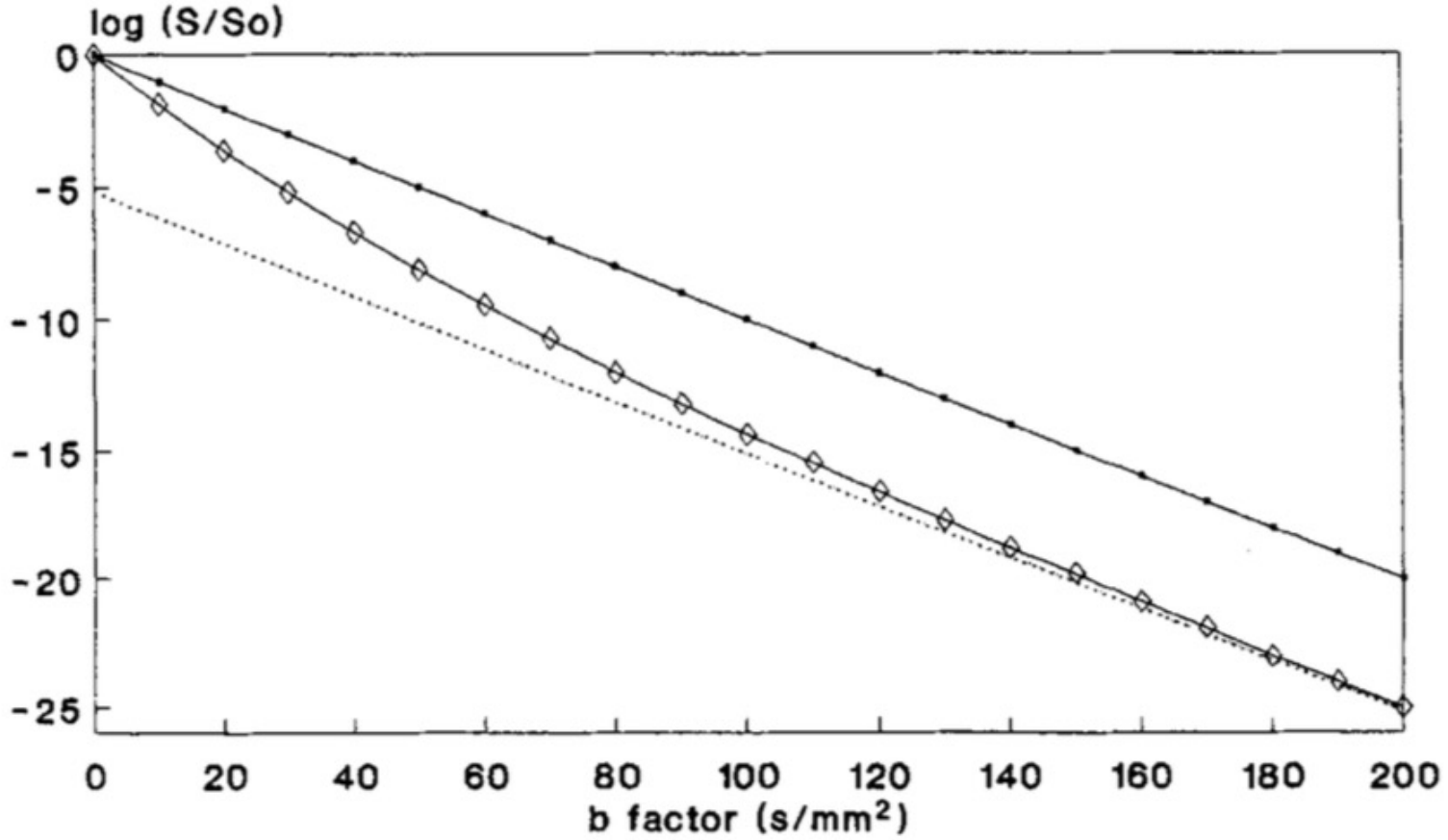

FIG. 2. Model of voxel. In a voxel, effects of both the flowing component and the static component must be taken into account. The first perfusion model was used ($D^* = 20 \times 10^{-3}$ mm^2/s) in this simulation. The capillary volume is typically 5 ml/100 mg of tissue. The logarithm of the signal attenuation is plotted against the b factor. The overall effect of perfusion is to shift the attenuation curve by a quantity $\log(1 - f)$, so that the intercept gives the perfusion factor f. The slope of the attenuation curve, as measured with large b values ($b > 100$ s/mm^2) gives the diffusion coefficient D. Perfusion and diffusion effects may be integrated in the "apparent diffusion coefficient," which is the slope of the attenuation curve obtained for smaller b values (typically between 0 and 100 s/mm^2). (■) Diffusion only; (◇) diffusion + perfusion; (· · ·) asymptote to diffusion.

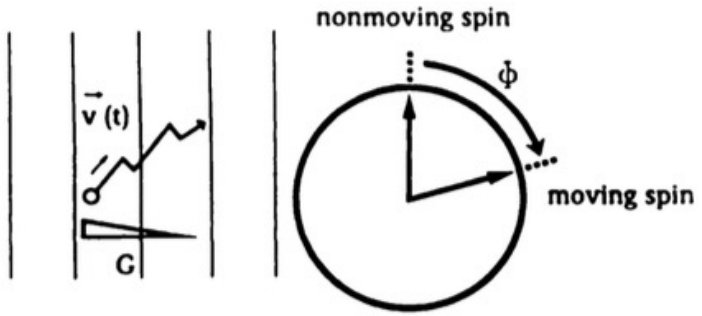

2a.

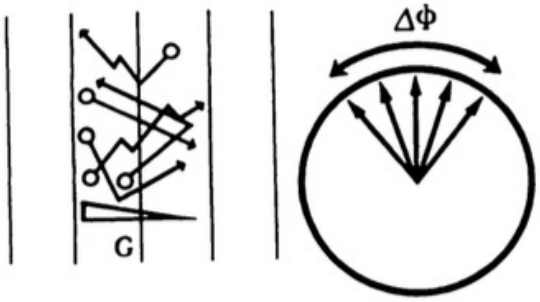

2b.

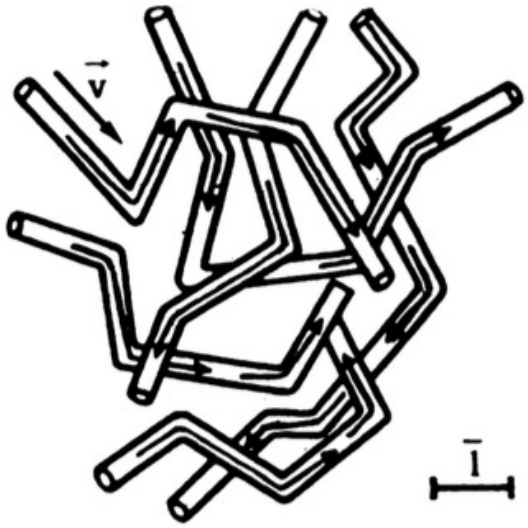

3a.

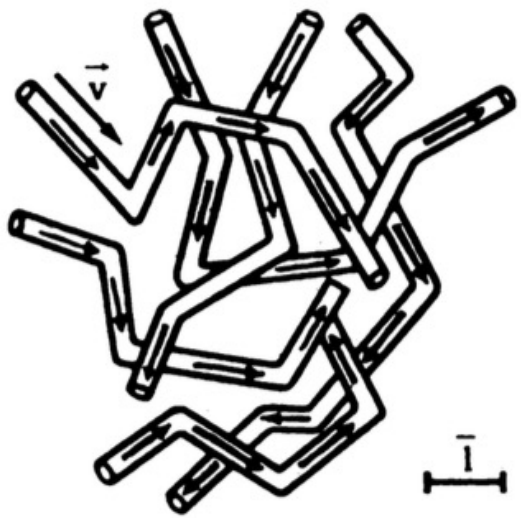

3b.

Figures 2, 3. **(2)** Effect of IVIM on the MR spin-echo signal. **(a)** Spin movements in the direction of a magnetic field gradient *G* produce phase shifts Φ of the transverse magnetization, as compared with nonmoving spins, due to changes in their precession frequency. **(b)** If spins present different movements in a given voxel, a distribution of phase shifts ΔΦ results. This loss of coherence in transverse magnetization decreases the echo signal amplitude, as a function of the differences in spin motions and of the field gradients used. In the case of molecular diffusion, for instance, the echo attenuation is an exponential function of the diffusion coefficient *D*. **(3)** For capillary flow, the spin-echo amplitude attenuation *F* is a function of blood velocity $\bar{v}$ and capillary geometry. Assuming that the capillary network can be described by a succession of straight capillary segments, the mean length of which is $\bar{l}$, two situations can be considered to determine *F*. **(a)** If blood flow changes segments several times during the spin-echo sequence, movement of water in capillaries looks like a diffusion process—that is, a random walk—but at a more complex level. A pseudodiffusion coefficient D^* can be defined, the value of which would be determined by $\bar{l}$ and $\bar{v}$. **(b)** If blood flow does not change segment during the spin-echo sequence, the echo attenuation law becomes different. This situation occurs when the capillary segments are longer, the blood velocity is slower, or the spin-echo delay is shorter. Nevertheless, the echo attenuation *F* can be calculated by assuming a random orientation of the capillary segments at the voxel level. In both these cases, the echo attenuation due to perfusion is always greater than that due to diffusion, potentially allowing them to be separated on a quantitative basis.

Biophysical Journal Volume 66 January 1994 259–267

MR Diffusion *Tensor* Spectroscopy and Imaging

Peter J. Basser,* James Mattiello,* and Denis LeBihan‡

*Biomedical Engineering and Instrumentation Program, National Center for Research Resources, and ‡Diagnostic Radiology Department, The Warren G. Magnuson Clinical Center, National Institutes of Health, Bethesda, Maryland 20892 USA

ABSTRACT This paper describes a new NMR imaging modality—MR diffusion *tensor* imaging. It consists of estimating an effective diffusion tensor, $\mathbf{D}_{\text{eff}}$, within a voxel, and then displaying useful quantities derived from it. We show how the phenomenon of anisotropic diffusion of water (or metabolites) in anisotropic tissues, measured noninvasively by these NMR methods, is exploited to determine fiber tract orientation and mean particle displacements. Once $\mathbf{D}_{\text{eff}}$ is estimated from a series of NMR pulsed-gradient, spin-echo experiments, a tissue's three orthotropic axes can be determined. They coincide with the eigenvectors of $\mathbf{D}_{\text{eff}}$, while the effective diffusivities along these orthotropic directions are the eigenvalues of $\mathbf{D}_{\text{eff}}$. Diffusion ellipsoids, constructed in each voxel from $\mathbf{D}_{\text{eff}}$, depict both these orthotropic axes and the mean diffusion distances in these directions. Moreover, the three scalar invariants of $\mathbf{D}_{\text{eff}}$, which are independent of the tissue's orientation in the laboratory frame of reference, reveal useful information about molecular mobility reflective of local microstructure and anatomy. Inherently, tensors (like $\mathbf{D}_{\text{eff}}$) describing transport processes in anisotropic media contain new information *within a macroscopic voxel* that scalars (such as the apparent diffusivity, proton density, T_1, and T_2) do not.

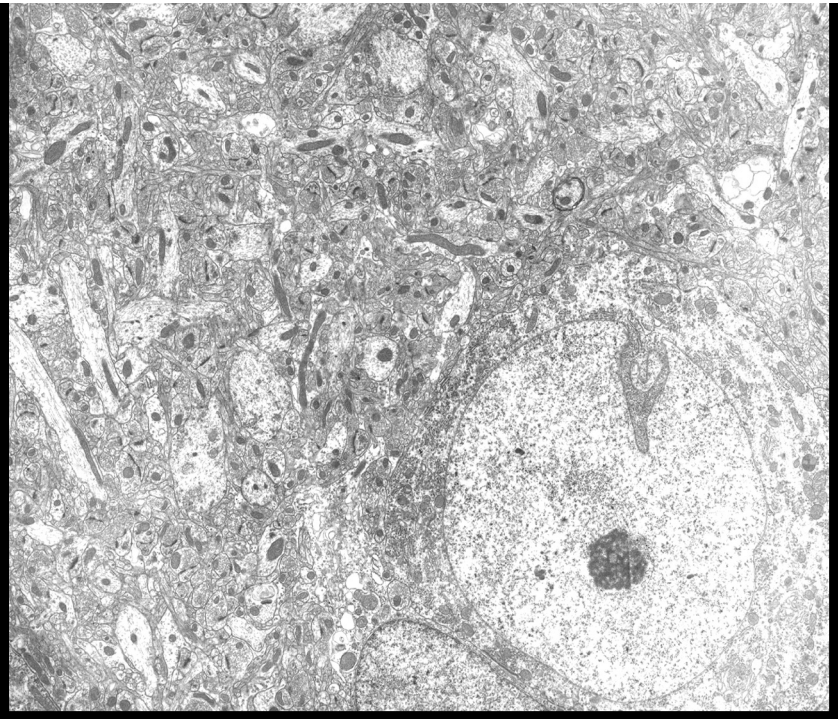

Gray matter
(Cortex)

isotropic
diffusion

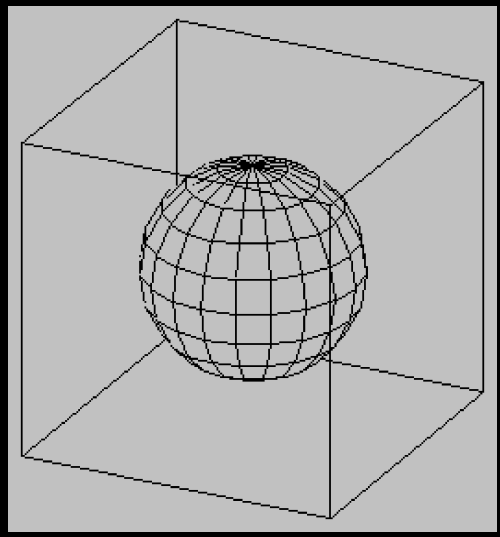

~ microns

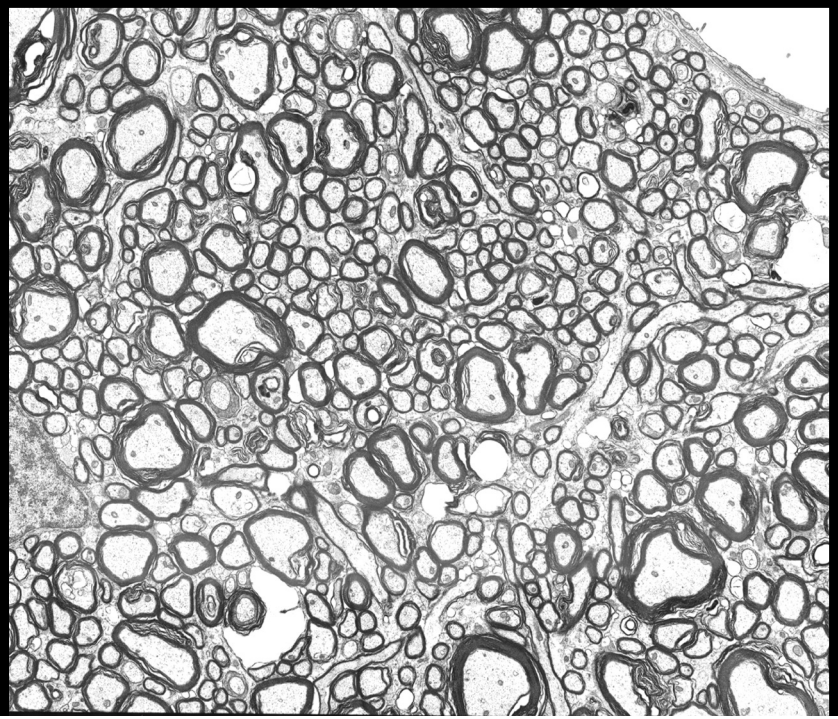

White matter
(Corpus callosum

*an*isotropic
diffusion

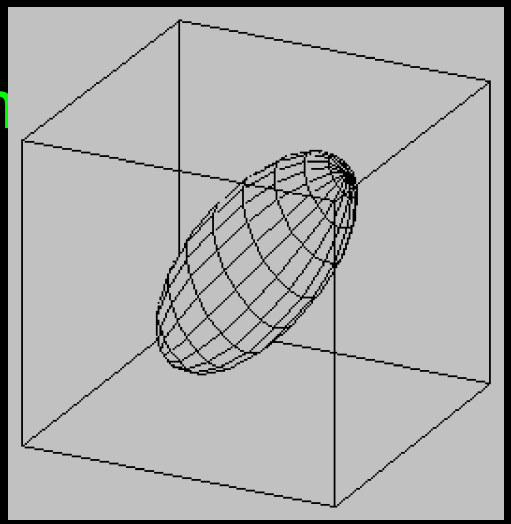

Diffusion Tensor MRI Flowchart

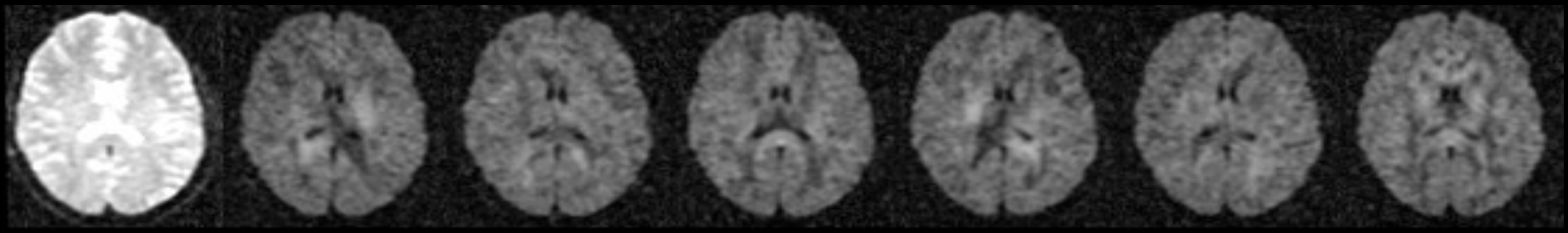

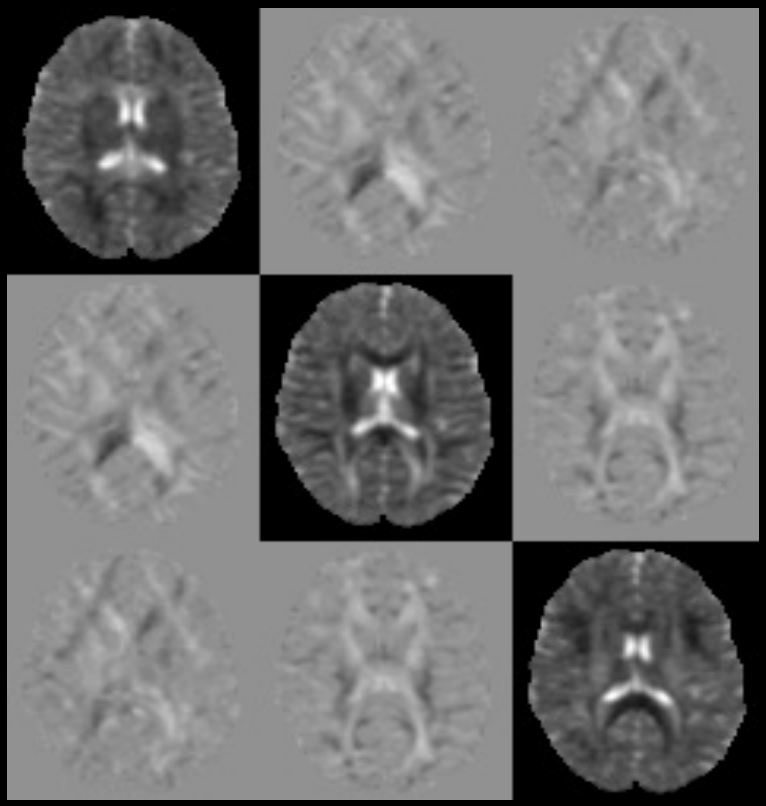

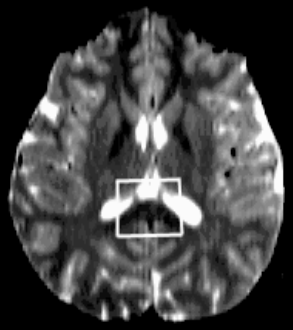

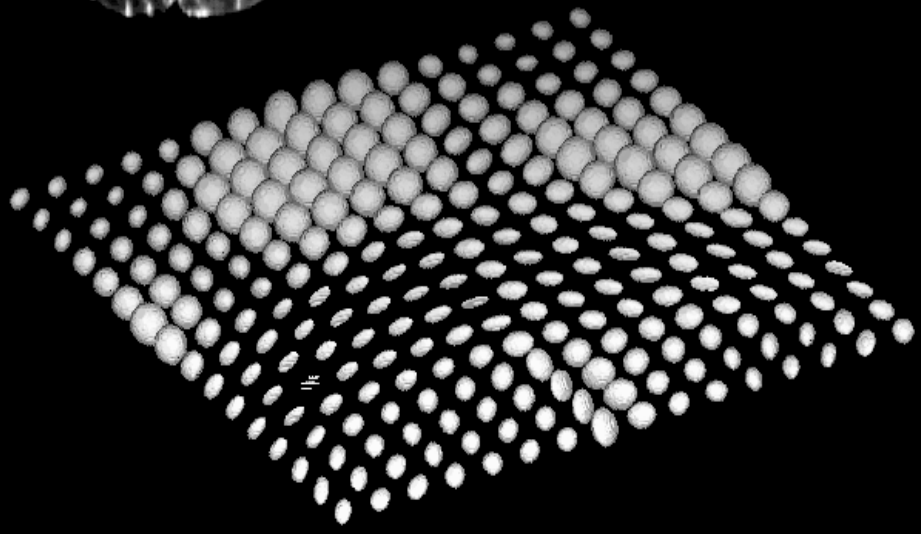

Diffusion Tensor MRI of the Human Brain.

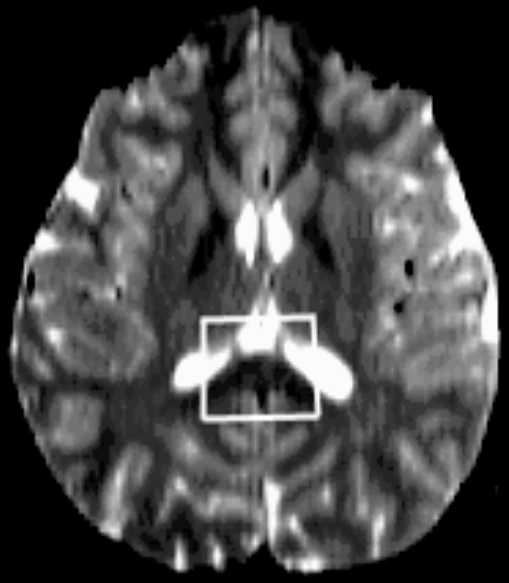

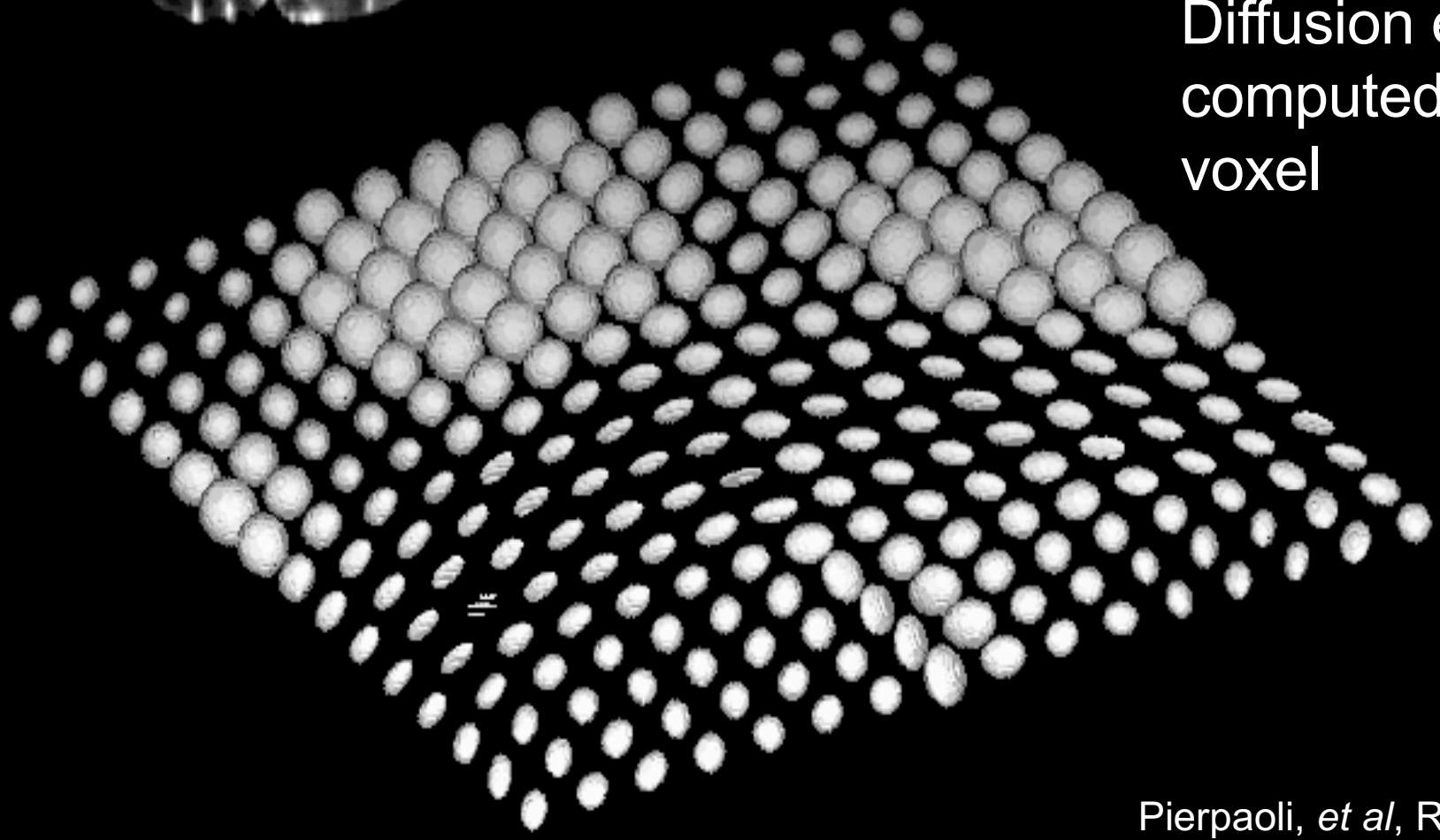

Diffusion ellipsoids computed in each voxel

Pierpaoli, *et al*, Radiology, 1996

High Angular Resolution Diffusion Imaging (HARDI)

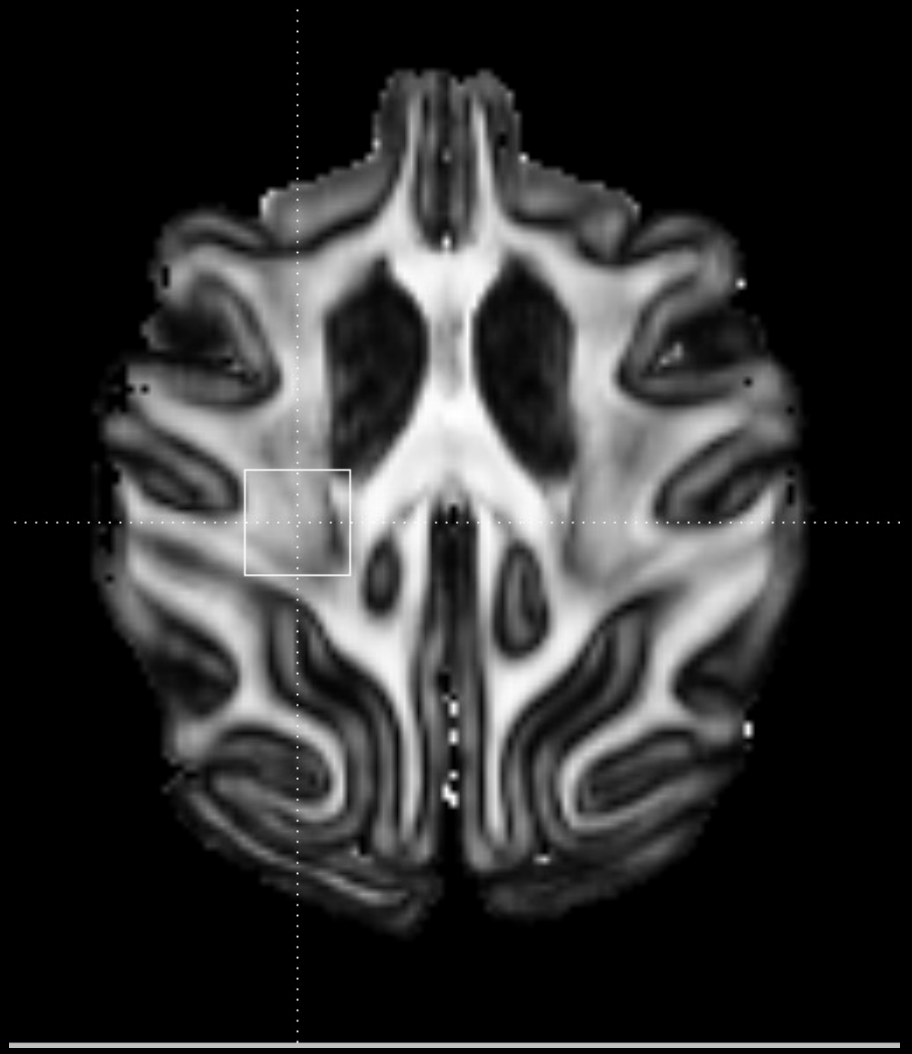

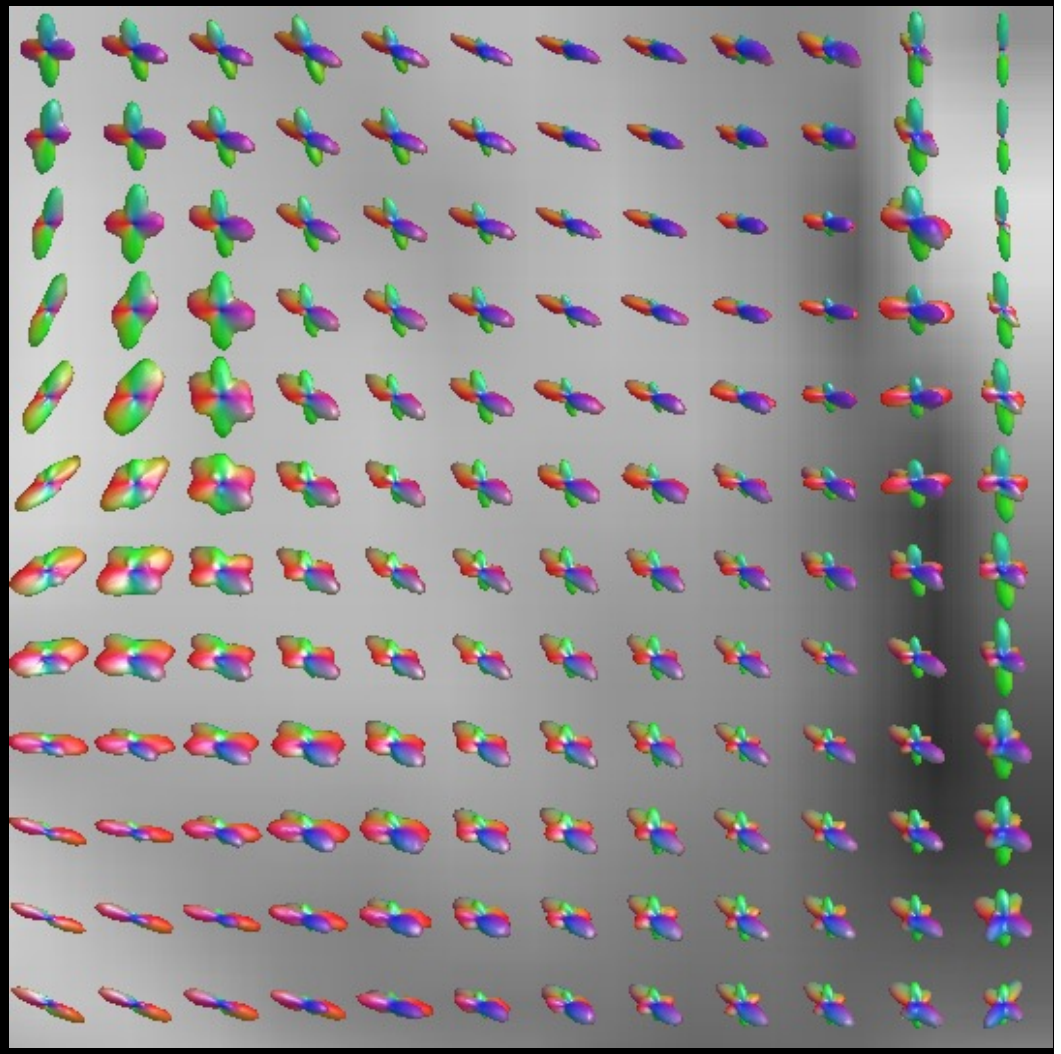

3D SHORE Courtesy of Evren Ozarslan

Trace(D) (averaged mean-squared displacement)

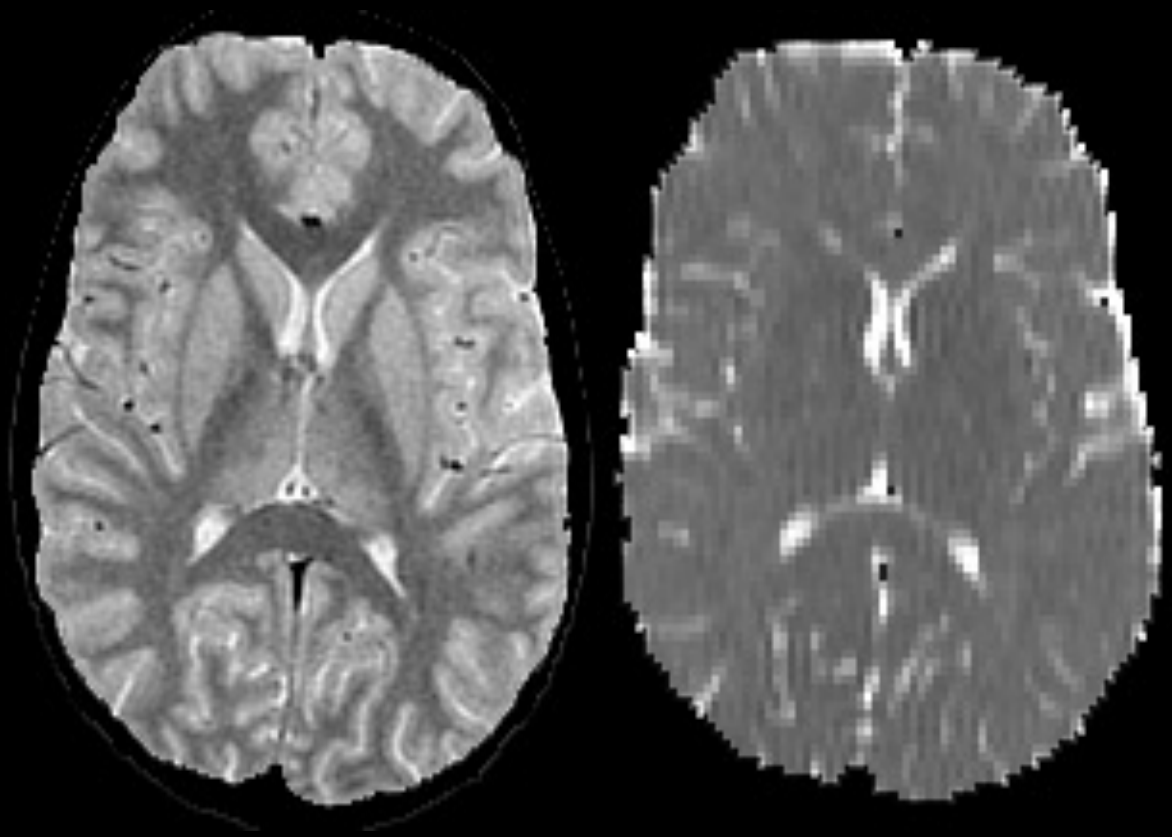

- Trace(**D**) is homogeneous in normal brain parenchyma

- Low inter-subject variability

T2 weighted image Trace(D) map (also called ADC or MD)

Early Detection of Stroke by Diffusion MRI

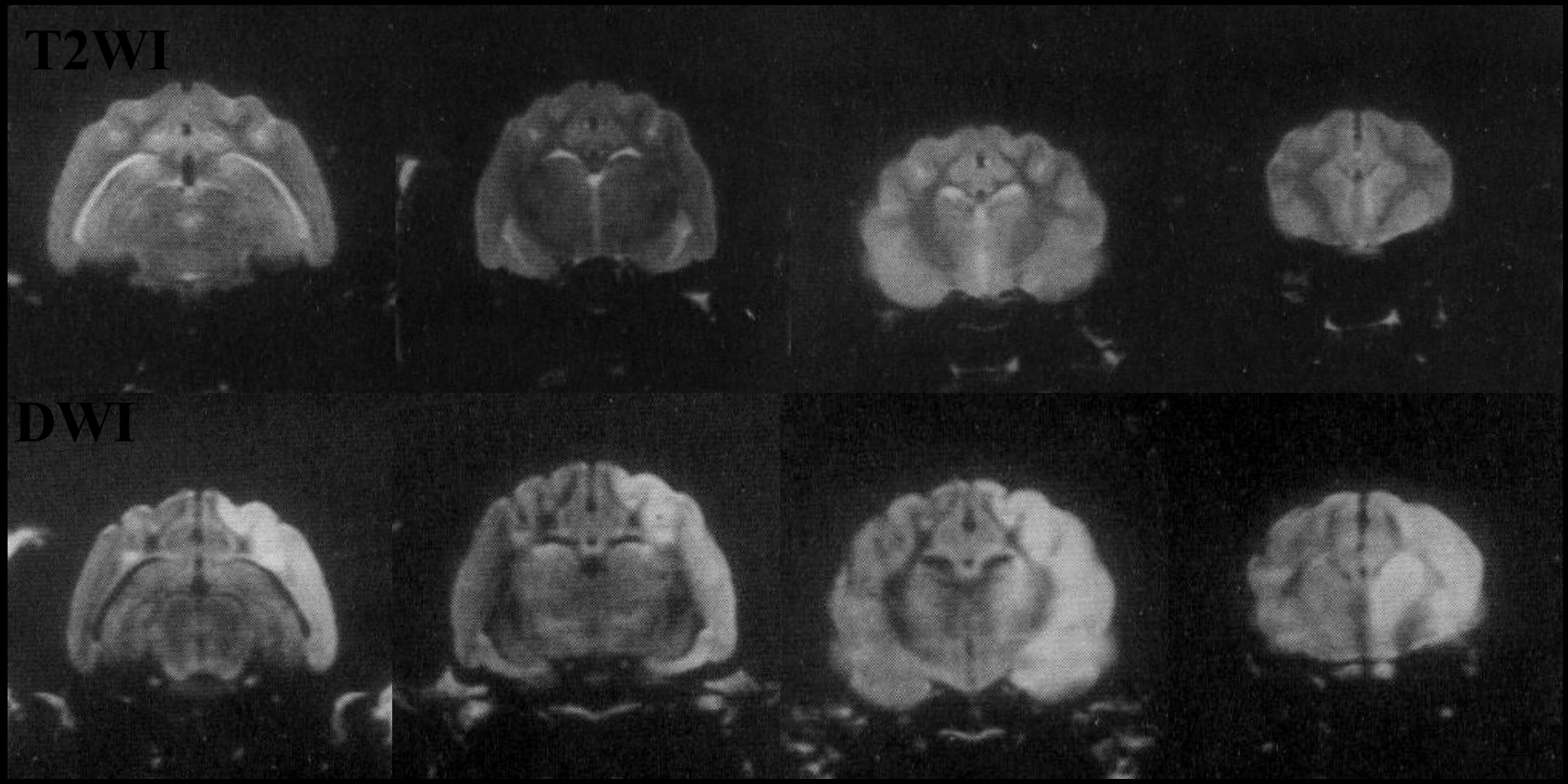

Mosley et.al, Magn Reson Med. 1990 May;14(2):330-46.

Kinetic of diffusion changes in reversible complete ischemia animal models

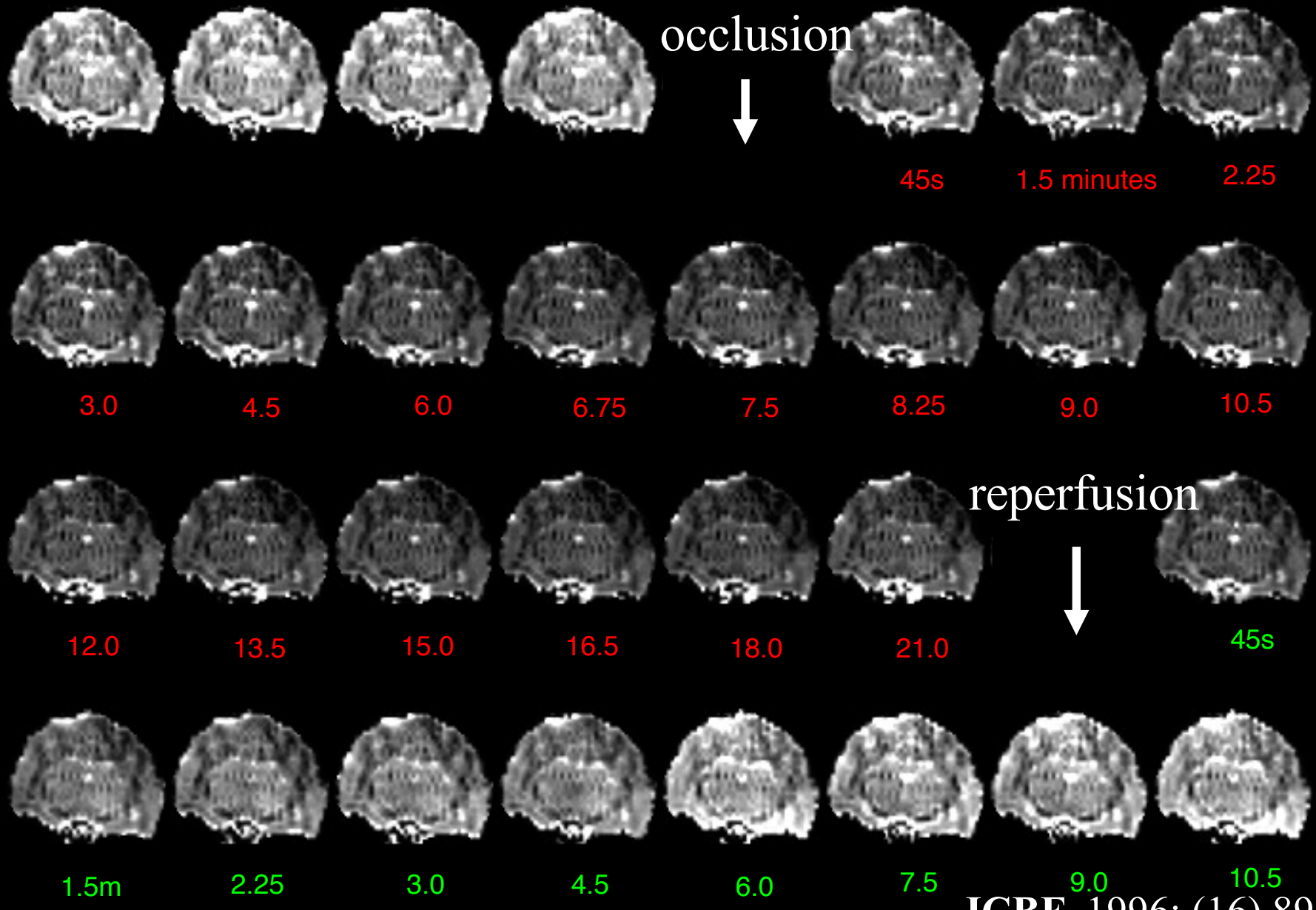

JCBF 1996; (16) 892-905.

Tissue characterization in stroke

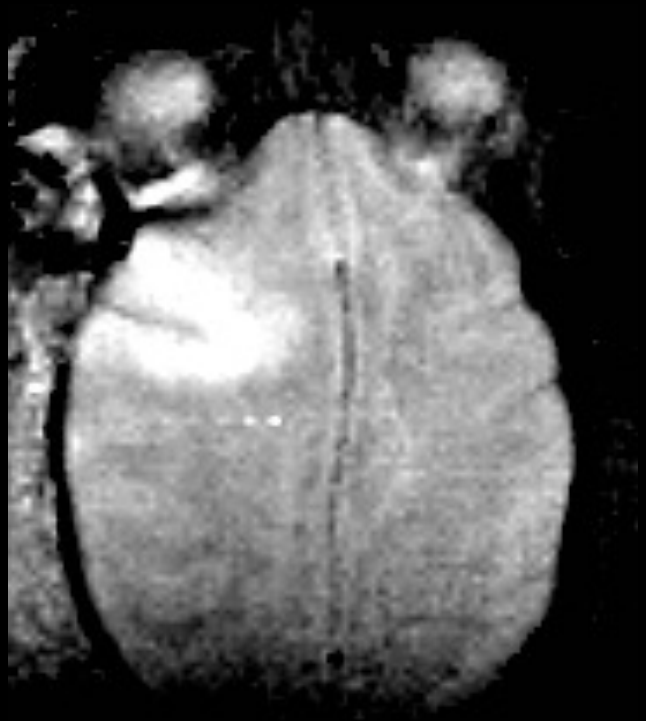

T2-weighted MRI

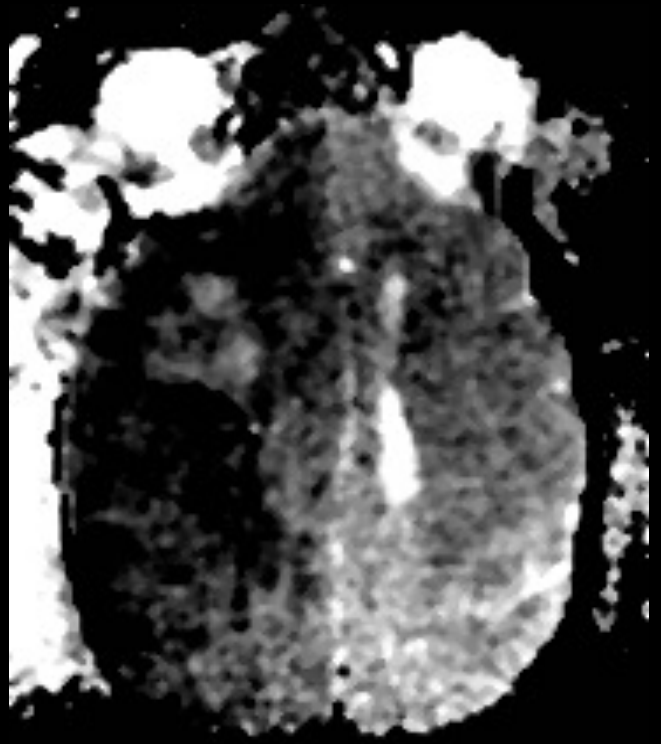

Trace (D)

Tissue characterization in stroke

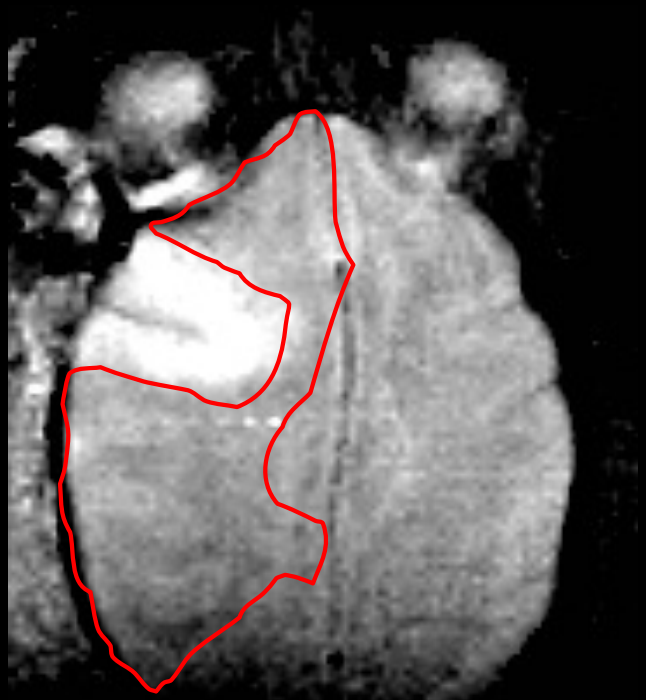

Acute
Ischemia
or stroke

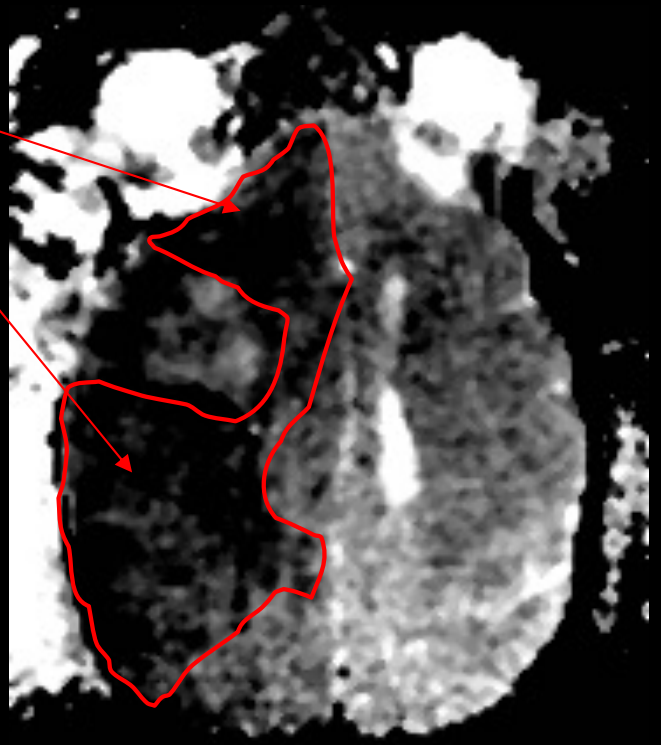

T2-weighted MRI

Trace (D)

Tissue characterization in stroke

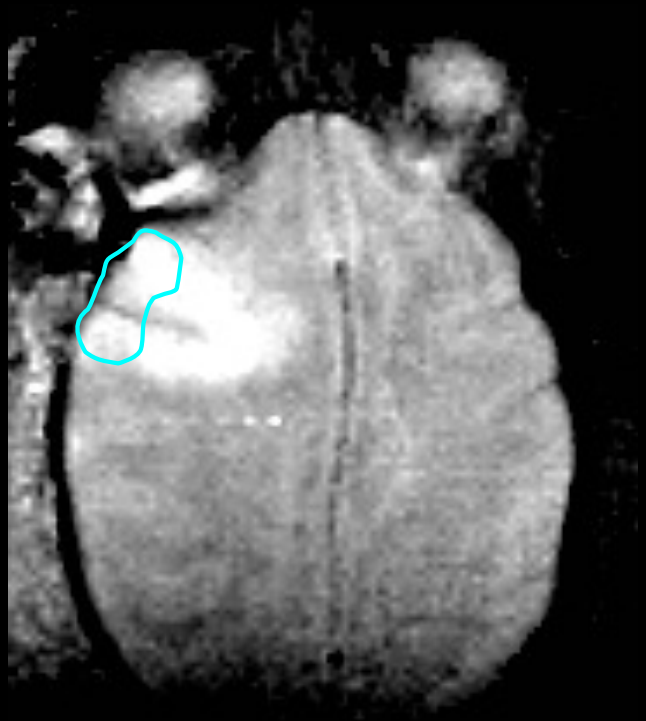

Stroke
intact
cells

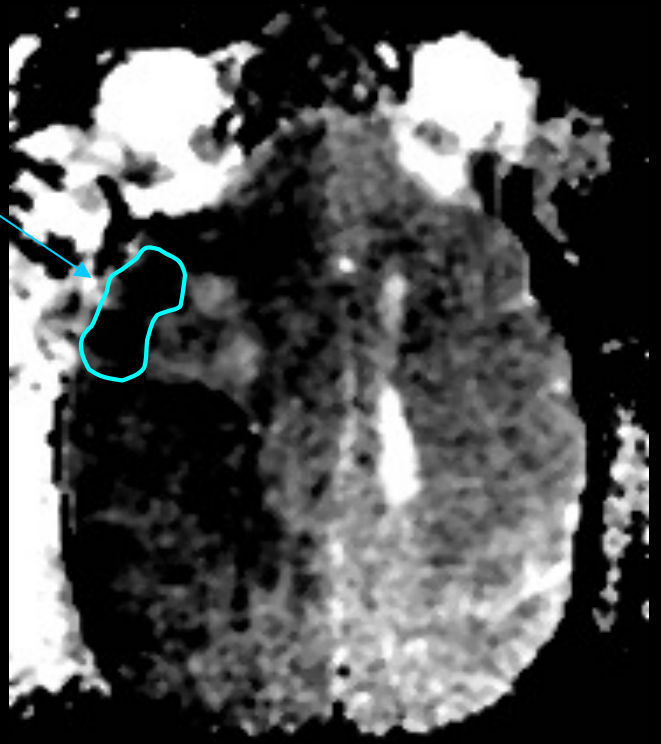

T2-weighted MRI

Trace (D)

Tissue characterization in stroke

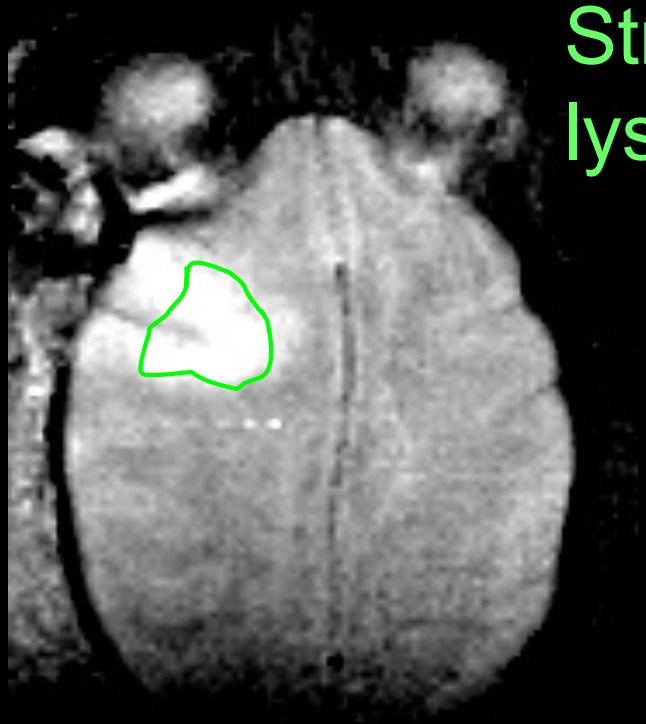

Stroke cell lysis

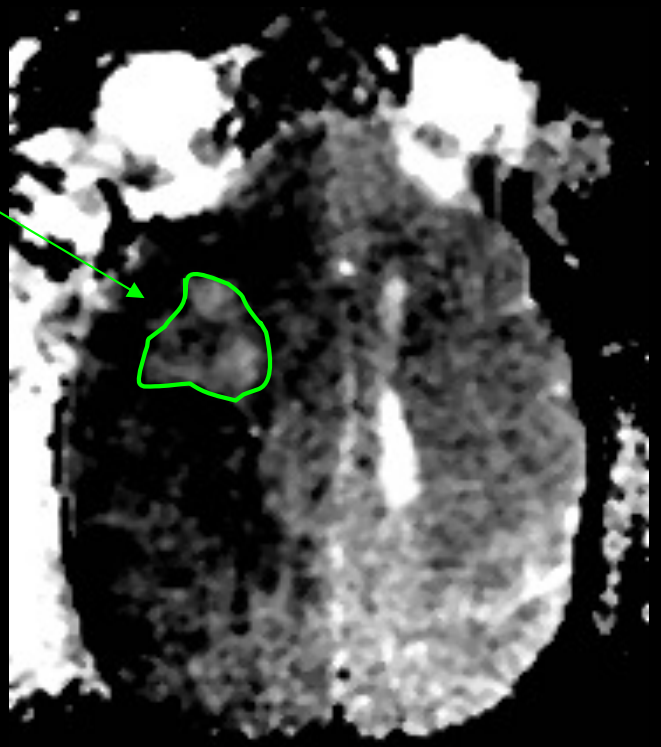

T2-weighted MRI

Trace (D)

SUMMARY. Tissue characterization in brain ischemia and stroke.

	T2WI	Diffusion
• Reduced perfusion	=	=
• Ischemia	=	- Trace(D)
• Acute infarct (no vasogenic edema)	=	- Trace(D)
• Subacute infarct (vasogenic edema)	+	- Trace(D)
• Chronic infarct (cell lysis)	+	+ Trace(D)
• Healthy tissue (vasogenic edema)	+	+ Trace(D)

Trace(**D**) differentiates between recent and old infarcts

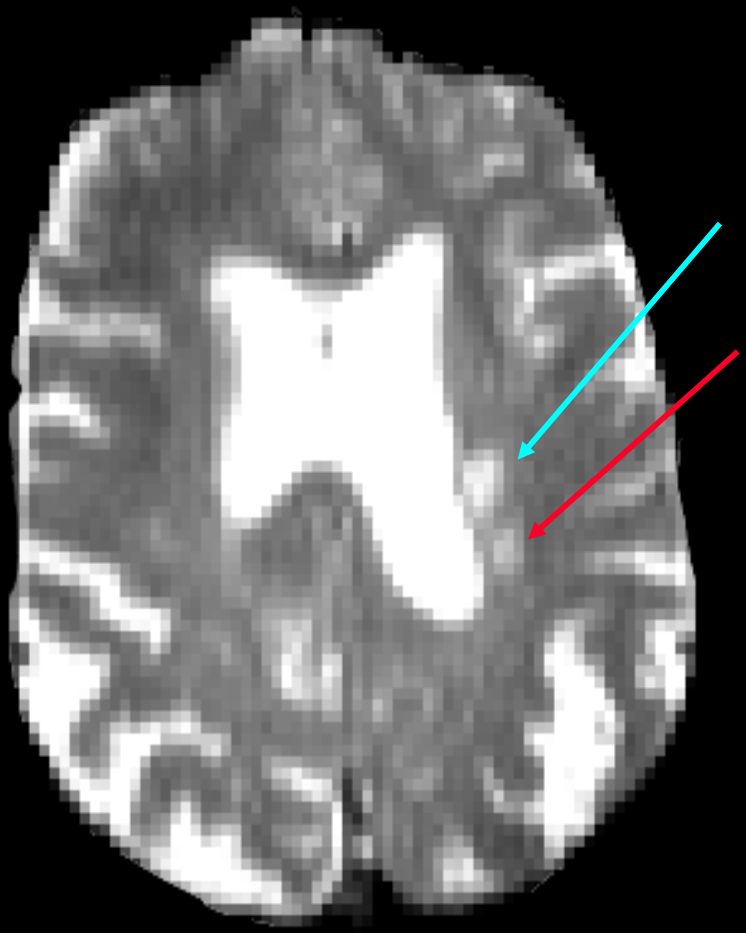

T2-weighted MRI

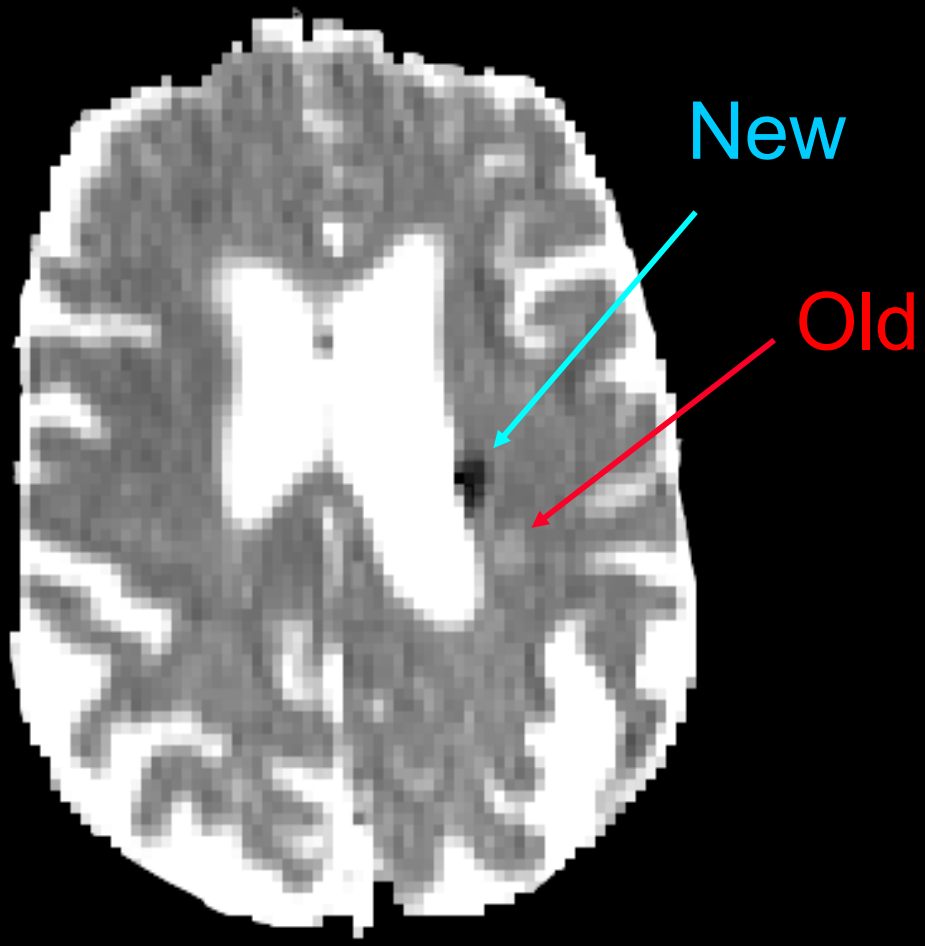

Trace(**D**)

Documenting tissue plasminogen activator(tPA) treatment outcome with diffusion and perfusion MRI

Pre tPA

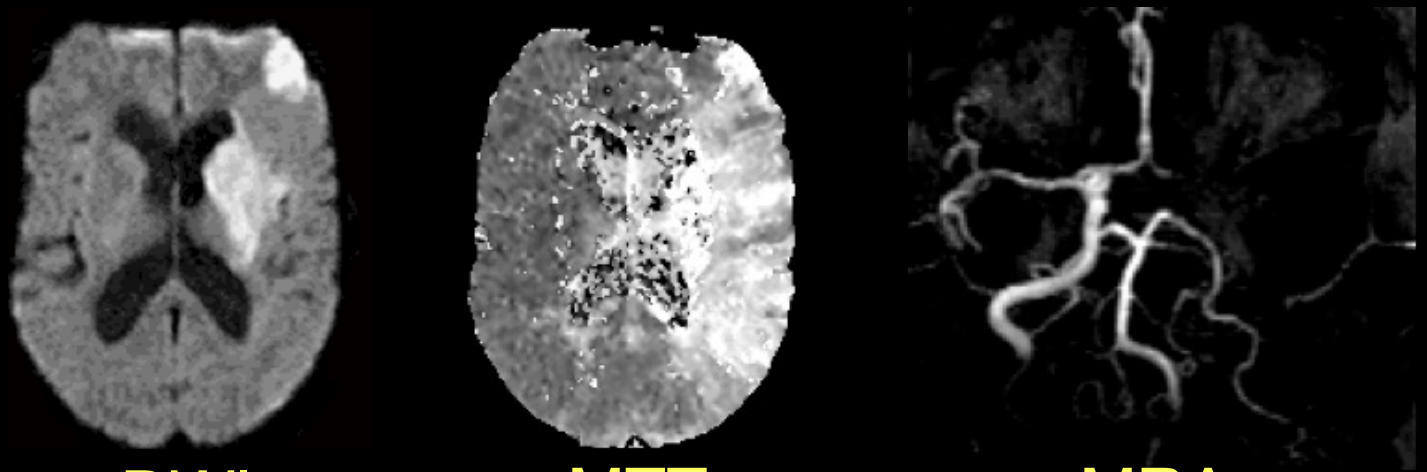

DWI MTT MRA

Post tPA

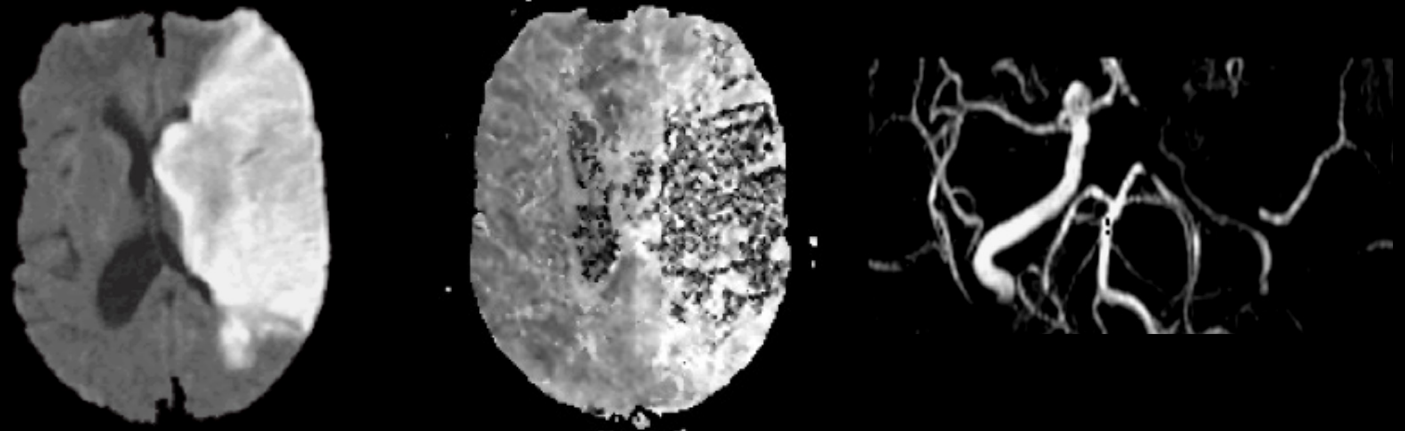

DWI MTT MRA

TRAUMATIC BRAIN INJURY

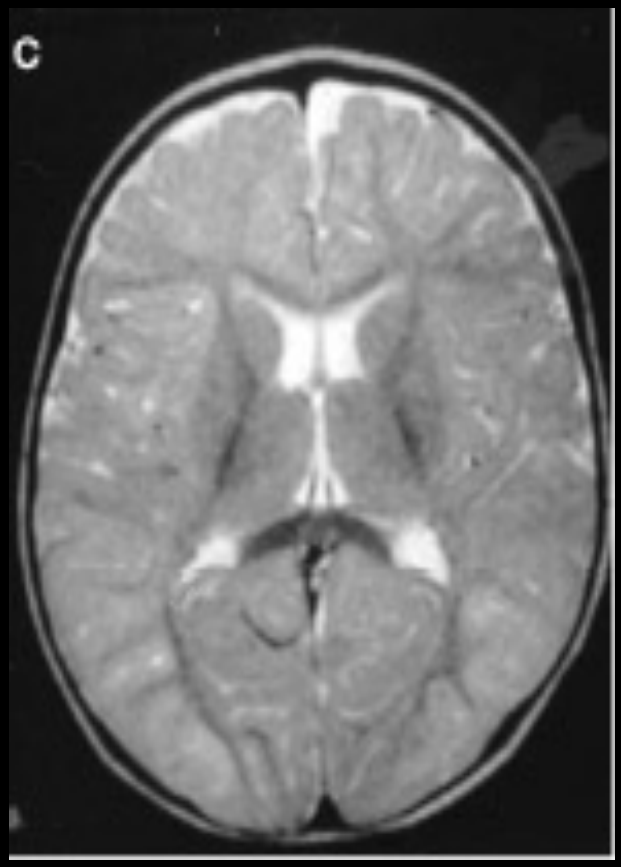

T2WI

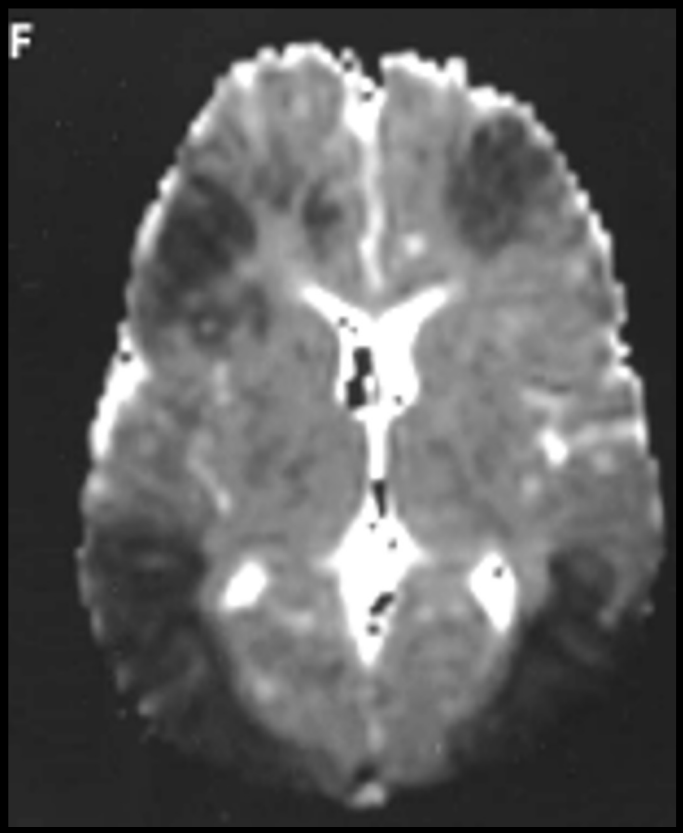

Trace(D)

7.5-month old boy who reportedly fell off the bed onto a carpeted floor. Scan performed 1 day after presentation.

Suh DY et al Neurosurgery, Vol. 49, No. 2, August 2001, 309-20

Biophysical hypothesis for Trace (or ADC) reduction in ischemia

In the normal brain: 80% intracellular water

$$ADC_{total} = ADC_{intra} * f_{intra} + ADC_{extra} * f_{extra}$$

Following ischemia: Na/K ATP-ase failure causes cell swelling

10% shift of water: $f_{extra} \rightarrow f_{intra}$

Results in a 30-50% decrease in ADC_{total}

Compartment shift hypothesis:

Intrinsic $ADC_{intra} << ADC_{extra}$

Extracellular tortuosity hypothesis:

ADC_{extra} decrease

Intracellular restriction hypothesis:

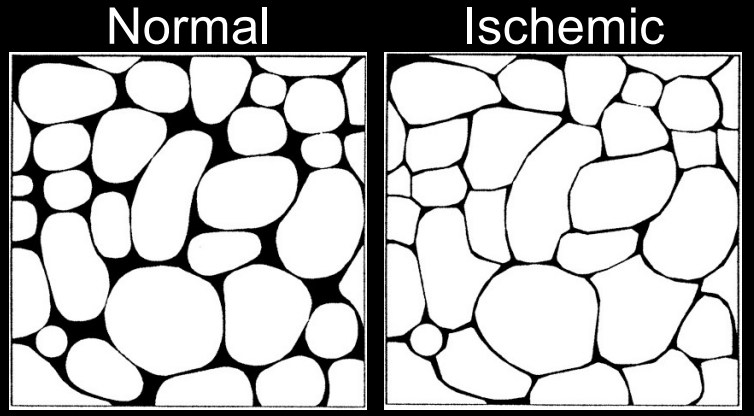

Chen KC. & Nicholson C. *PNAS* 2000

Diffusivity of Cs+ (intracellular surrogate) decreased by ~75% following global ischemia. (Goodman, et al. *MRM* 2008)

Slide courtesy of Matt Budde

Hypothesis by Matt Budde, et al., PNAS, 2010

Neurite beading is sufficient to decrease ADC_{intra} by restricting water mobility along each neurite.

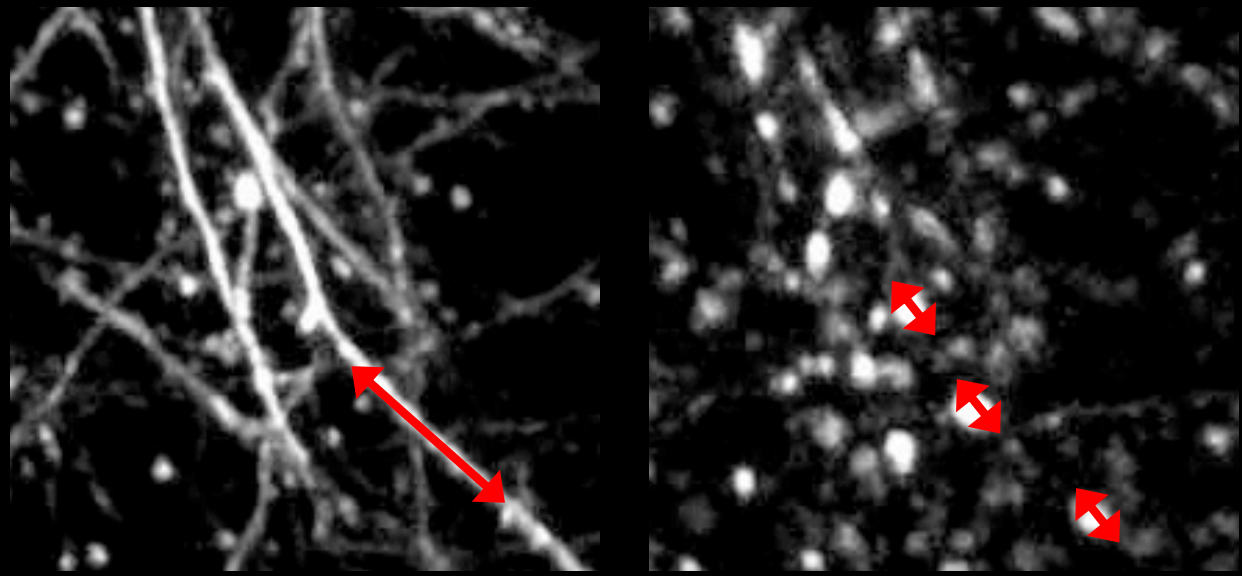

Approach

Derive a biophysical model of beading in neurites

Simulate diffusion MR experiment in 3D geometrical surfaces

Validate model in mammalian tissues

Slide courtesy of Matt Budde

What can we learn from other imaging modalities?

In vivo two-photon microscopy (Murphy T, et al. *J Neurosci* 2008)

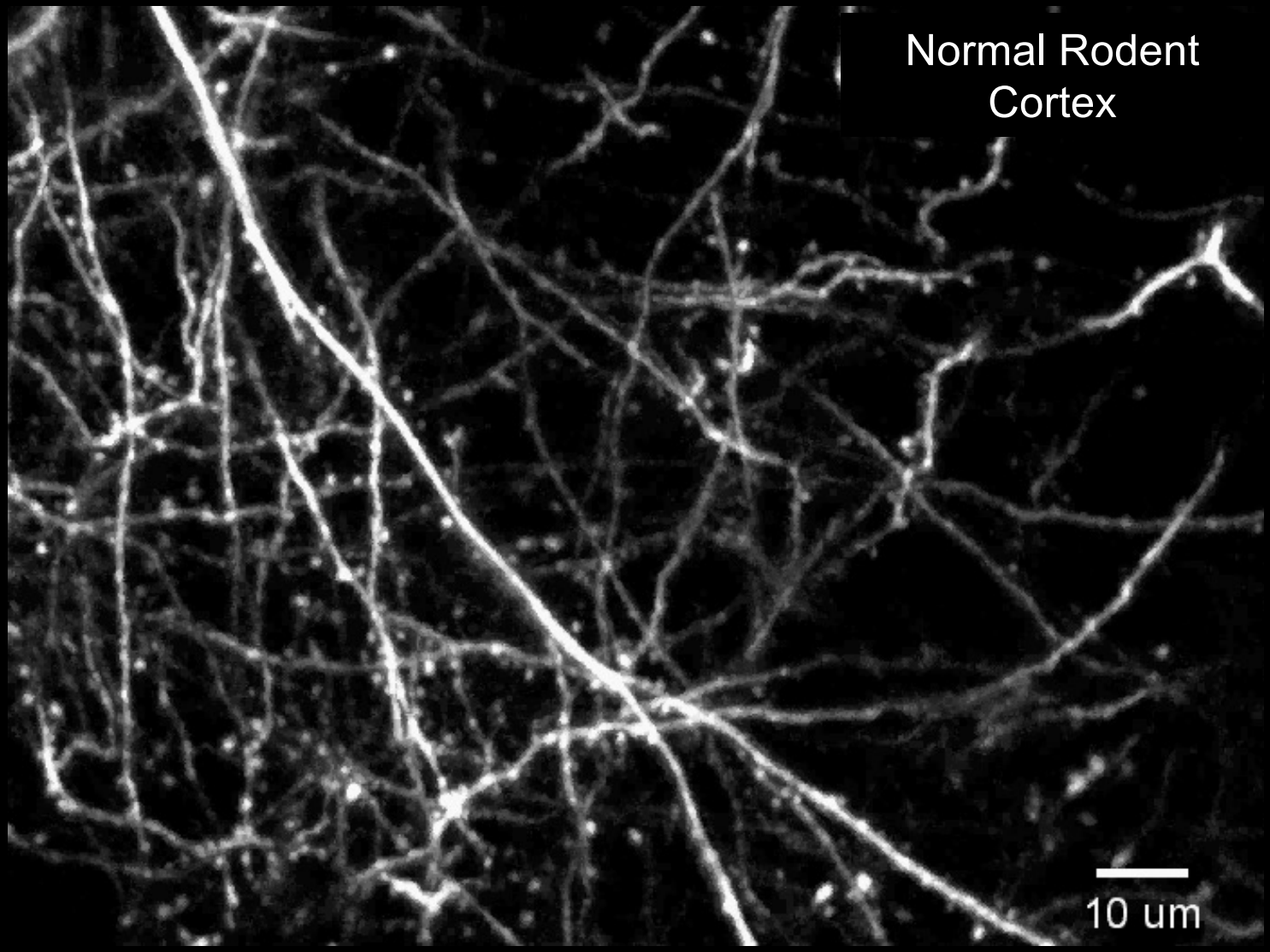

Slide courtesy of Matt Budde

Neurite beading occurs abruptly after ischemia…

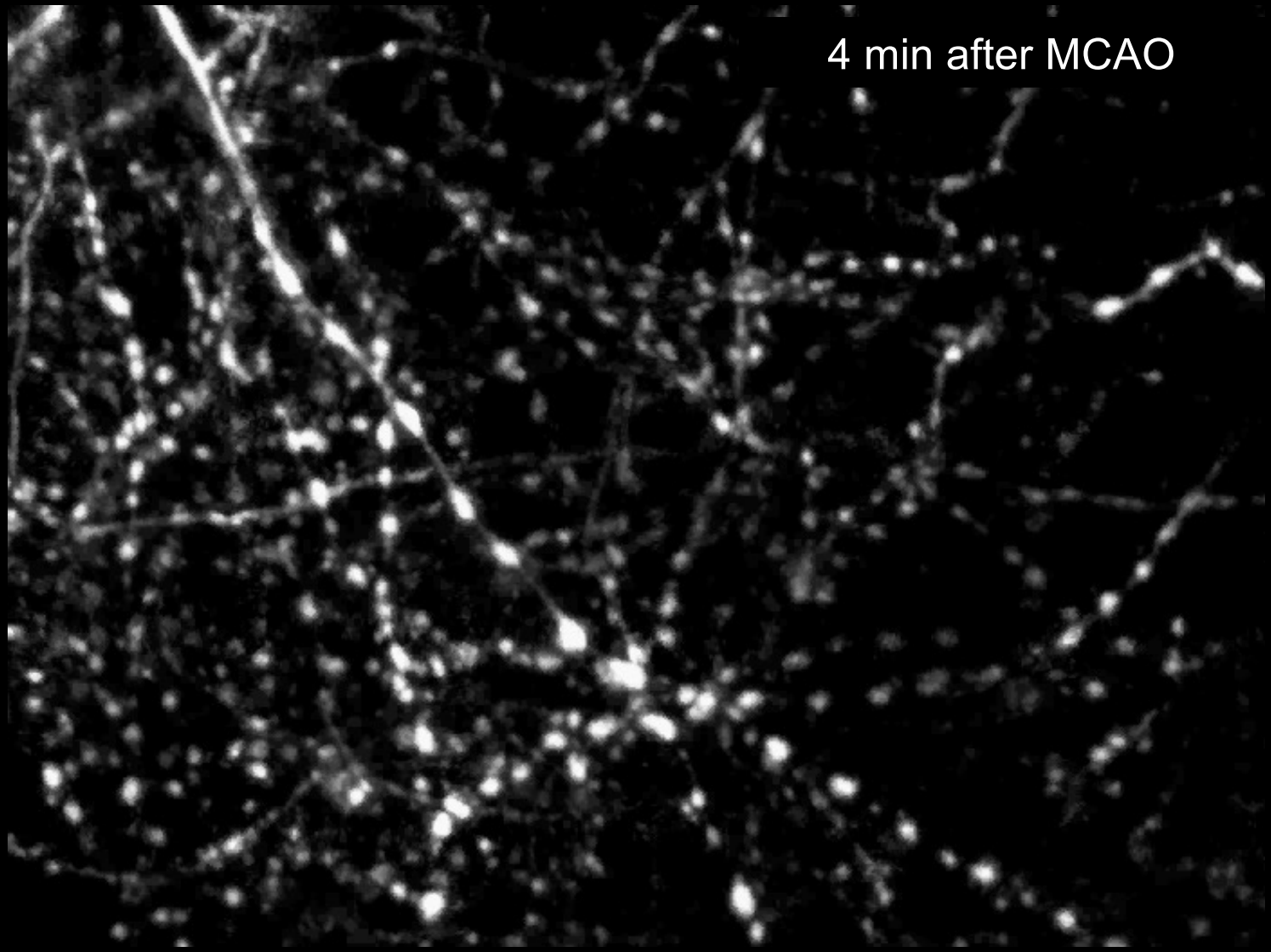

Slide courtesy of Matt Budde

…and resolves upon reperfusion.

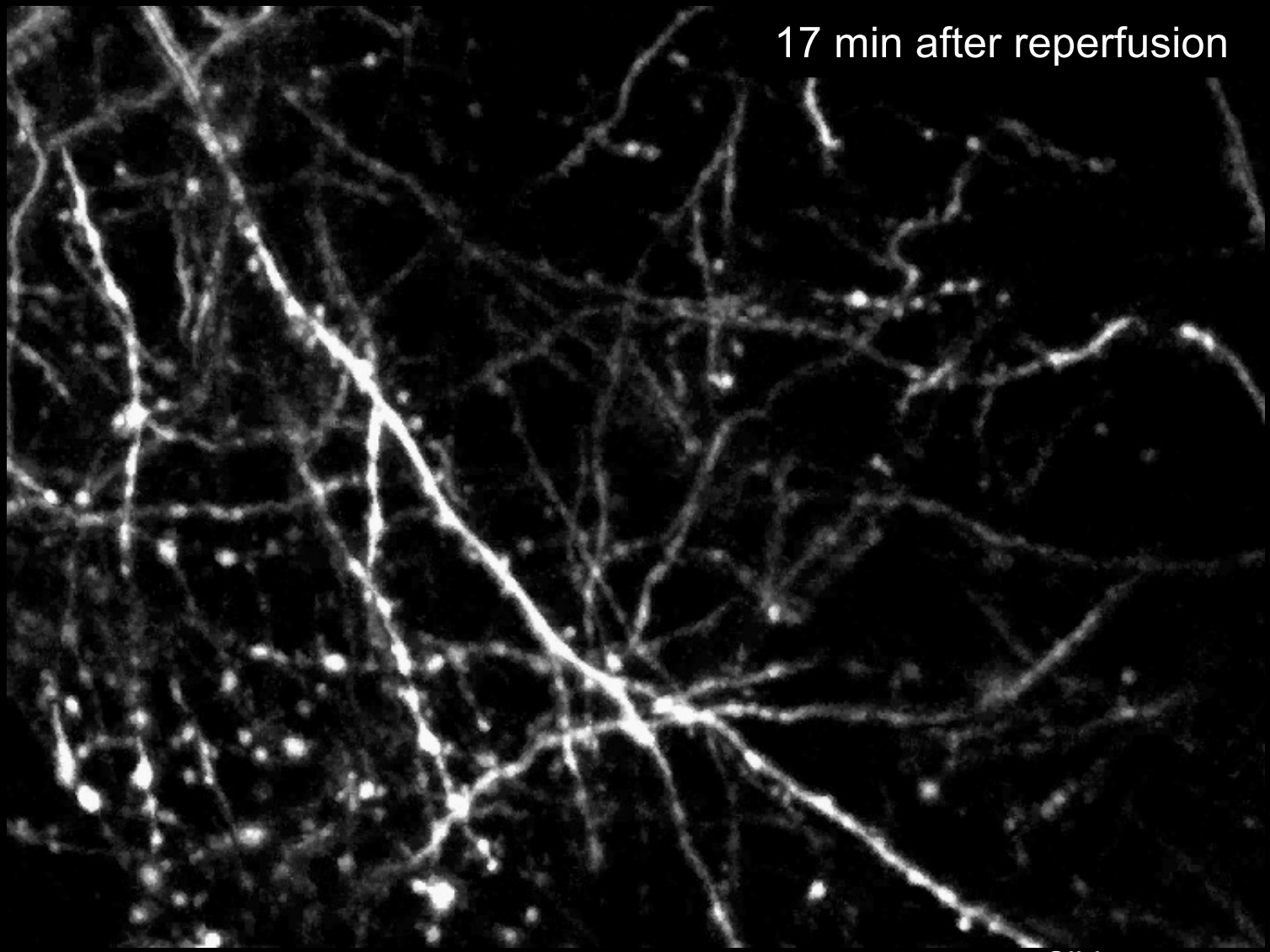

Slide courtesy of Matt Budde

Diffusion anisotropy (shape of displacement profile)

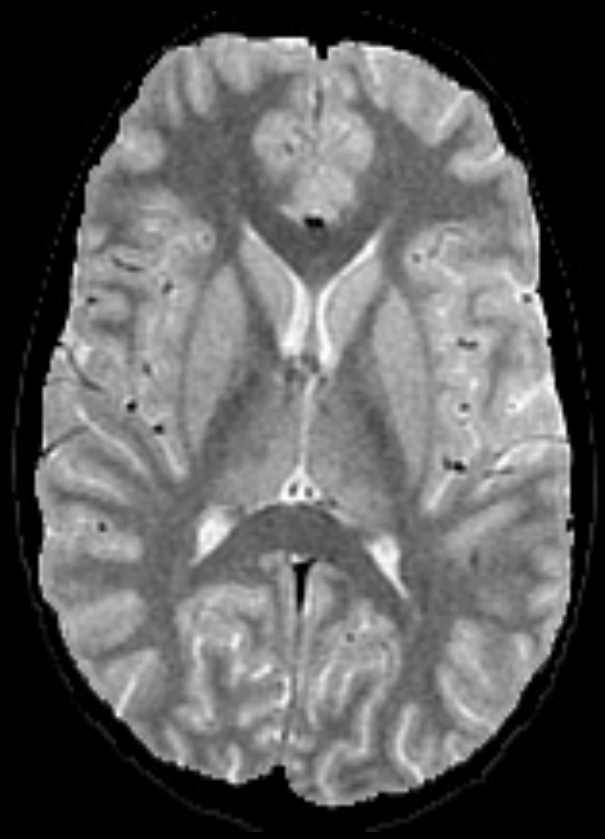

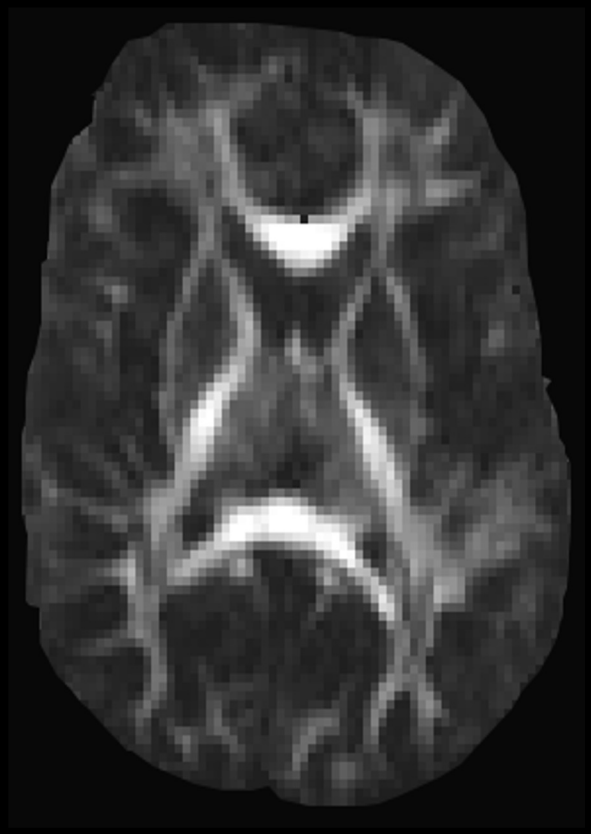

T2 weighted image Anisotropy map

- Diffusion anisotropy is highly variable in normal white matter

- Differences in anisotropy reflect differences in white matter architecture

Intra-voxel orientational coherence of white matter fibers is an important factor in determining diffusion anisotropy

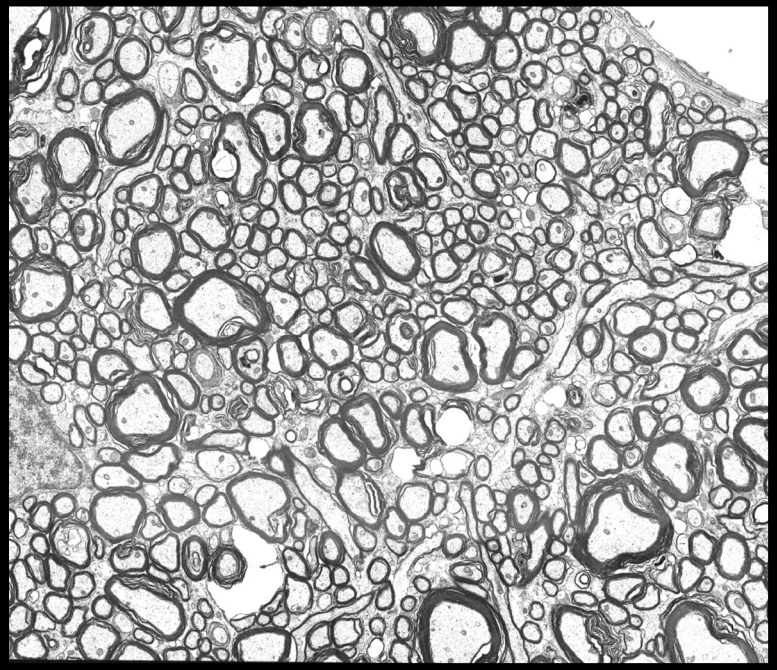

White matter
(Corpus callosum)

anisotropic
diffusion

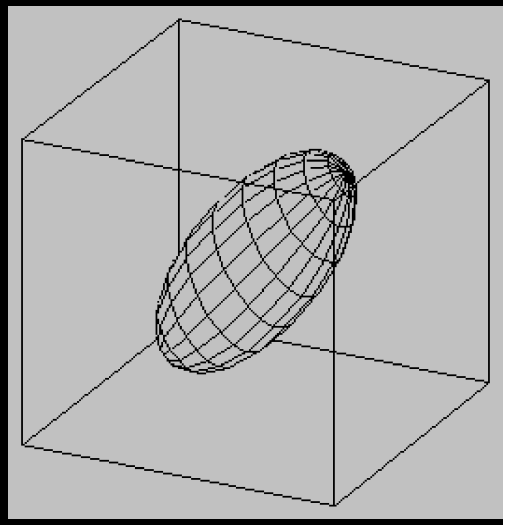

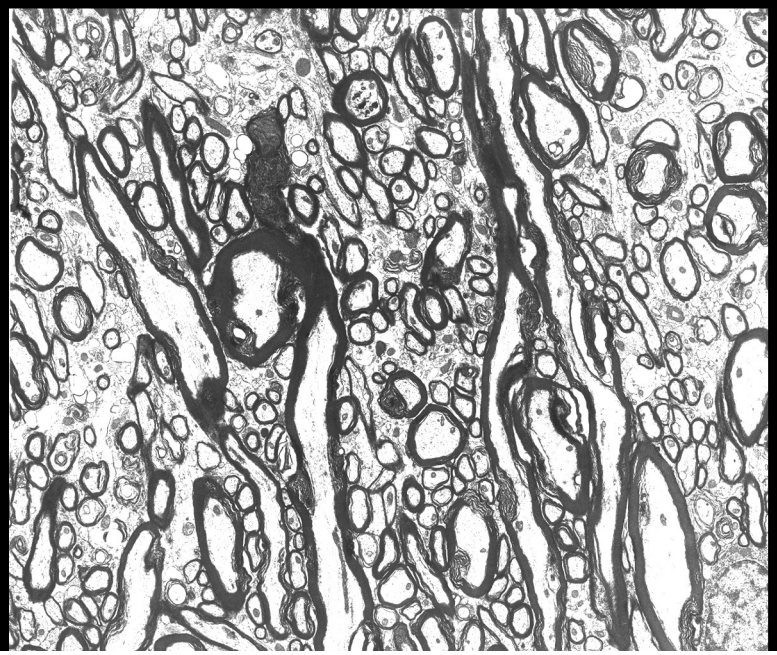

Subcortical
White matter

more isotropic
diffusion

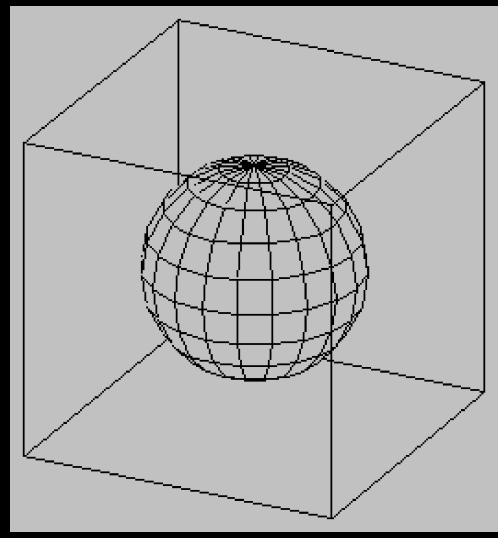

Pierpaoli, *et al*, Radiology, 1996

Fiber orientation

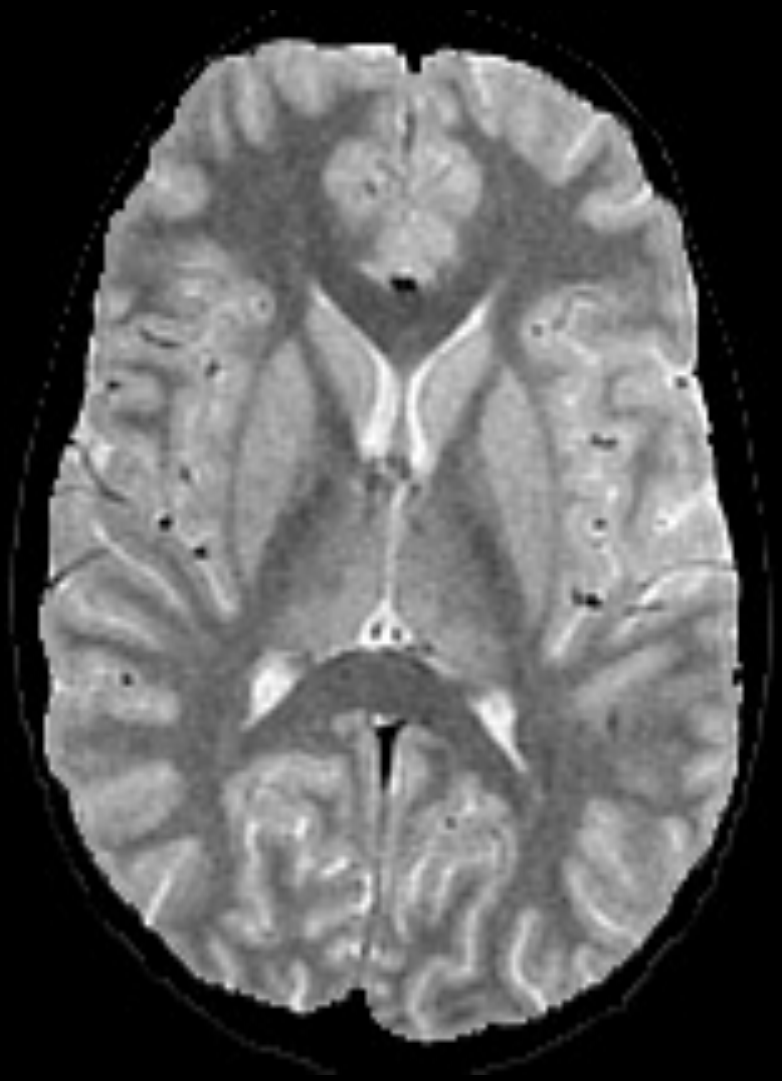

T2 weighted image

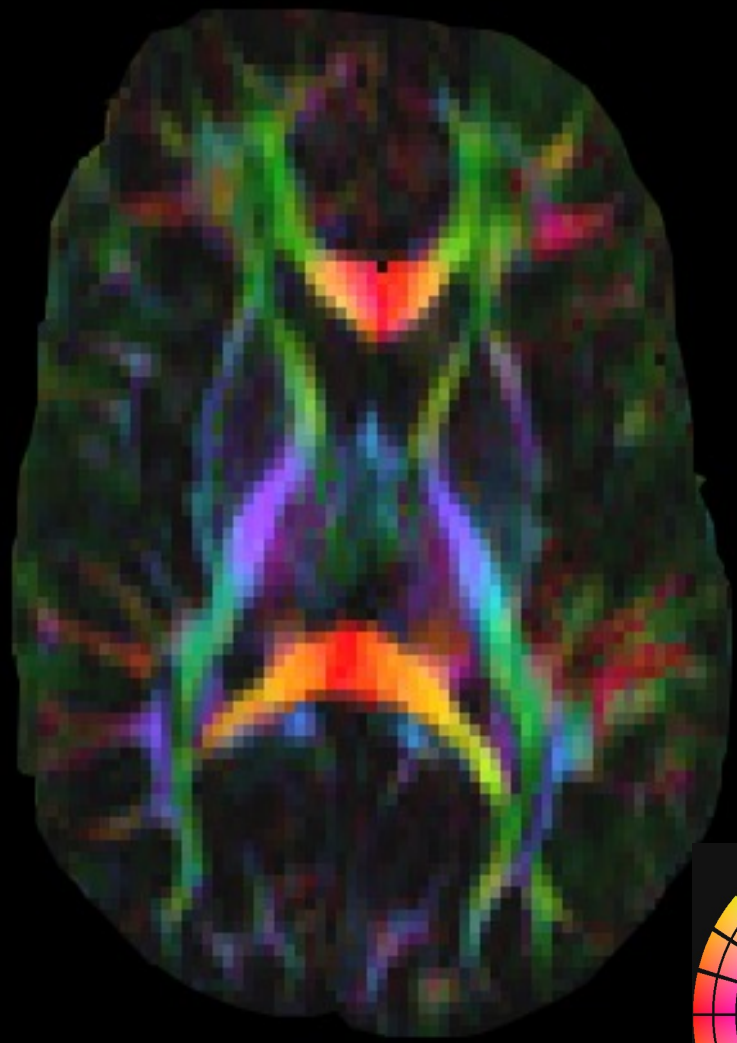

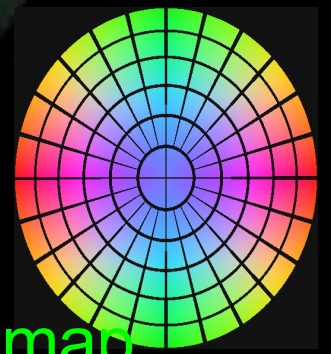

Color fiber orientation map

Pajevic and Pierpaoli, MRM 1999

DTI vs. conventional structural MRI

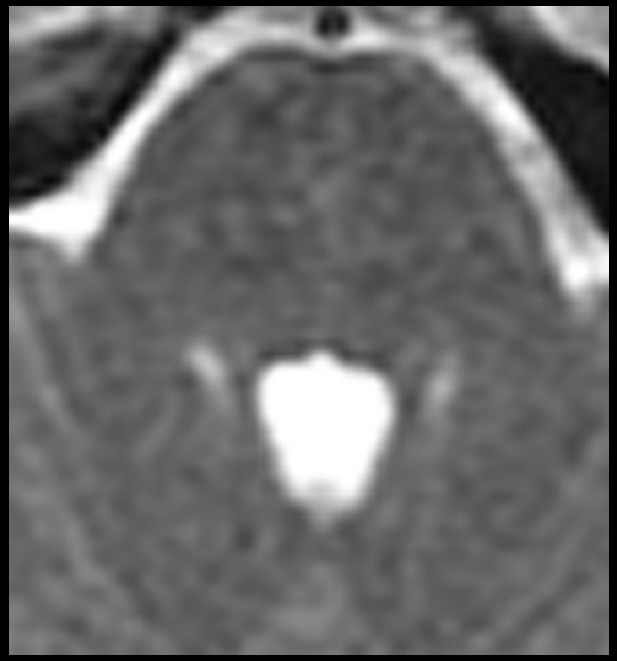

High resolution T2-weighted structural MRI

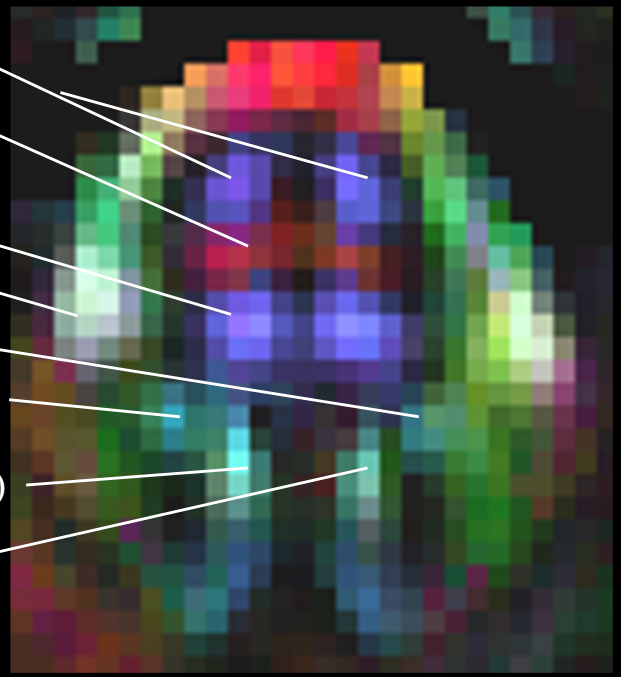

DTI fiber orientation map

Pajevic and Pierpaoli, MRM 1999

Color maps of Association Pathways

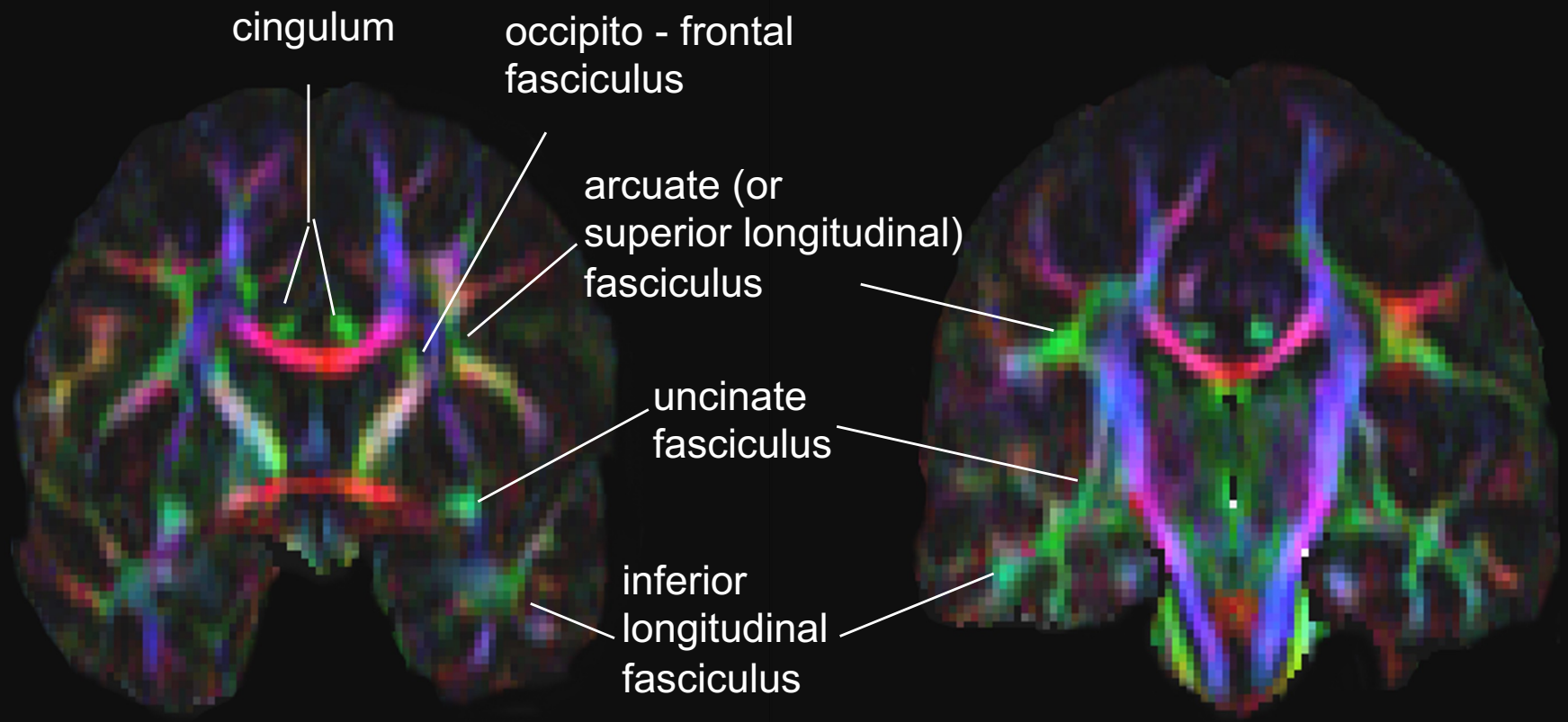

Pajevic and Pierpaoli, MRM 1999

Degeneration of pontocerebellar pathways in Multiple System Atrophy

Healthy subject

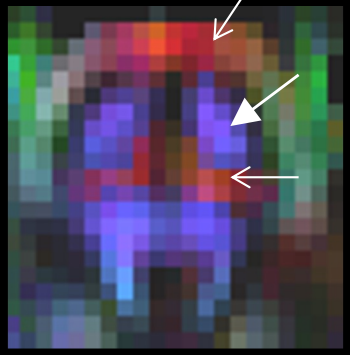

MSA patient

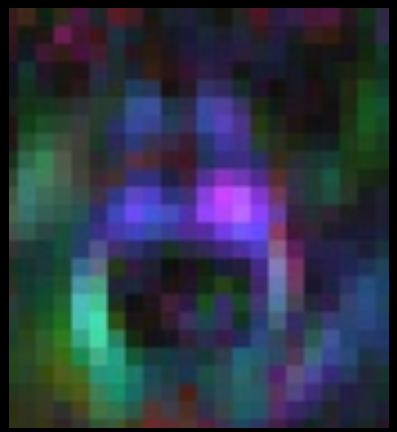

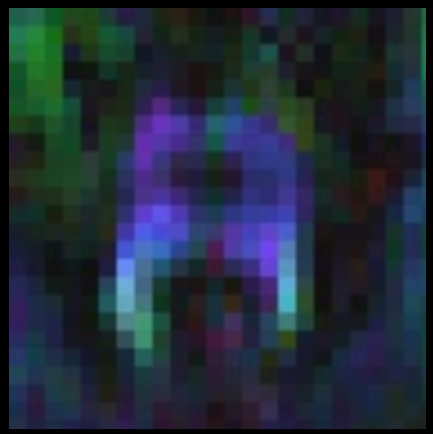

SECONDARY WHITE MATTER DEGENERATION

Primary lesion in the Internal Capsule

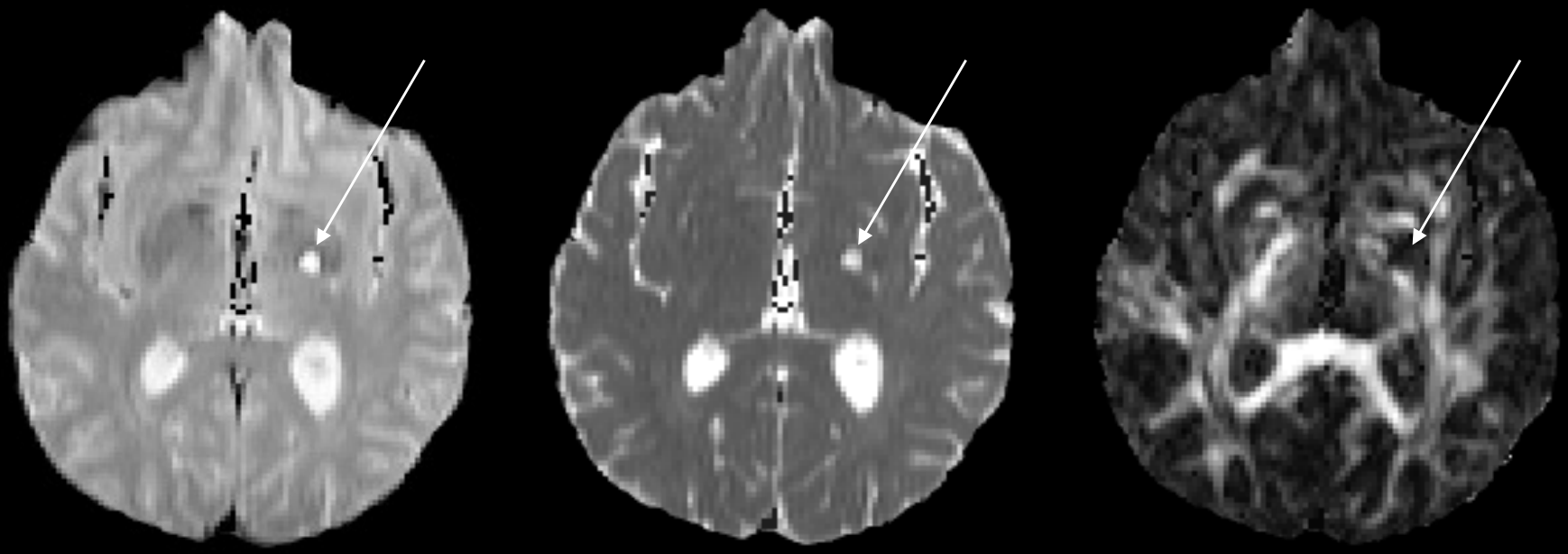

T2WI

Trace(D)

Anisotropy

NeuroImage **13,** 1174–1185 (2001)

Secondary degeneration in the Cerebral Peduncle

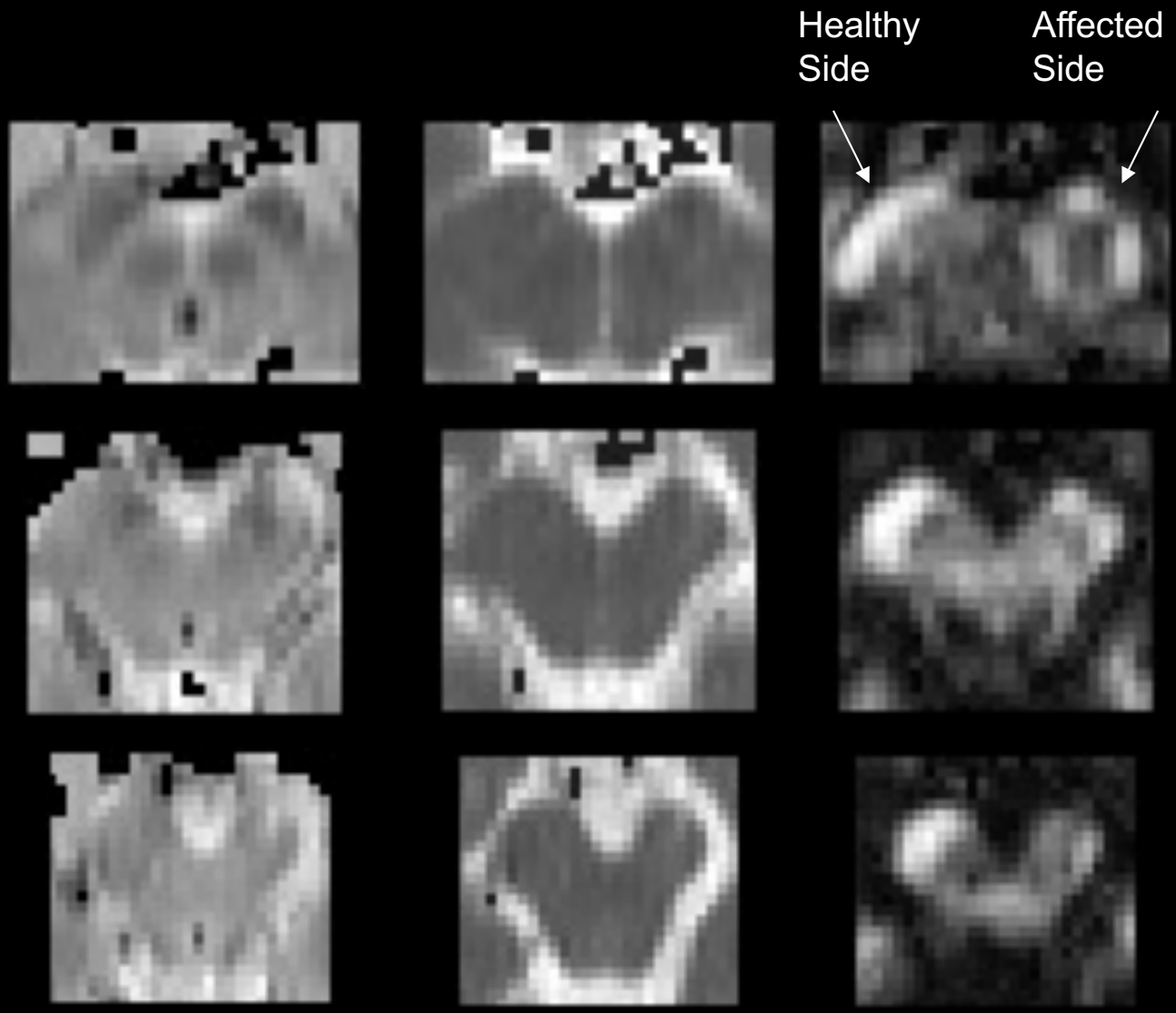

NeuroImage **13,** 1174–1185 (2001)

Secondary degeneration in the Rostral Pons

T2WI

Trace(D)

Anisotropy

NeuroImage **13,** 1174–1185 (2001)

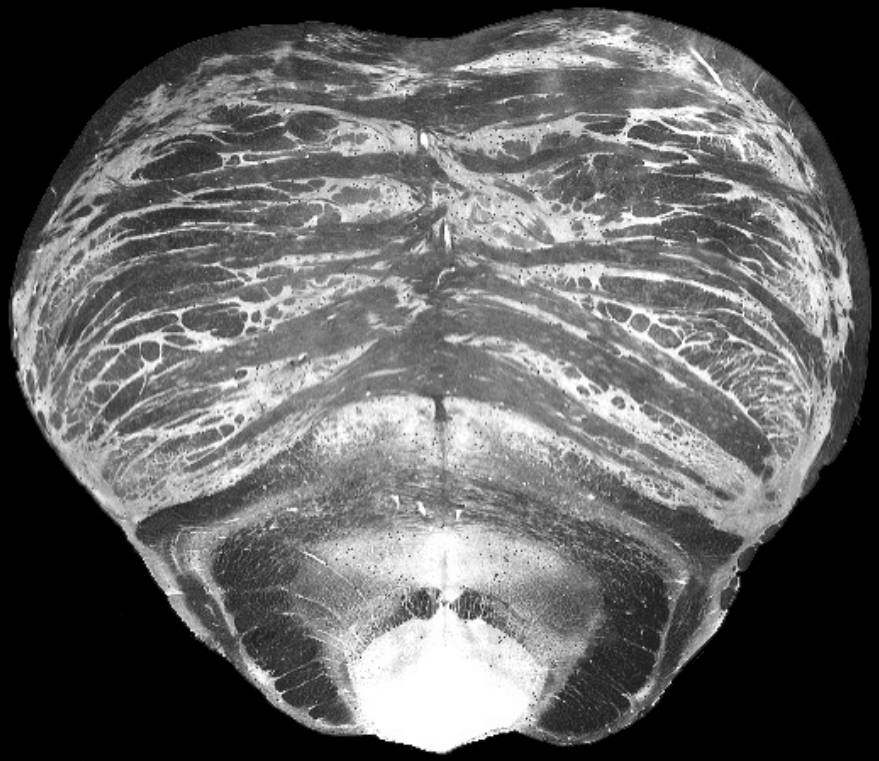

Summary of findings in Wallerian degeneration

	Primary lesion	**Wallerian degeneration in regions of isolated fiber bundles**	**Wallerian degeneration in regions of intersecting pathways**
D_{av} = Trace(D)/3	Large increase	Small increase	Small increase
Diffusion anisotropy	Large decrease	Large decrease	Small decrease. No changes or slight increase possible
Diffusivity parallel to the fibers ($\lambda 1$)	Increase	Decrease	Small change
Diffusivity perpendicular to the fibers ($\lambda 2$ and $\lambda 3$)	Increase	Increase	Small change
Apparent fiber orientation ($\varepsilon 1$)	Inconsistent changes due to loss of anisotropy	Inconsistent changes due to loss of anisotropy	Consistent changes dictated by the orientation of remaining pathways unaffected by Wallerian degeneration

Diffusion MRI “tractography”

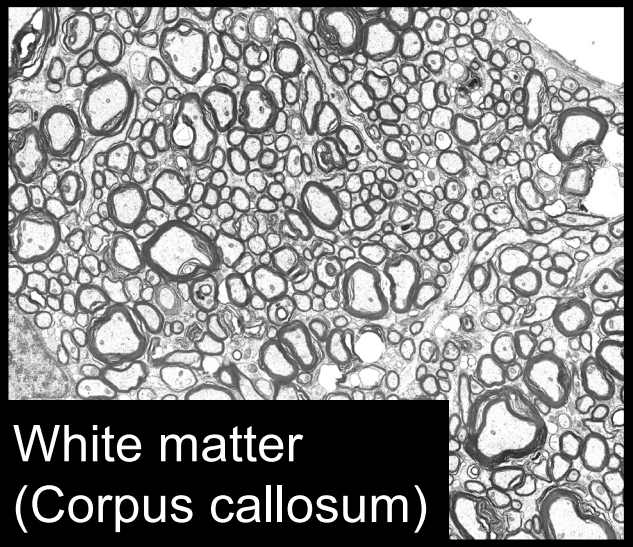

White matter
(Corpus callosum)

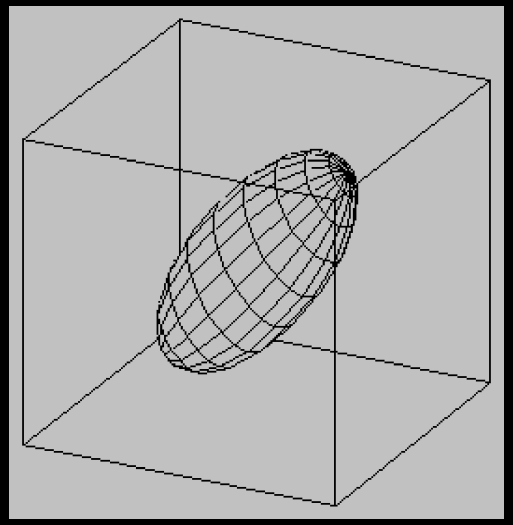

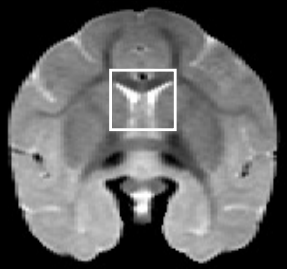

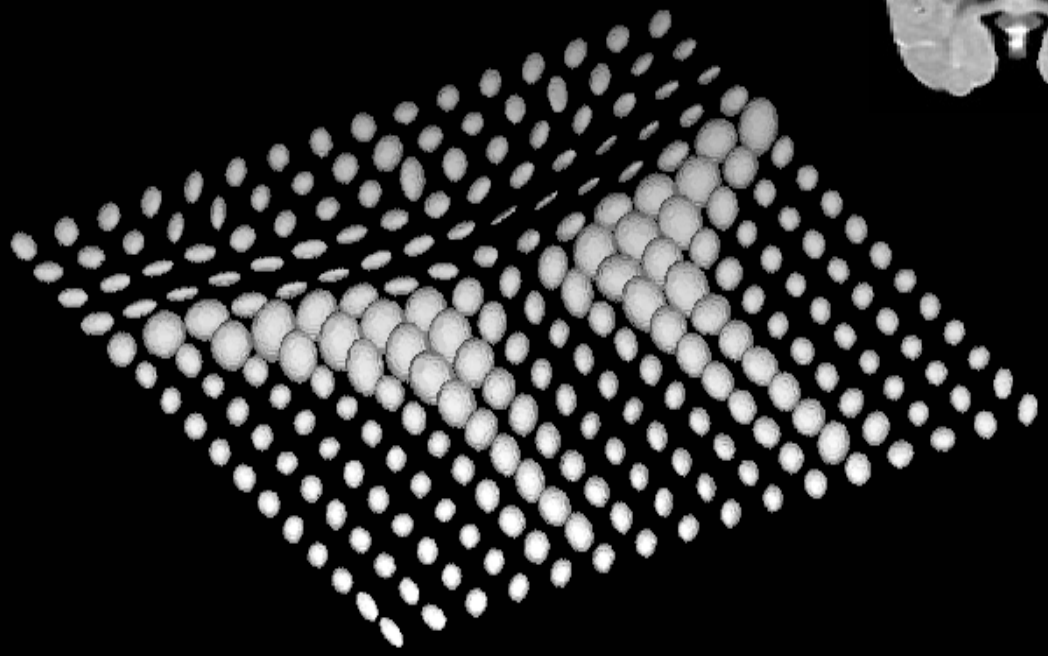

Diffusion MRI “tractography”

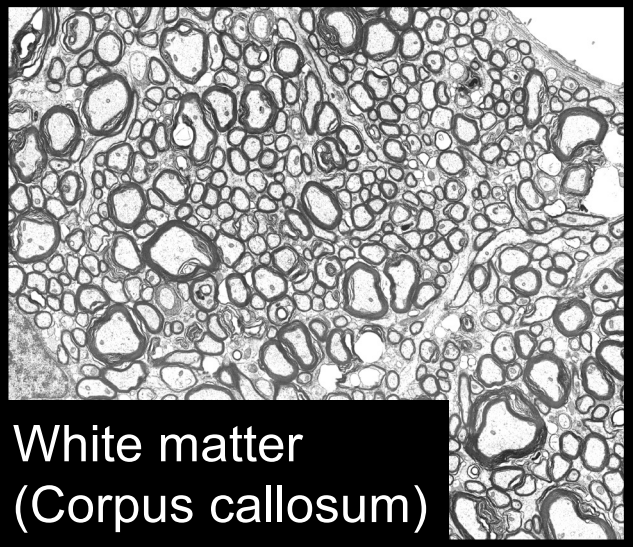

White matter
(Corpus callosum)

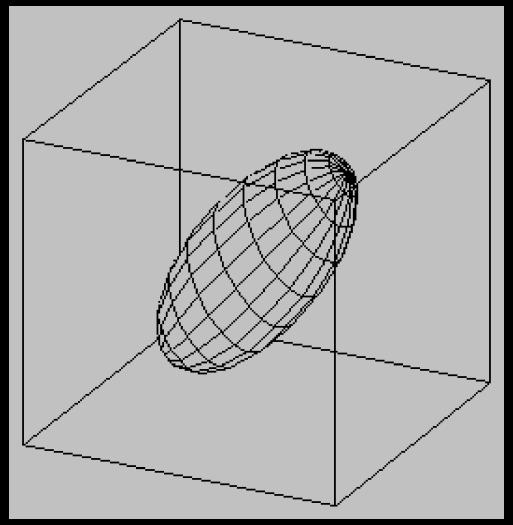

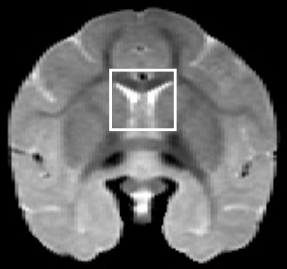

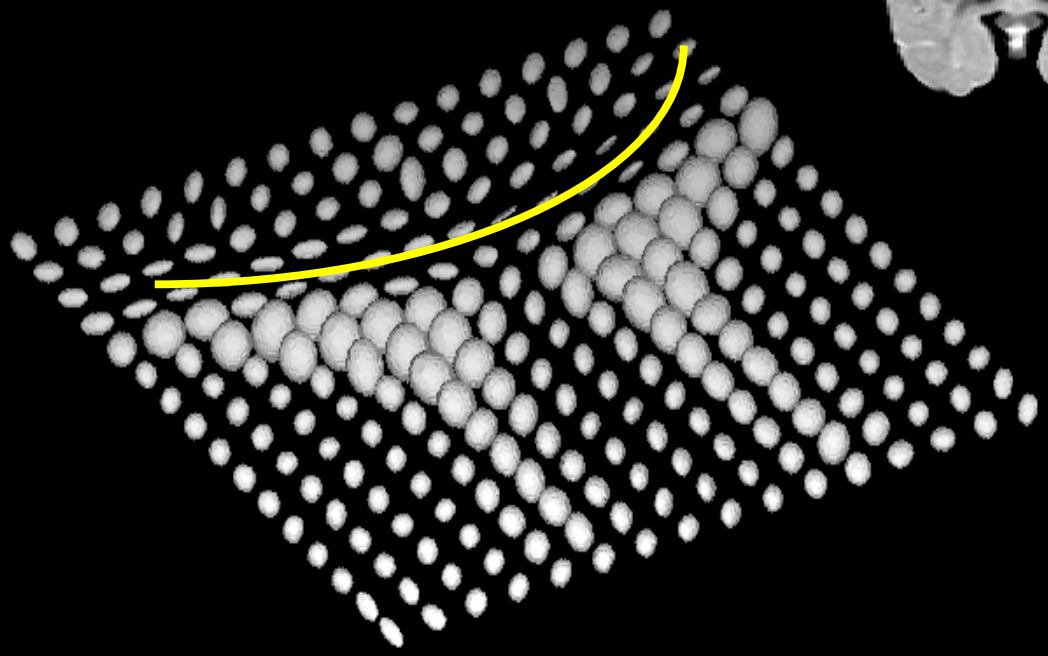

Deterministic Diffusion MRI tractography

Seminal contributions:

Conturo *et al*. PNAS, 1999
Mori *et al*. Annals Neurology, 1999
Basser *et al*., MRM 2000
Pupon *et al*., Neuroimage, 2000

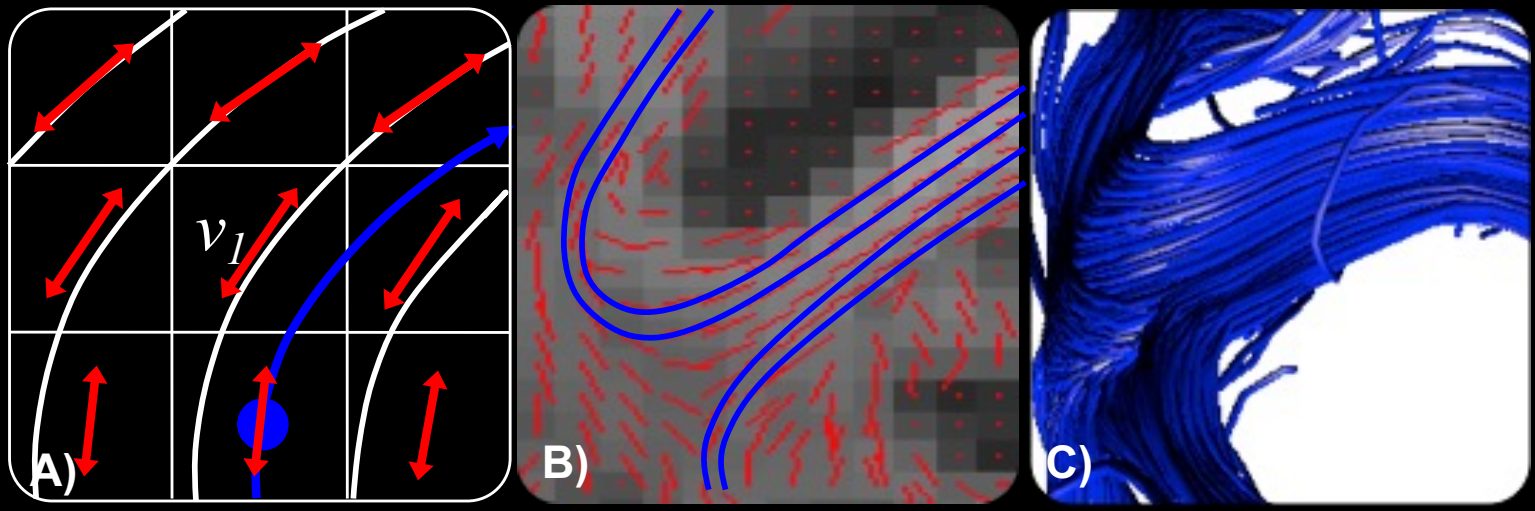

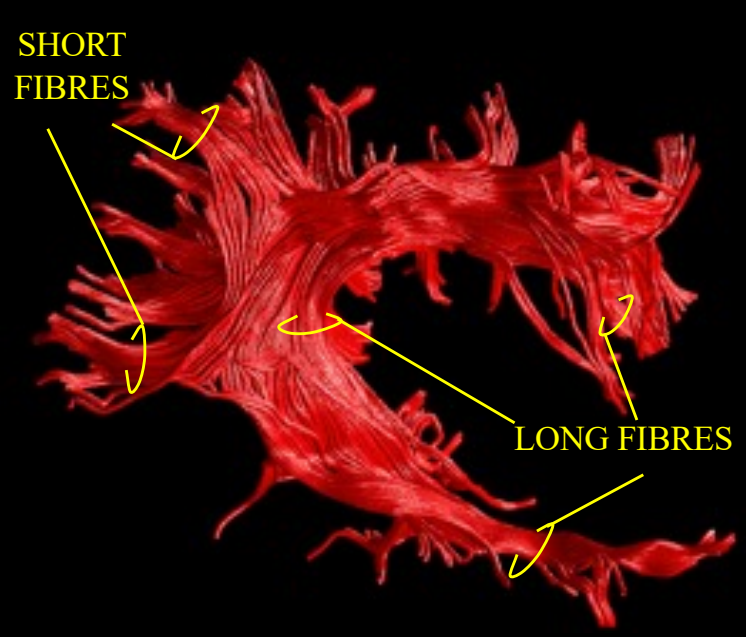

Virtual In-Vivo Dissection

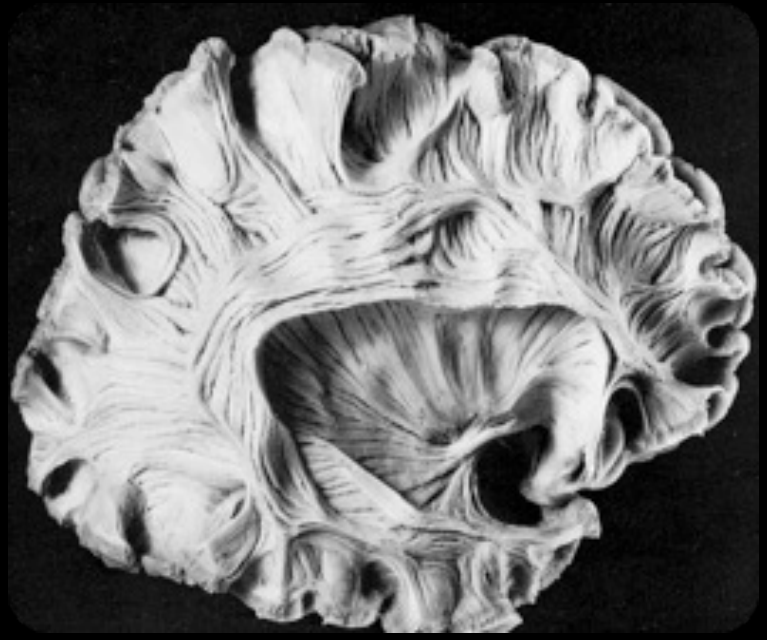

Post-Mortem Dissection

The Klingler method of tract dissection

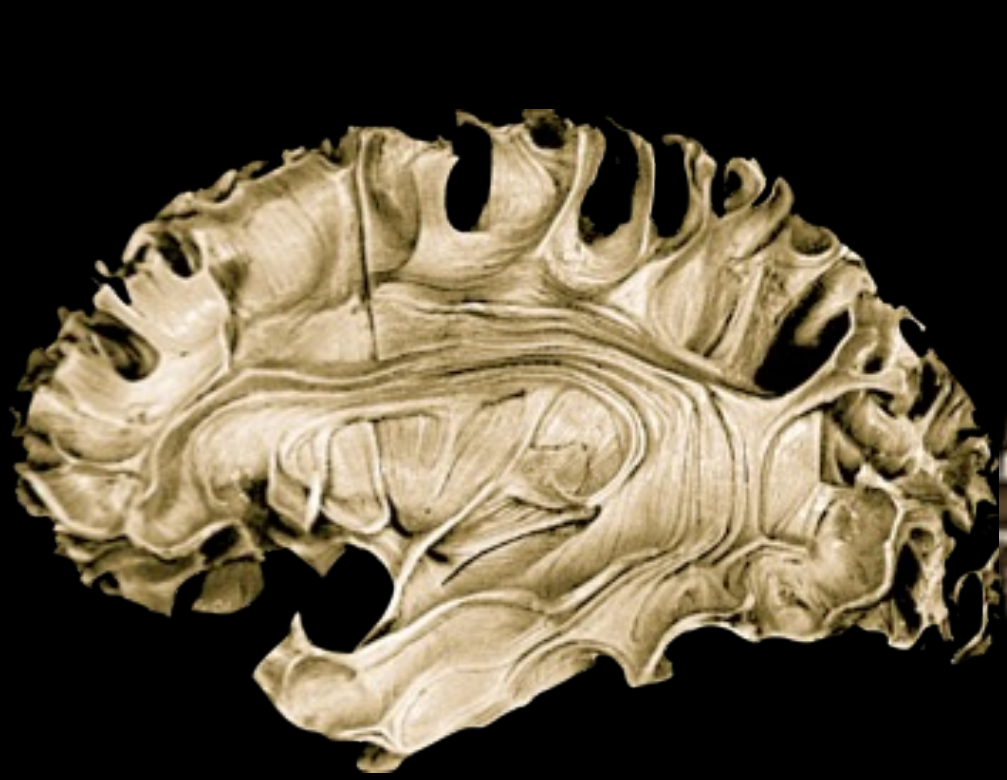

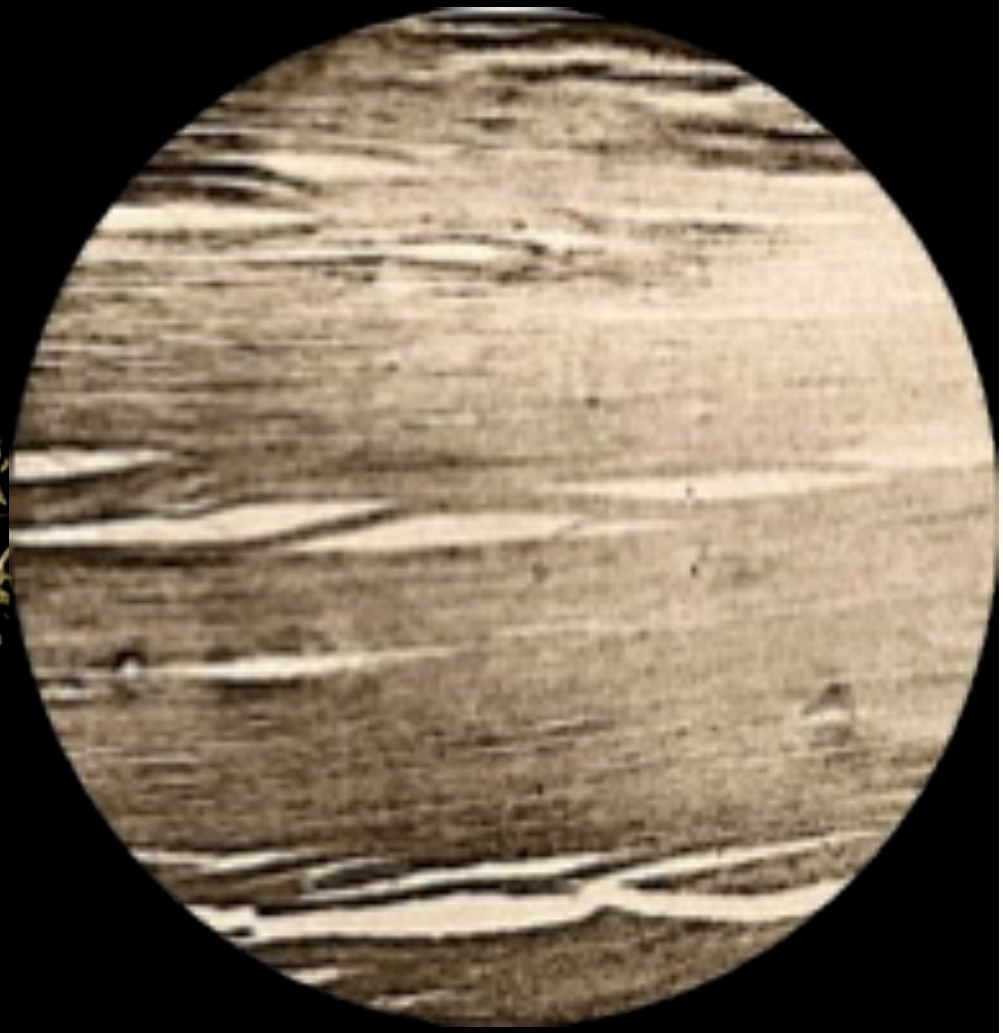

From Catani's chapter in Diffusion MRI (Oxford University Press)

Superior Longitudinal Fasciculus

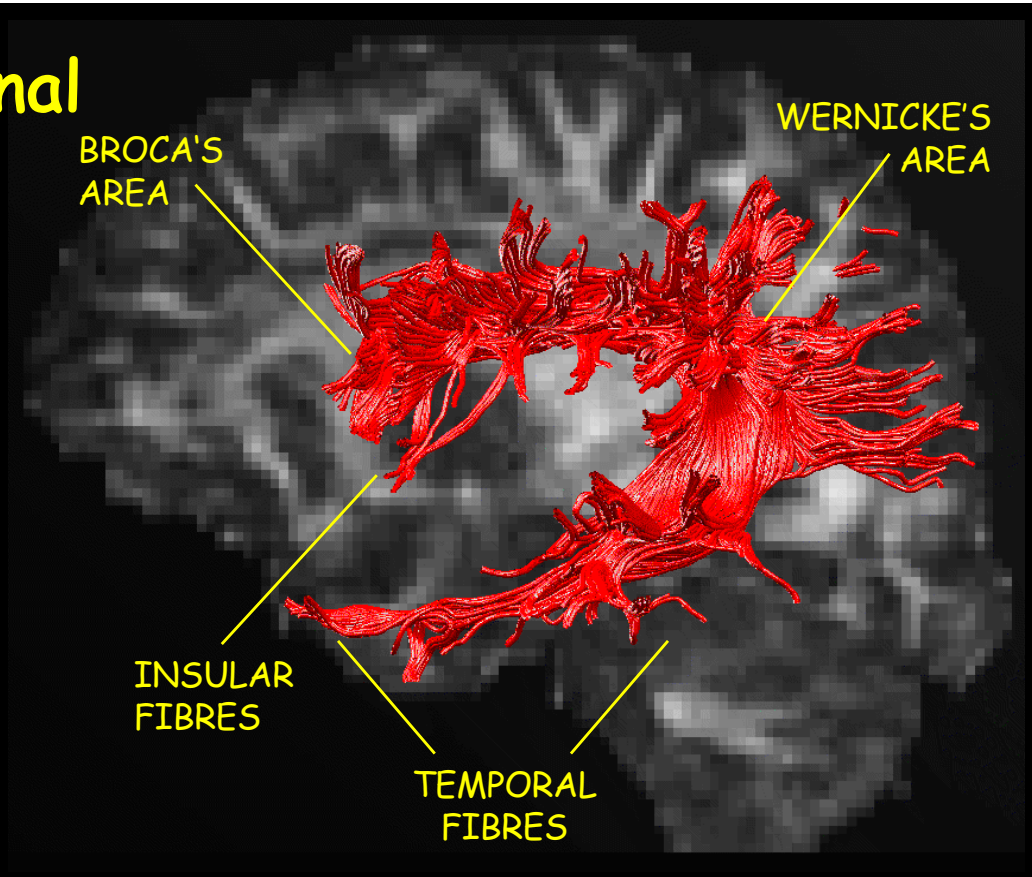

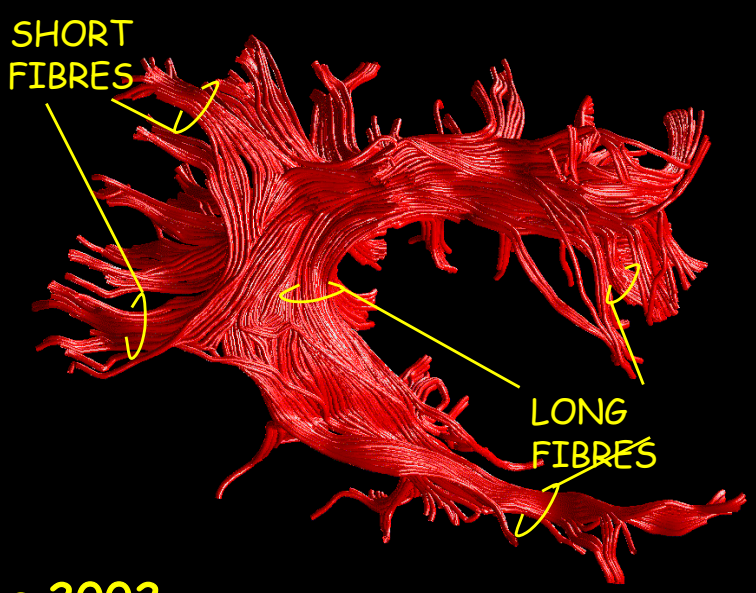

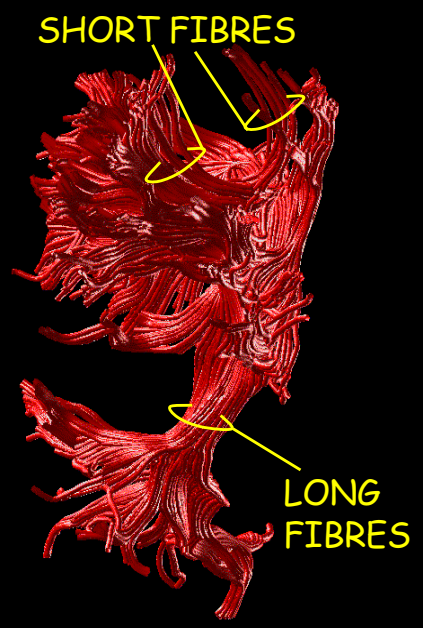

Catani et al. NeuroImage 2002

perisylvian language networks Catani et al PNAS 2007

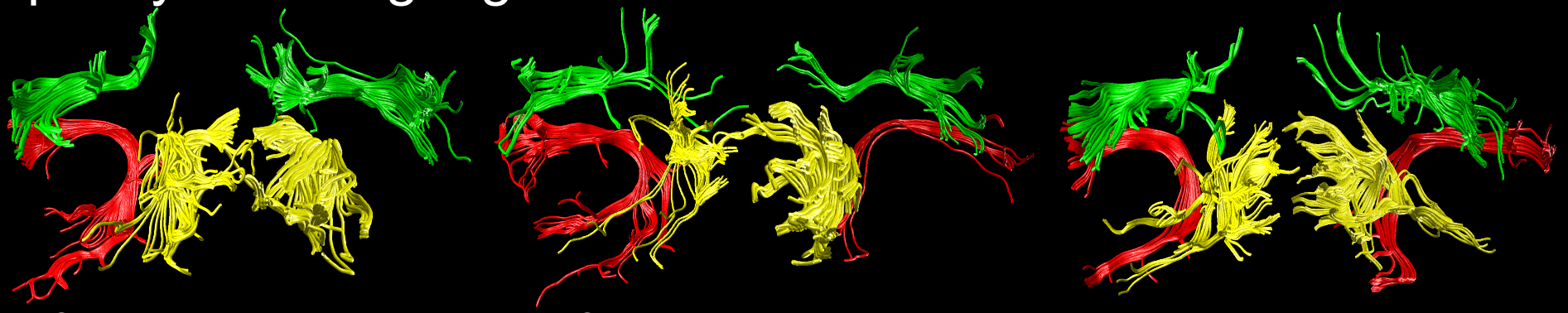

A)

Group 1 strong left lateralization (~60%)

Group 2 bilateral, left lateralization (~20%)

Group 3 bilateral, symmetrical (~20%)

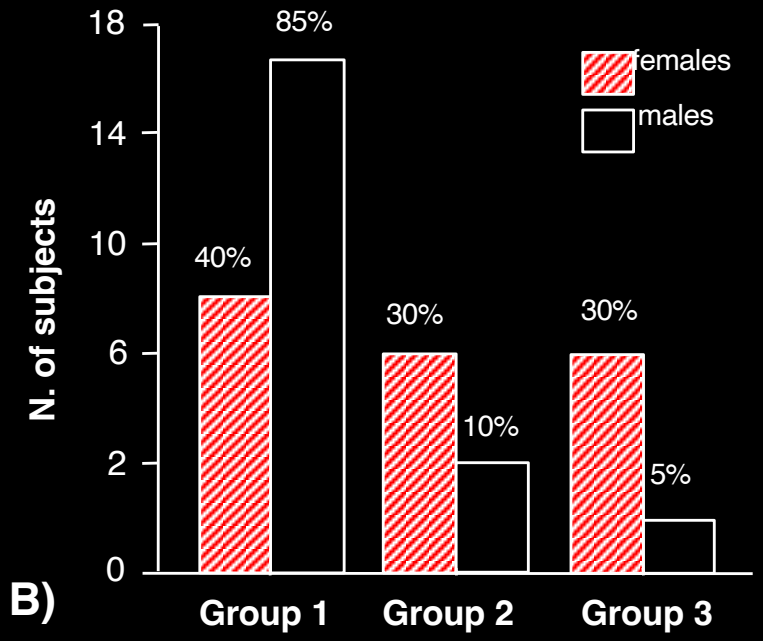

B)

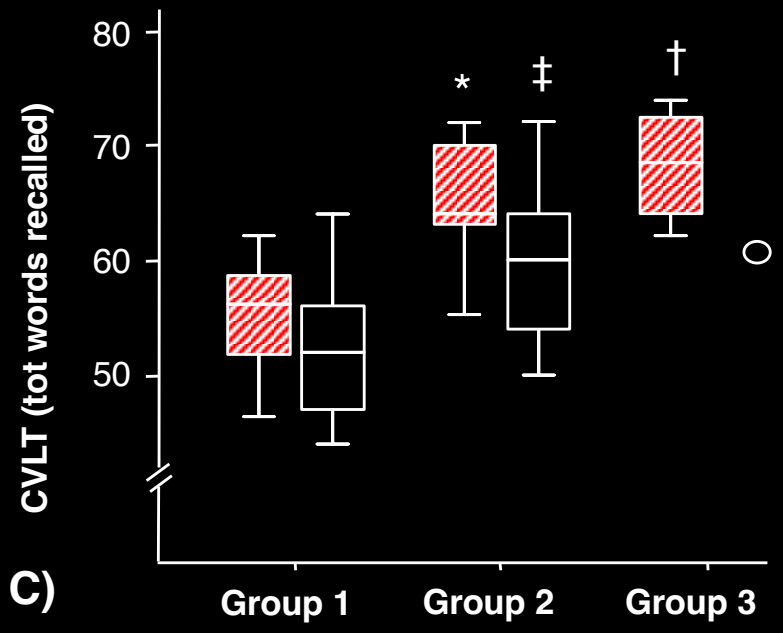

C)

DT_MRI tractography in presurgical assessment of tumors

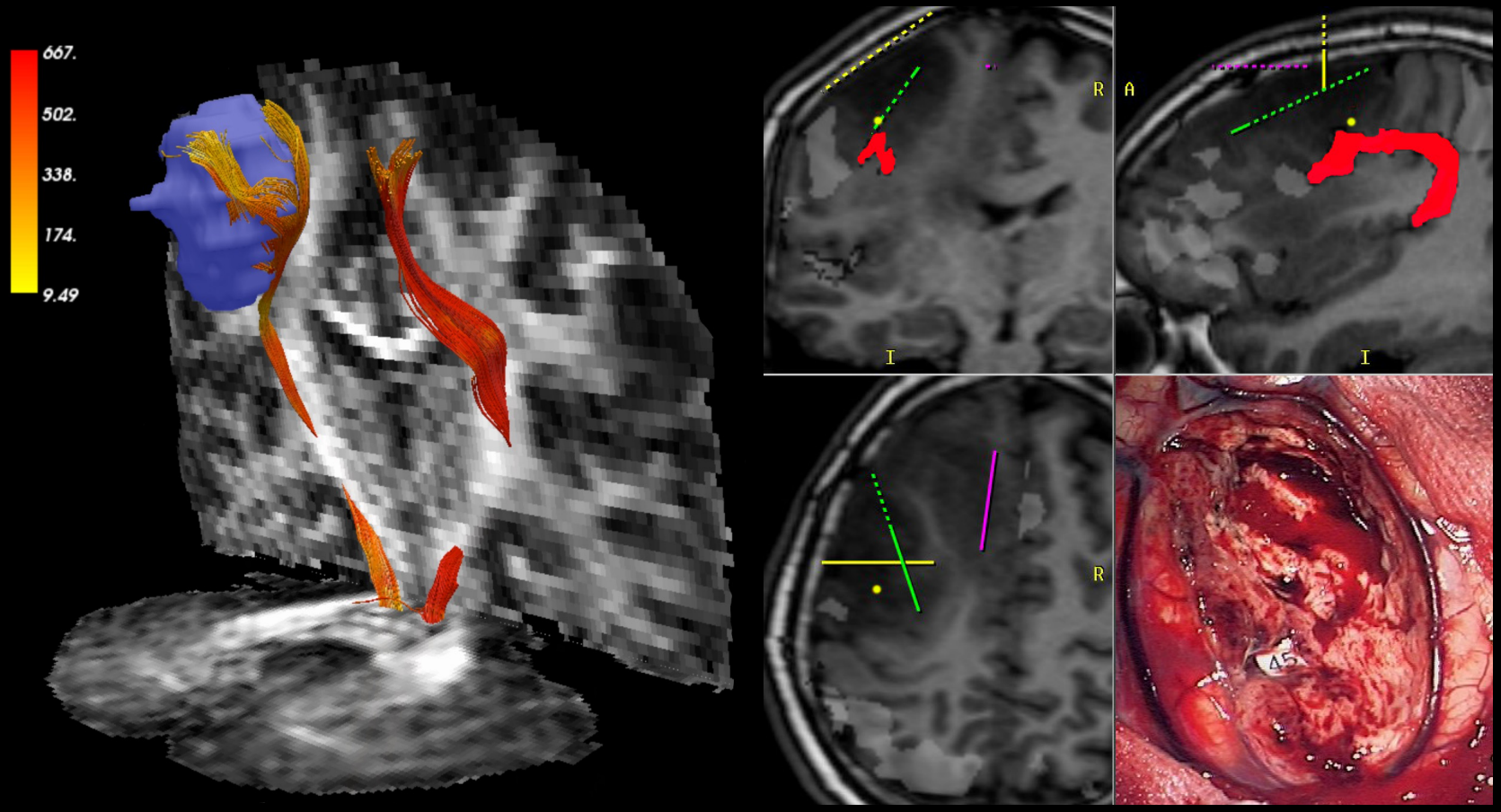

Probabilistic Diffusion MRI tractography

Seminal contributions:

Pajevic and Basser, 2000
Beherens *et al*., 2003
Parker *et al* , 2003
Lazar *et al*., 2005
Jones *et al*., 2005

Probabilistic Diffusion MRI tractography

Key Concepts:

Taking into account uncertainty (effects of noise)

Still considering a single fiber population in a voxel

Provides information on reproducibility of tracts,
but it does not improve anatomical accuracy

Example of probabilistic tractography using the Fast Marching Tractography Method By Parker et al.

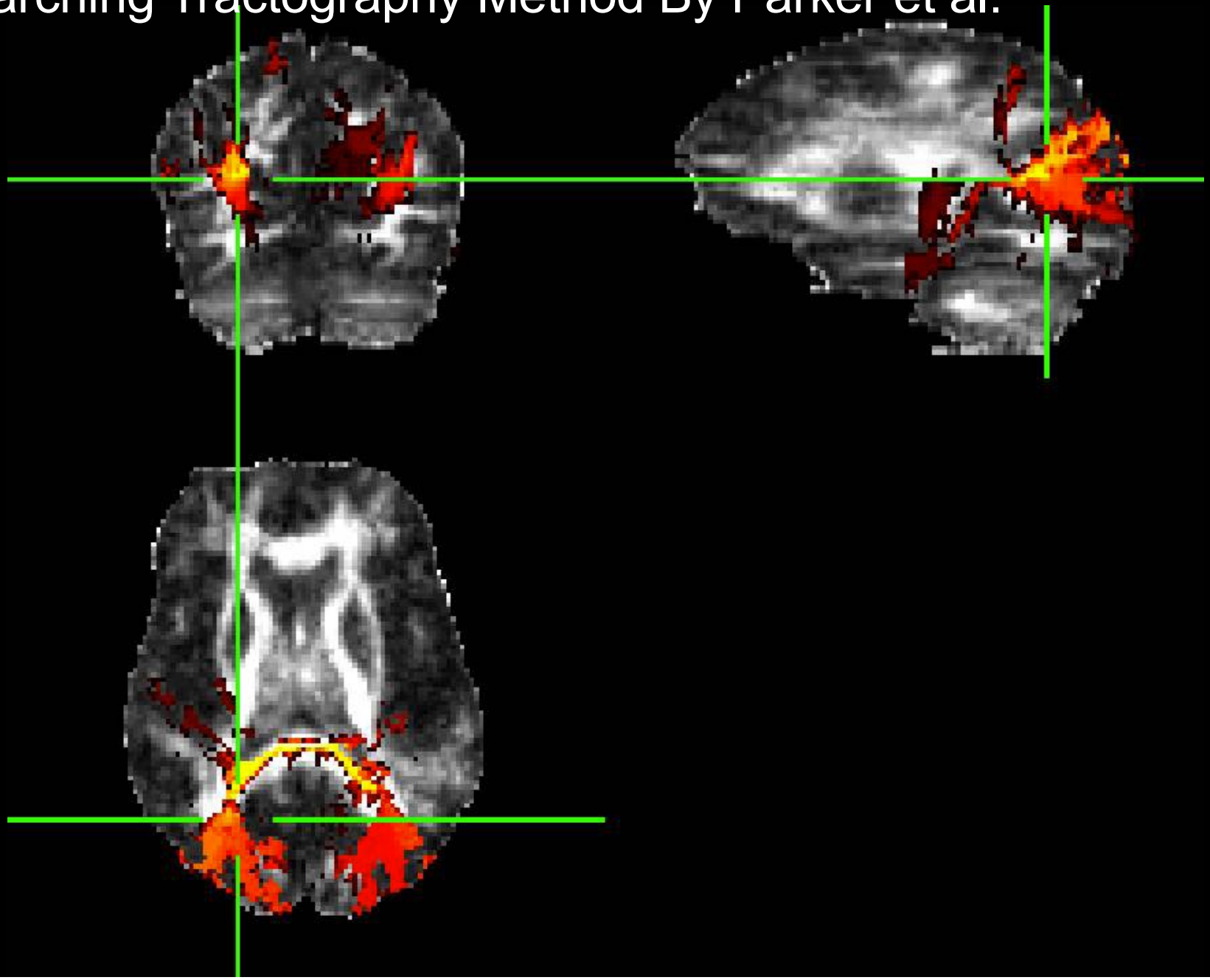

Tractography from HARDI methods

Spherical harmonics

L. Frank, 2000

q-space, DSI

P. T. Callaghan, et al 1988
D. G. Cory and A. N. Garroway 1990
M. D. King, 1994
Y. Assaf and Y. Cohen, 1999
DS Tuch, JW Belliveau, TG Reese, VJ Wedeen, 1998
VJ Wedeen, 2000

Multiple fiber populations in a voxel

Diffusion tensor model

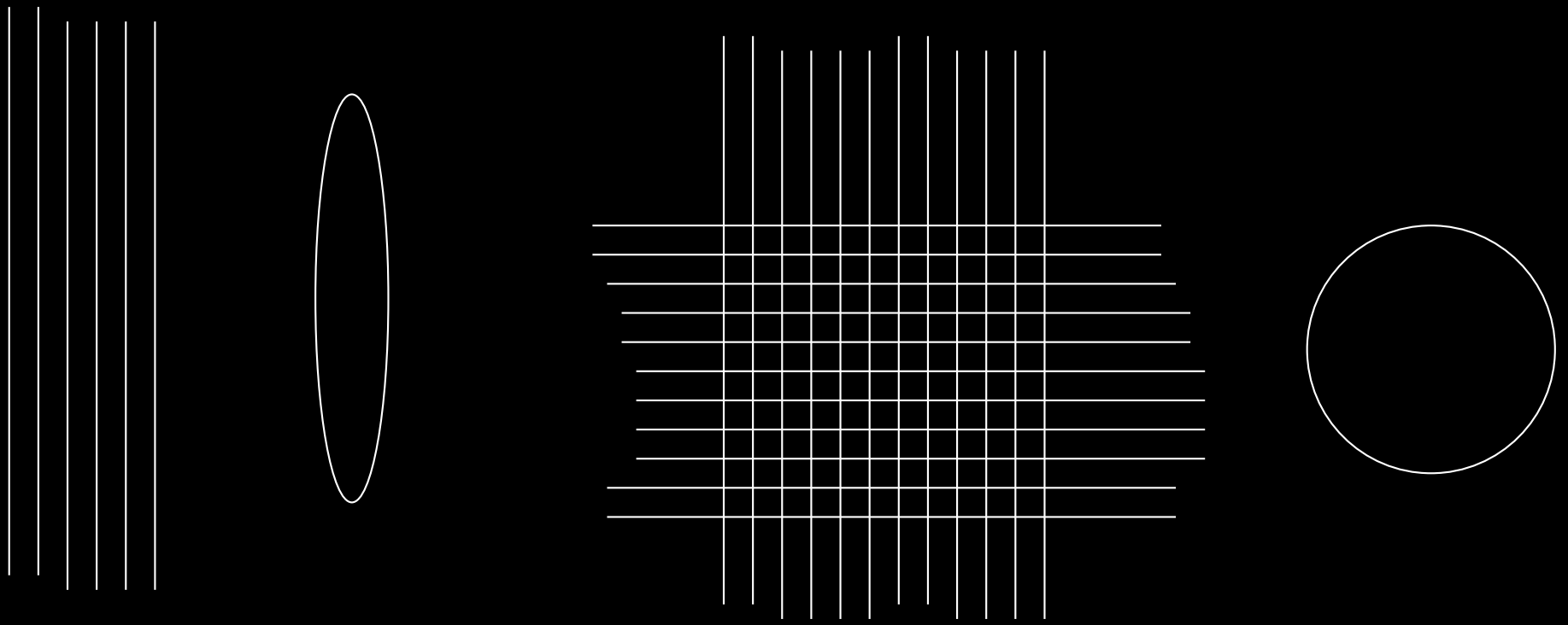

Multiple fiber populations in a voxel

Model “independent”: q-space, DSI

Higher order models: spherical harmonics

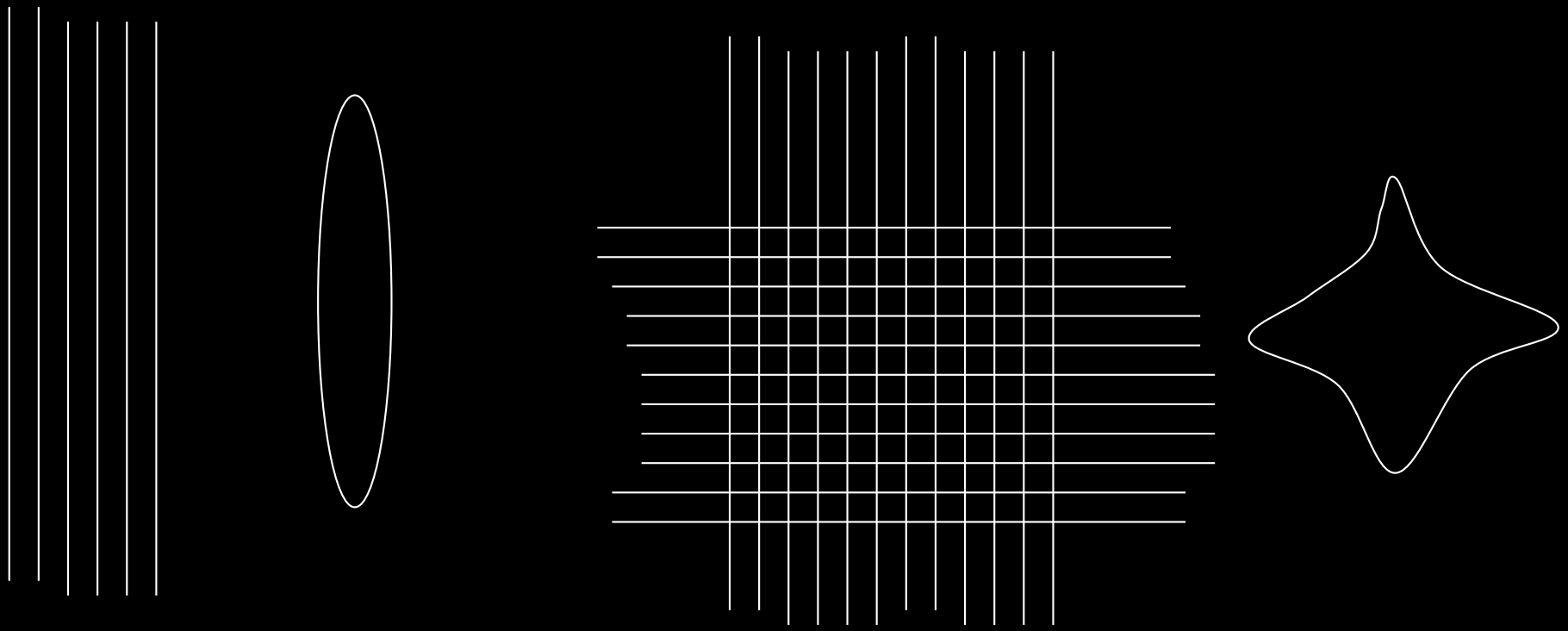

Diffusion Orientation Transform - Results

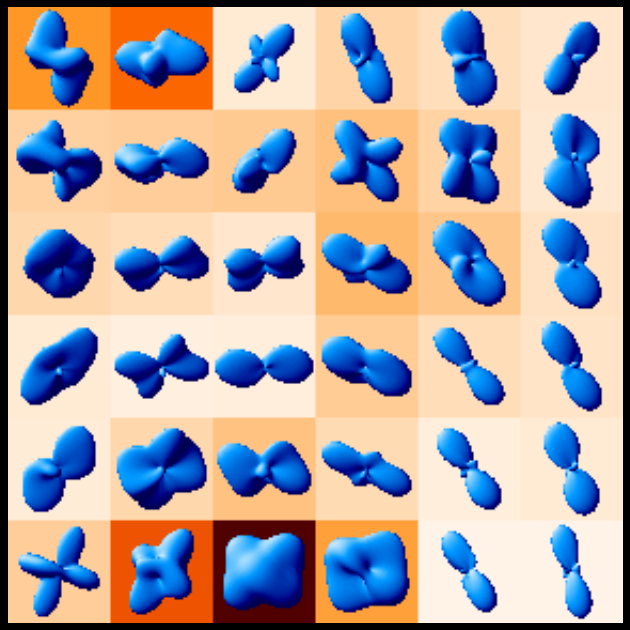

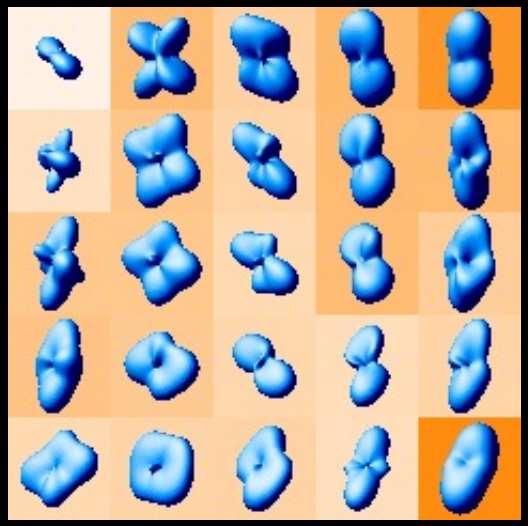

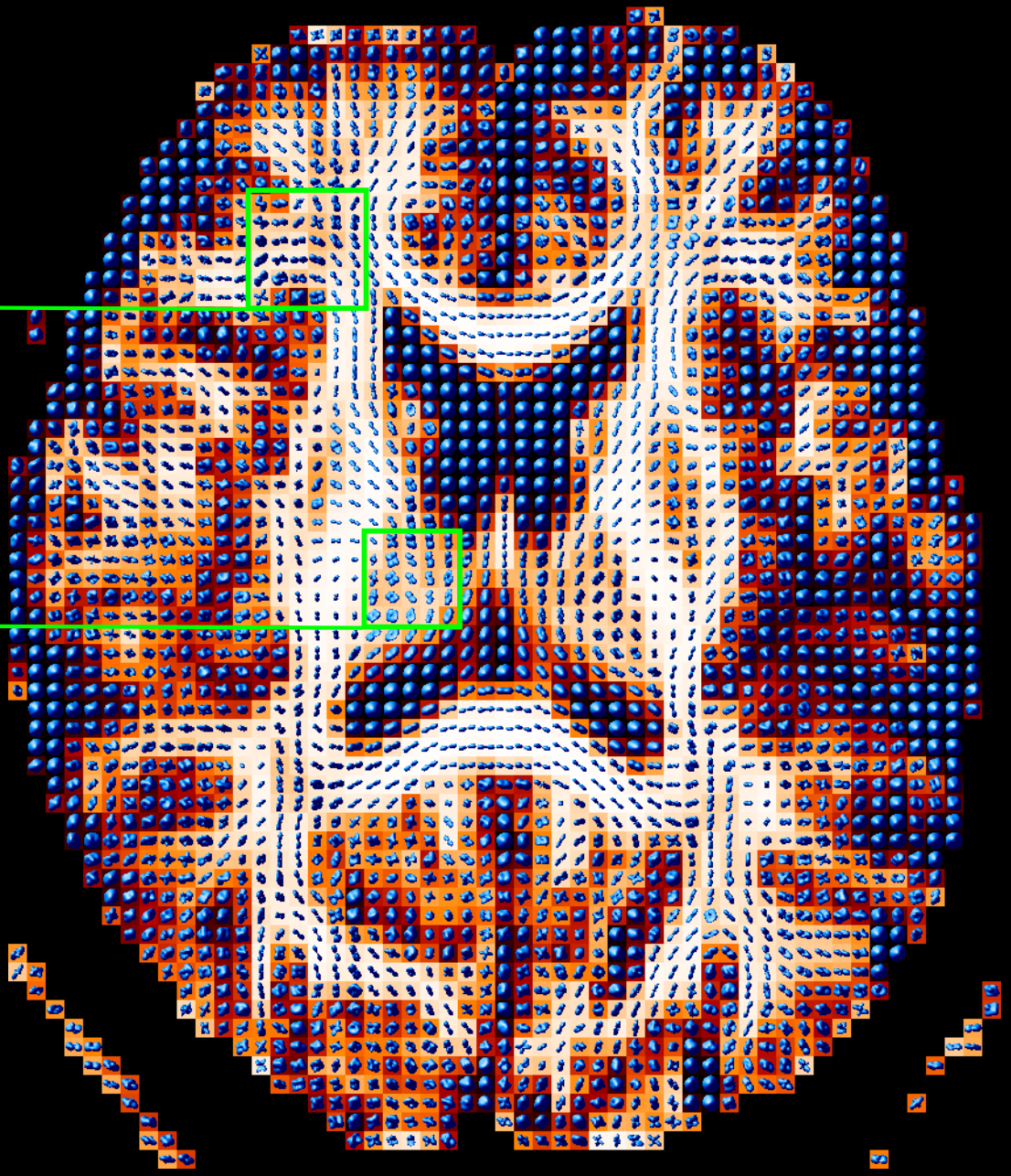

* E. Özarslan, T.M. Shepherd, B.C. Vemuri, S.J. Blackband and T.H. Mareci, NeuroImage, 31:1086-1103, 2006.

Solving multiple fiber populations

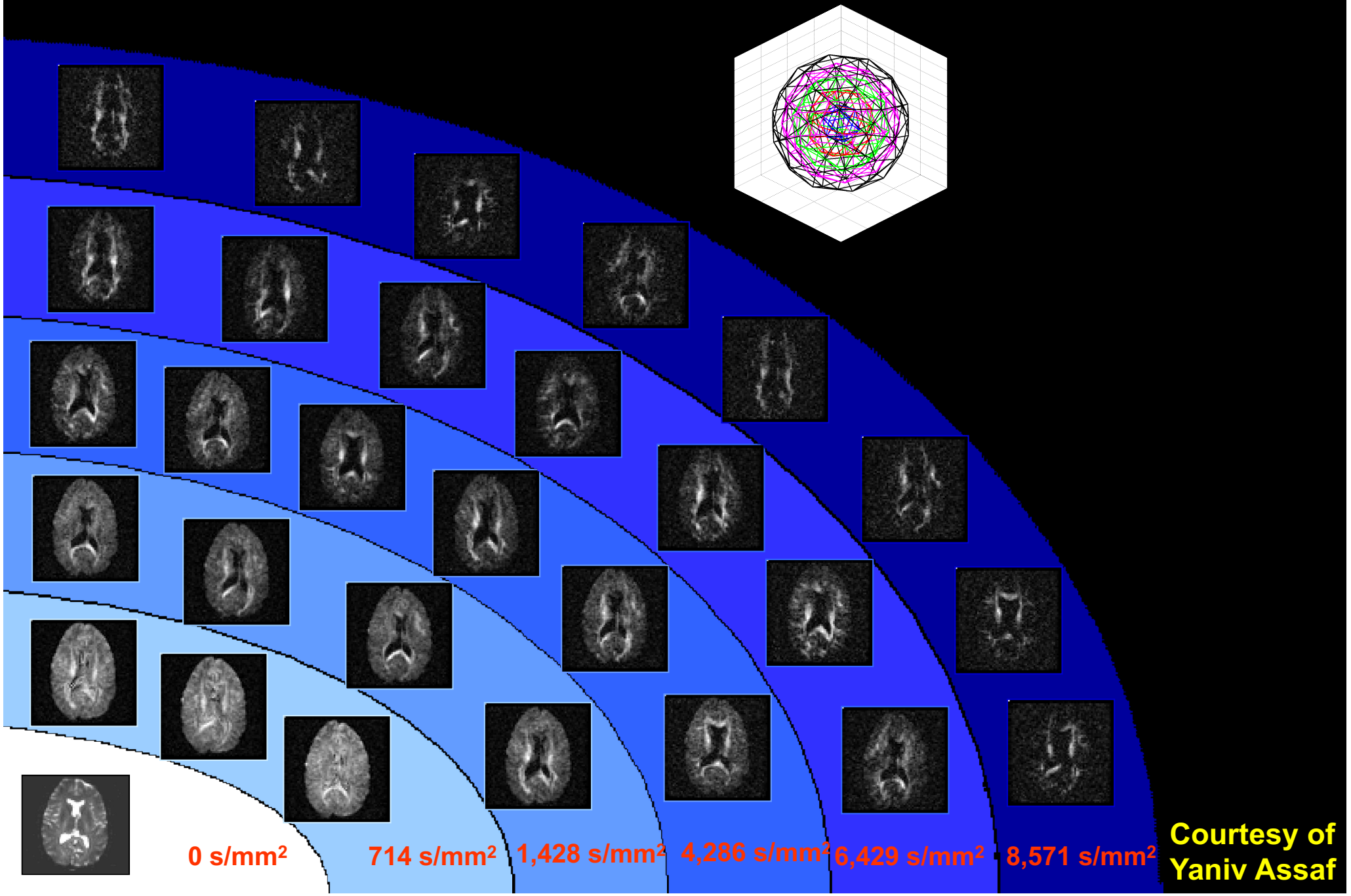

Courtesy of Yaniv Assaf

Hindered Compartment

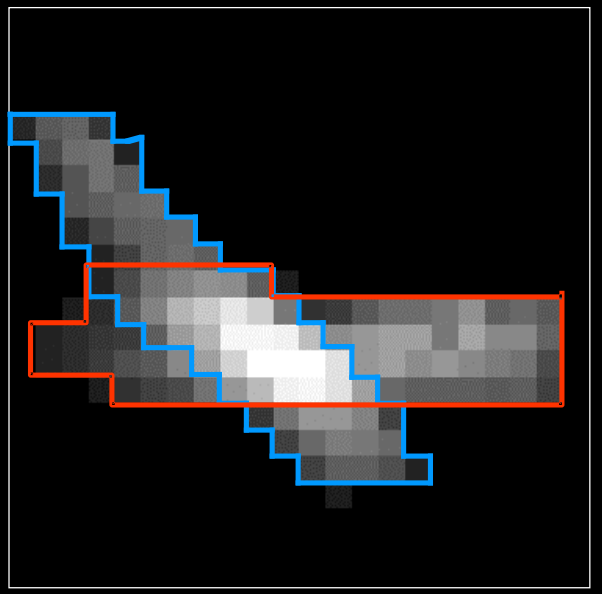

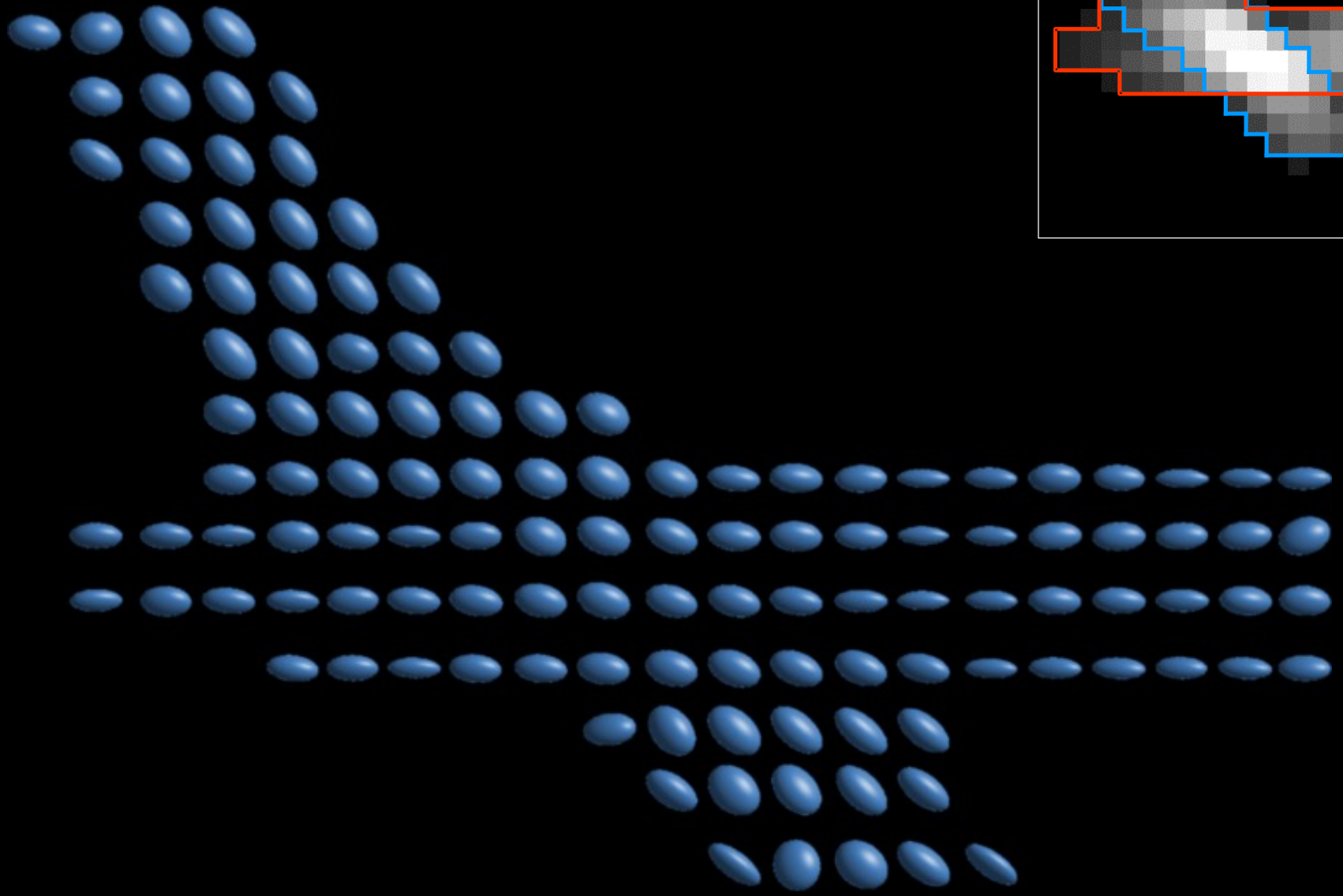

Restricted Compartment

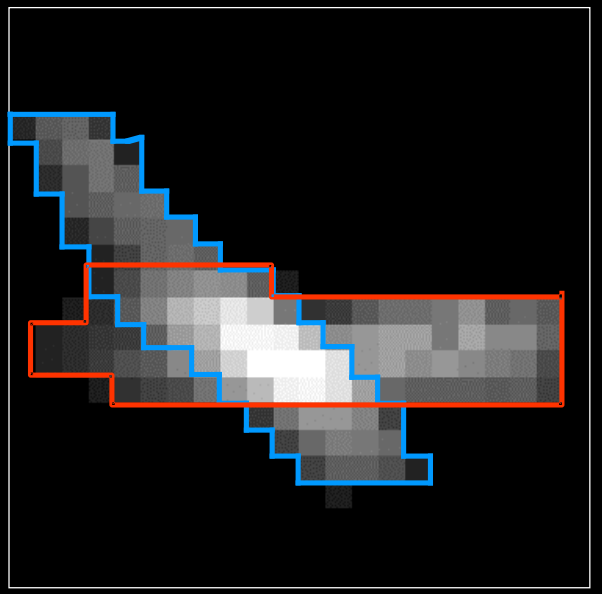

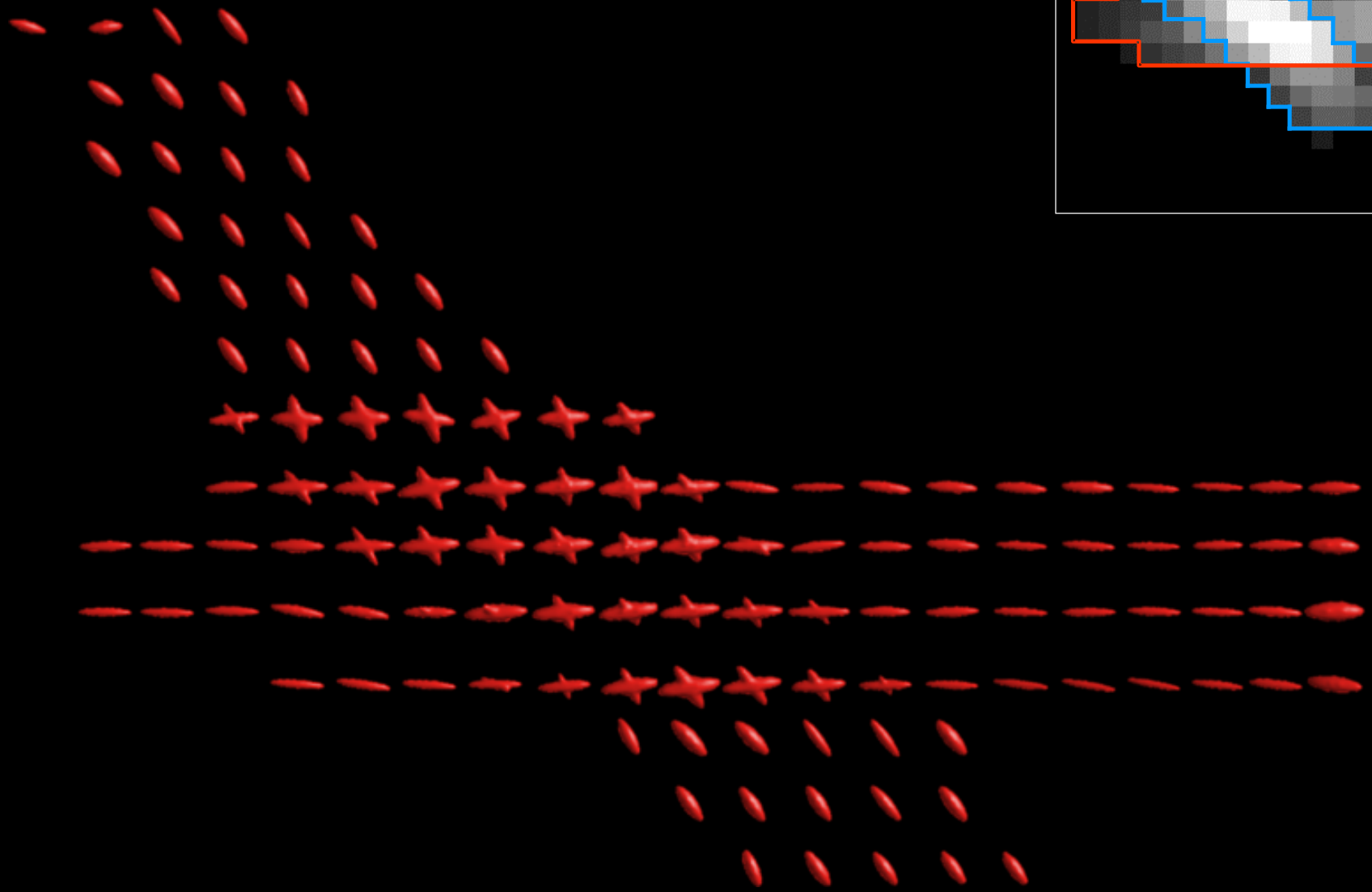

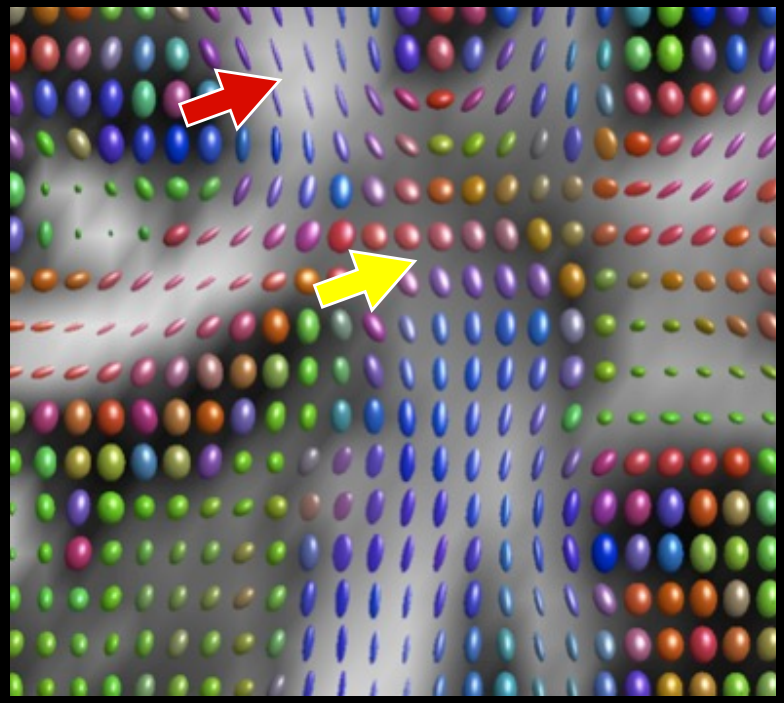

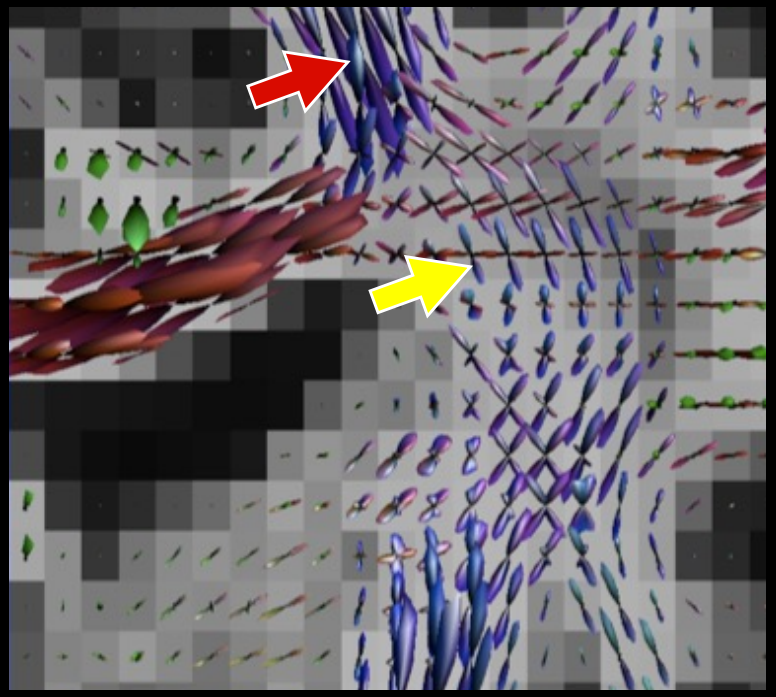

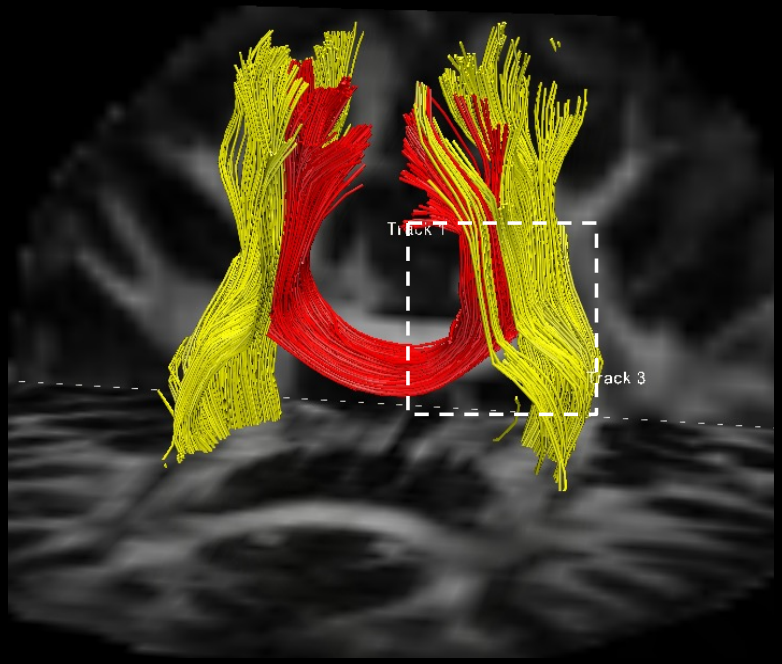
Track 1
Track 3

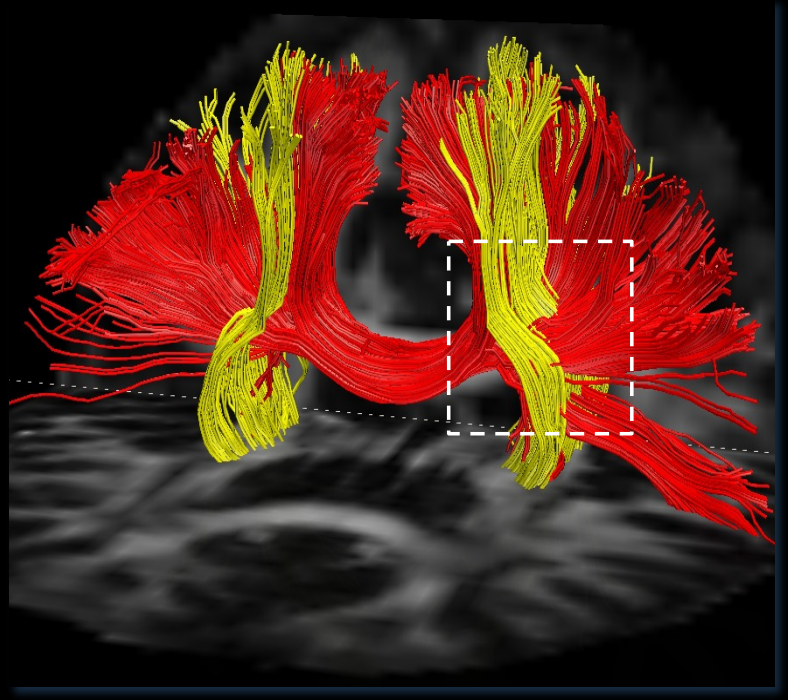

Challenges in using diffusion MRI tractography

Knowledge of the diffusion propagator in each voxel is sufficient to trace white matter fibers reliably ?

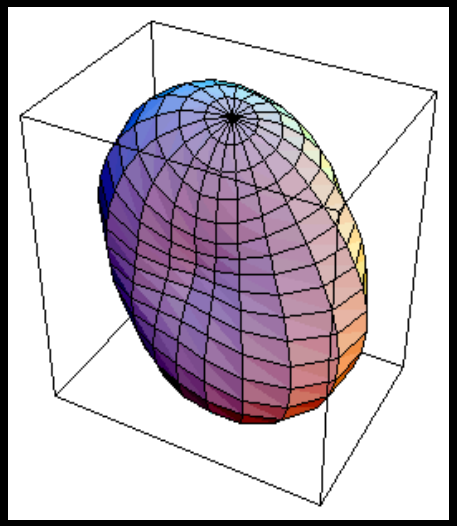

?

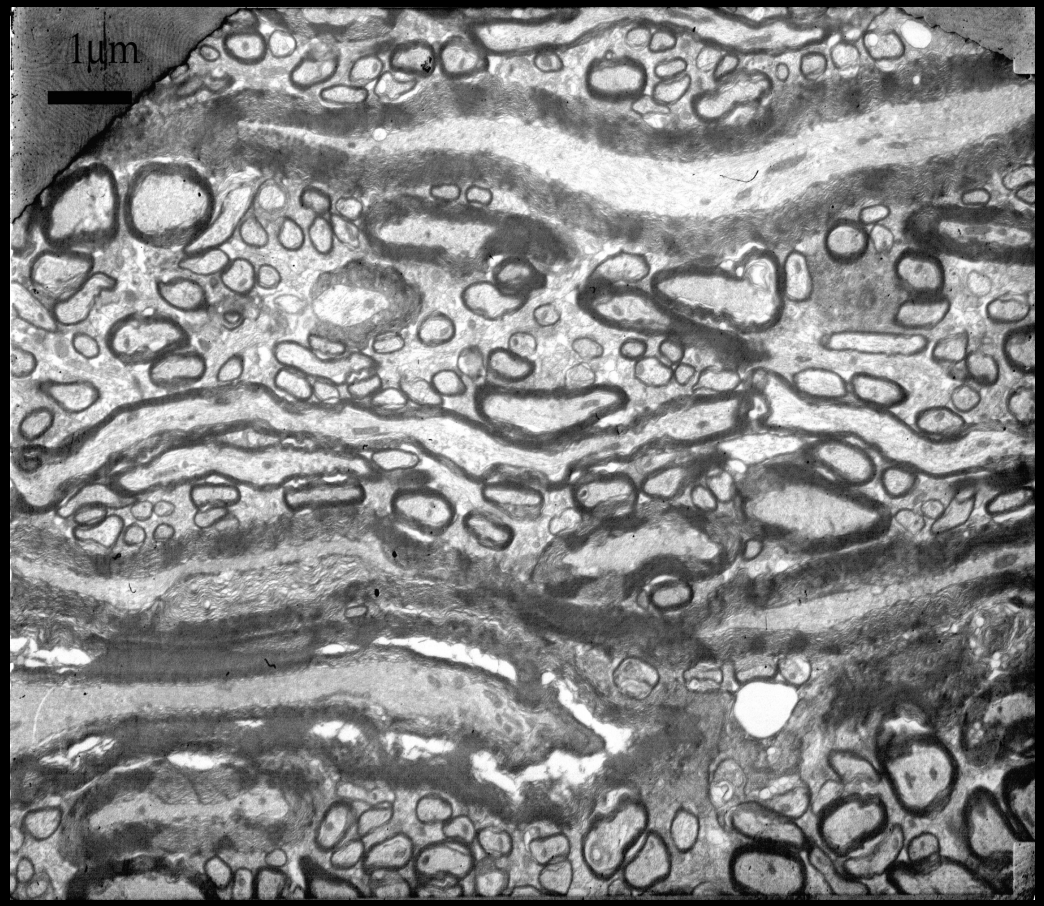

Anatomical Validation of Diffusion MRI tractography

Human brain: a-priori anatomical knowledge by experts

Animal brain: tracers

- Tractography validation in animal models:
  - Macaque (Schmahmann et al., 2007)
  - Macaque (Jbabdi et al., 2013)
  - Minipig (Dyrby et al., 2007)
  - Mice (Jiang et al., 2005)
- However….
  - Studies are qualitative
  - Focused on sensitivity (True positives), ignoring specificity (False positives)
  - Using constraints: e.g. way points, multiple ROIs
  - Empirical search of best parameters

Anatomical accuracy of brain connections derived from diffusion MRI tractography is inherently limited

Cibu Thomas[a,b,1], Frank Q. Ye[c,d], M. Okan Irfanoglu[a,b], Pooja Modi[a], Kadharbatcha S. Saleem[e], David A. Leopold[c,d], and Carlo Pierpaoli[a,b]

[a]Program on Pediatric Imaging and Tissue Sciences, Eunice Kennedy Shriver National Institute of Child Health and Human Development, Bethesda, MD, 20892; [b]Center for Neuroscience and Regenerative Medicine, Uniformed Services University of the Health Sciences, Bethesda, MD 20814; [c]Neurophysiology Imaging Facility, National Institute of Mental Health, National Institute of Neurological Disorders and Stroke, and National Eye Institute, Bethesda, MD 20892; [d]Section on Cognitive Neurophysiology and Imaging and [e]Section on Cognitive Neuroscience, Laboratory of Neuropsychology, National Institute of Mental Health, Bethesda, MD, 20892

Edited* by Leslie G. Ungerleider, National Institute of Mental Health, Bethesda, MD, and approved September 22, 2014 (received for review March 26, 2014)

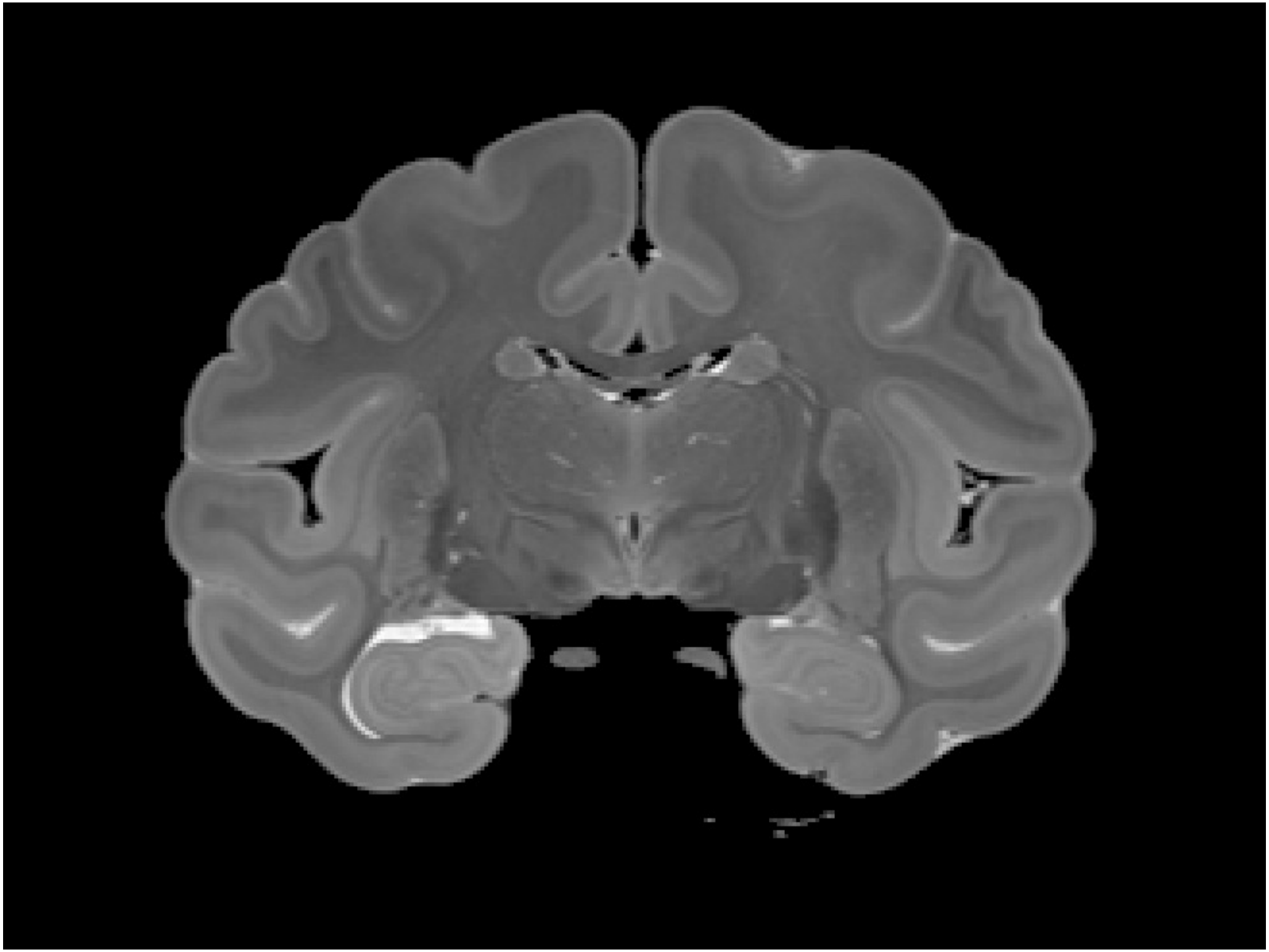

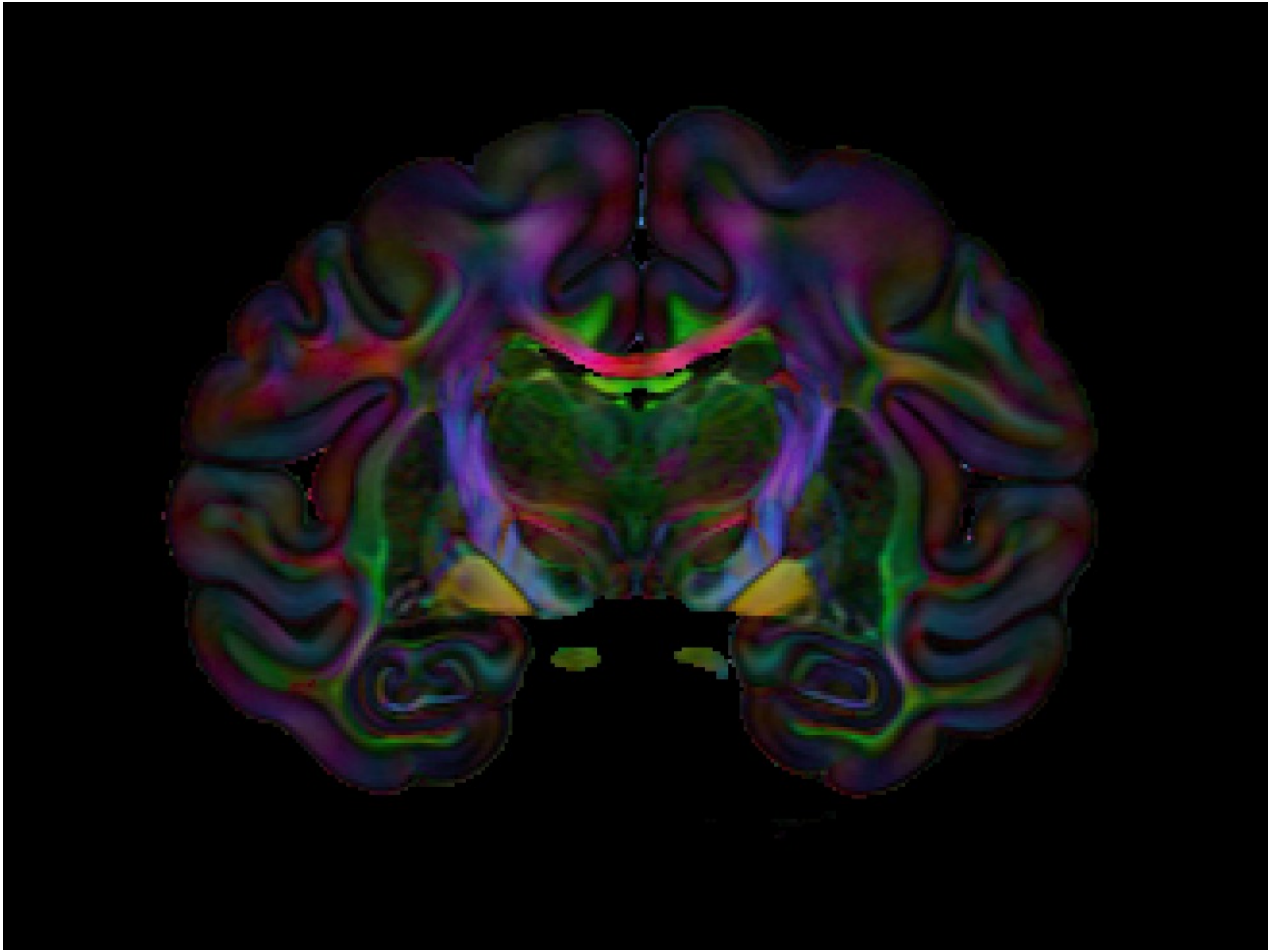

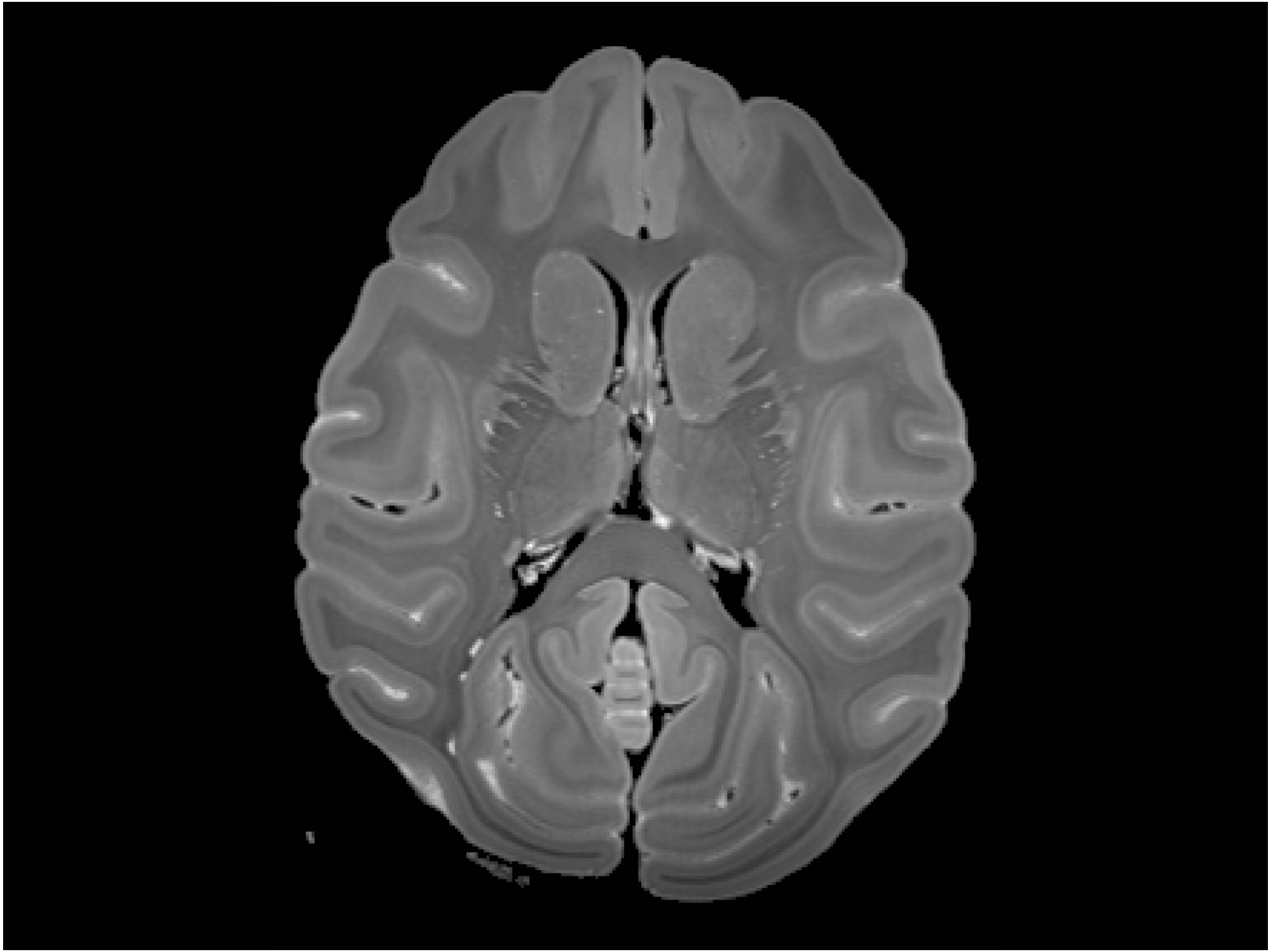

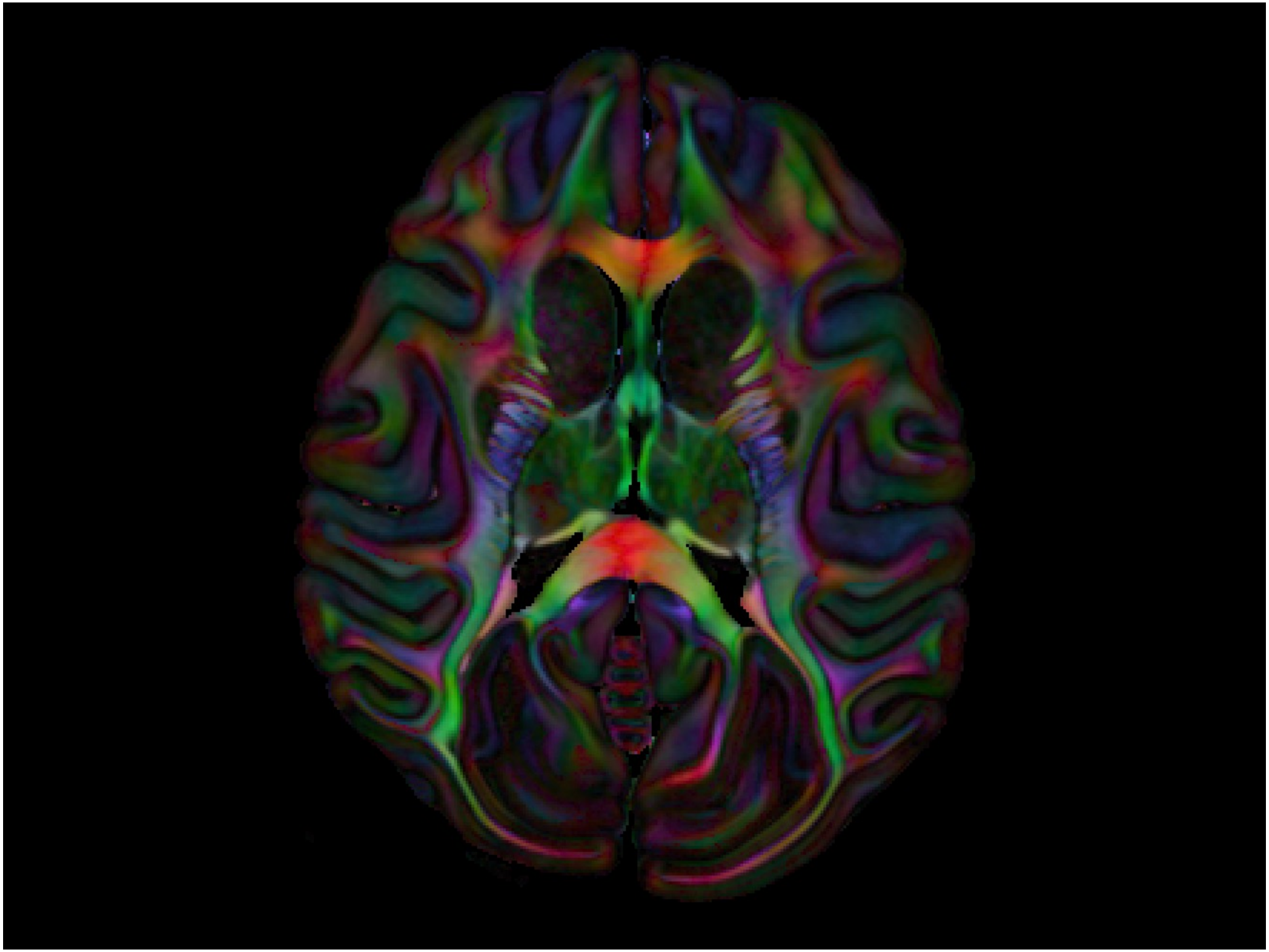

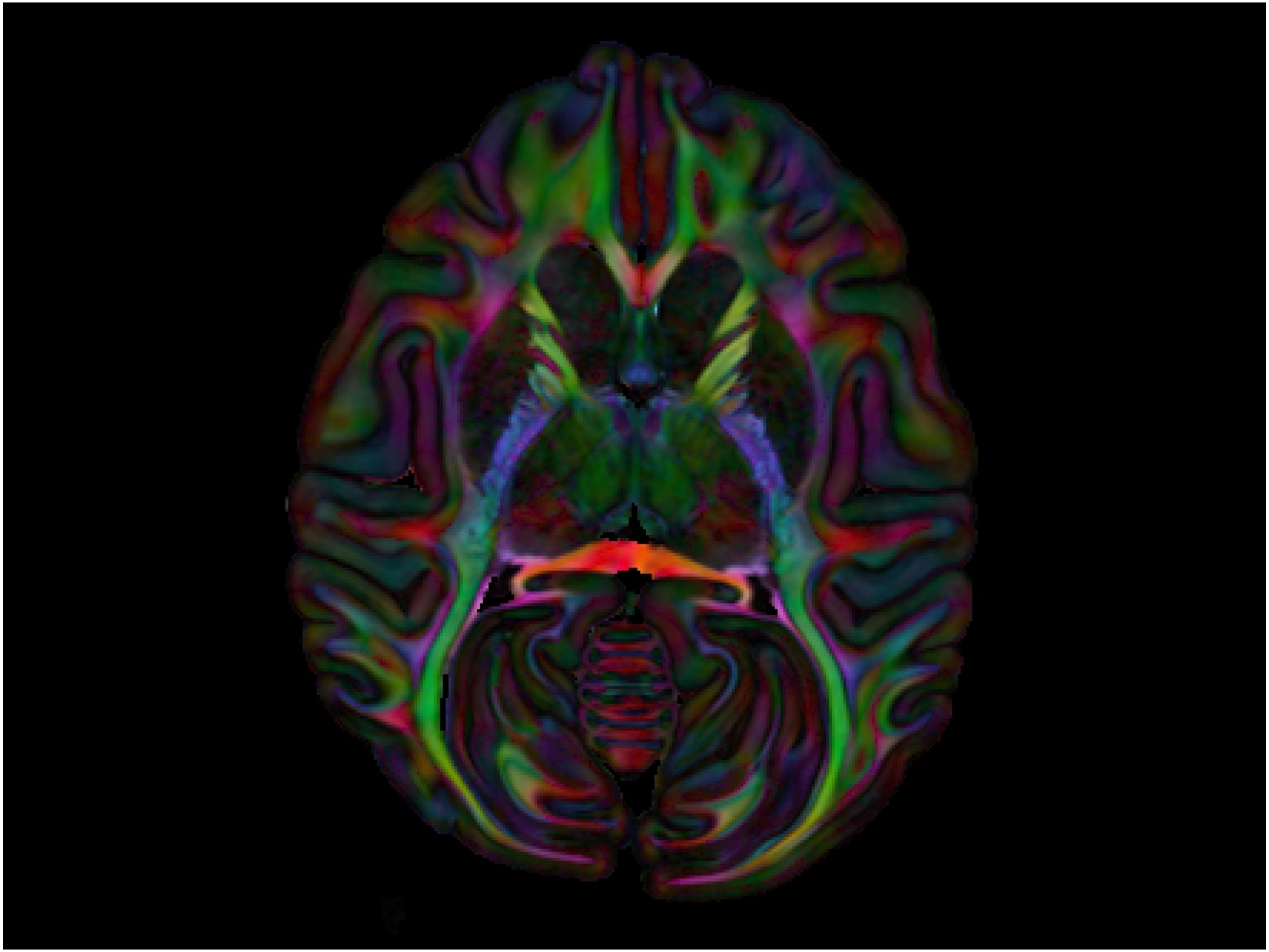

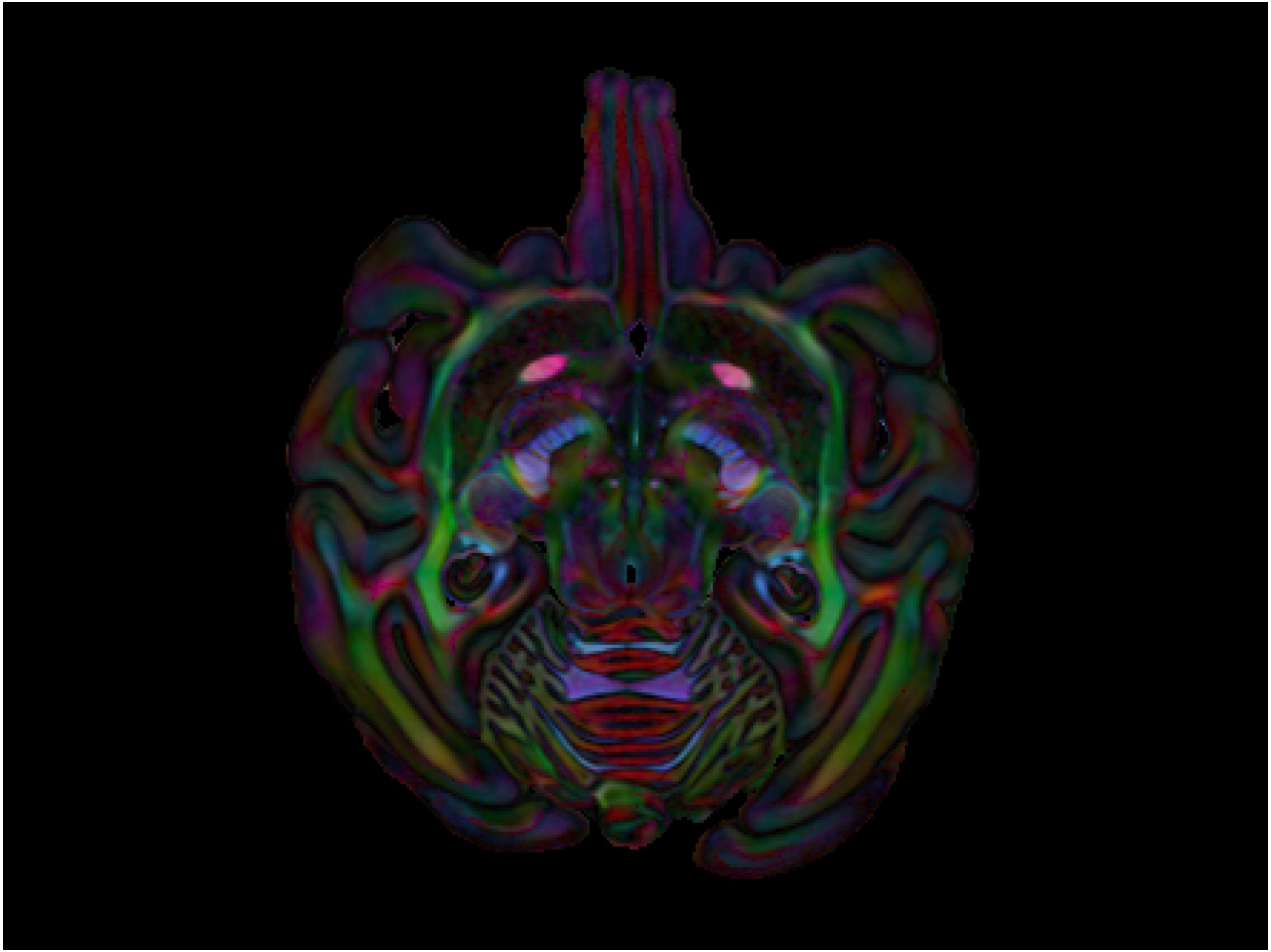

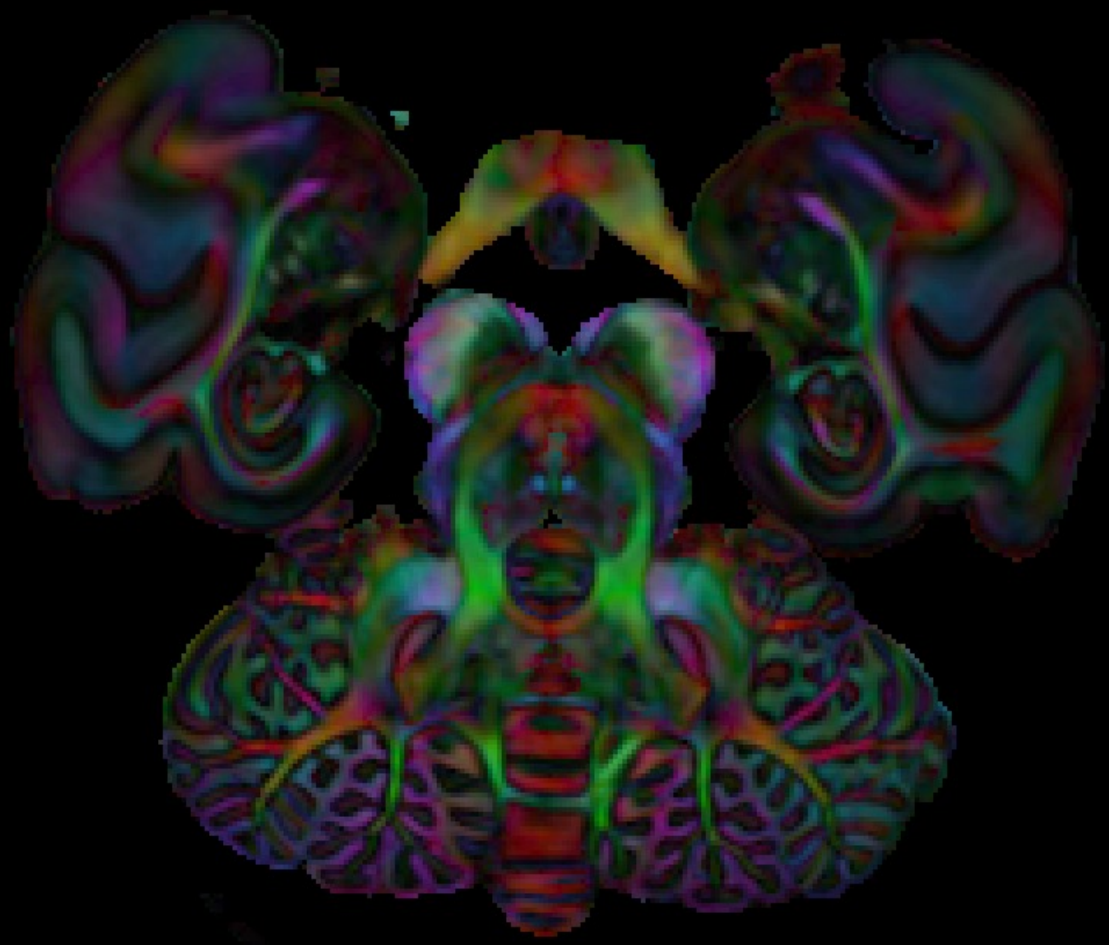

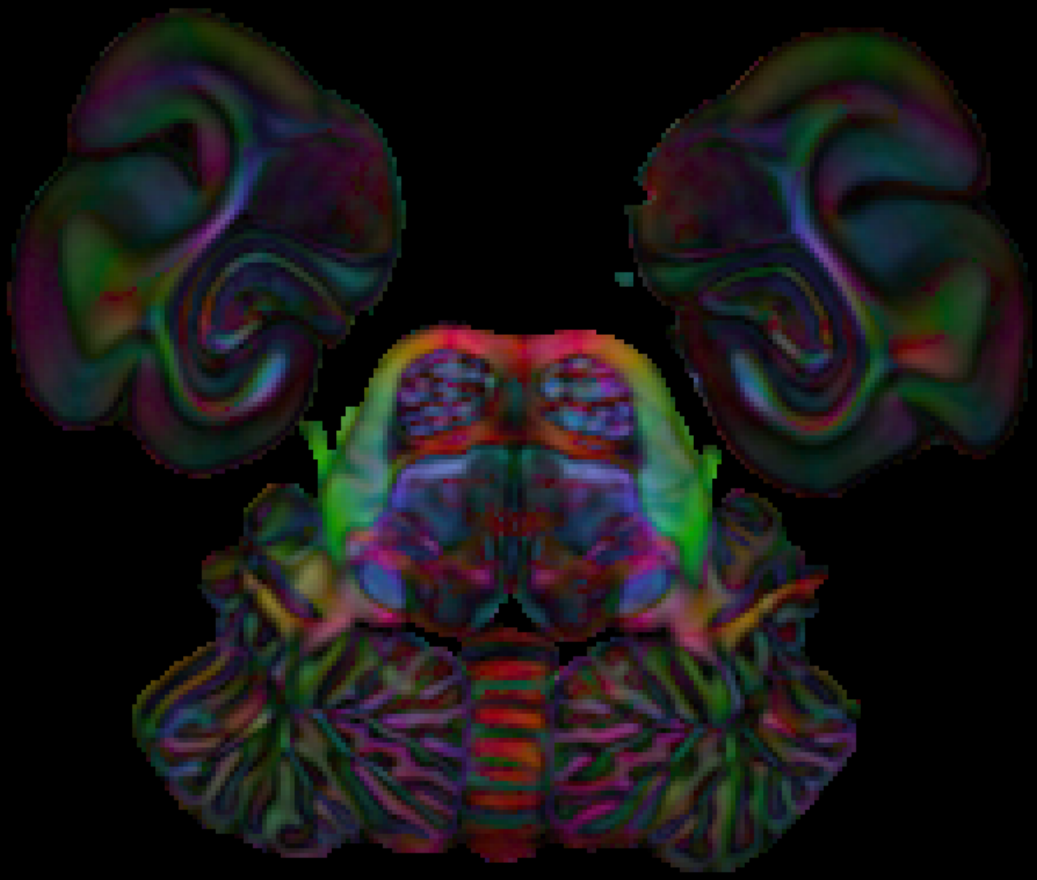

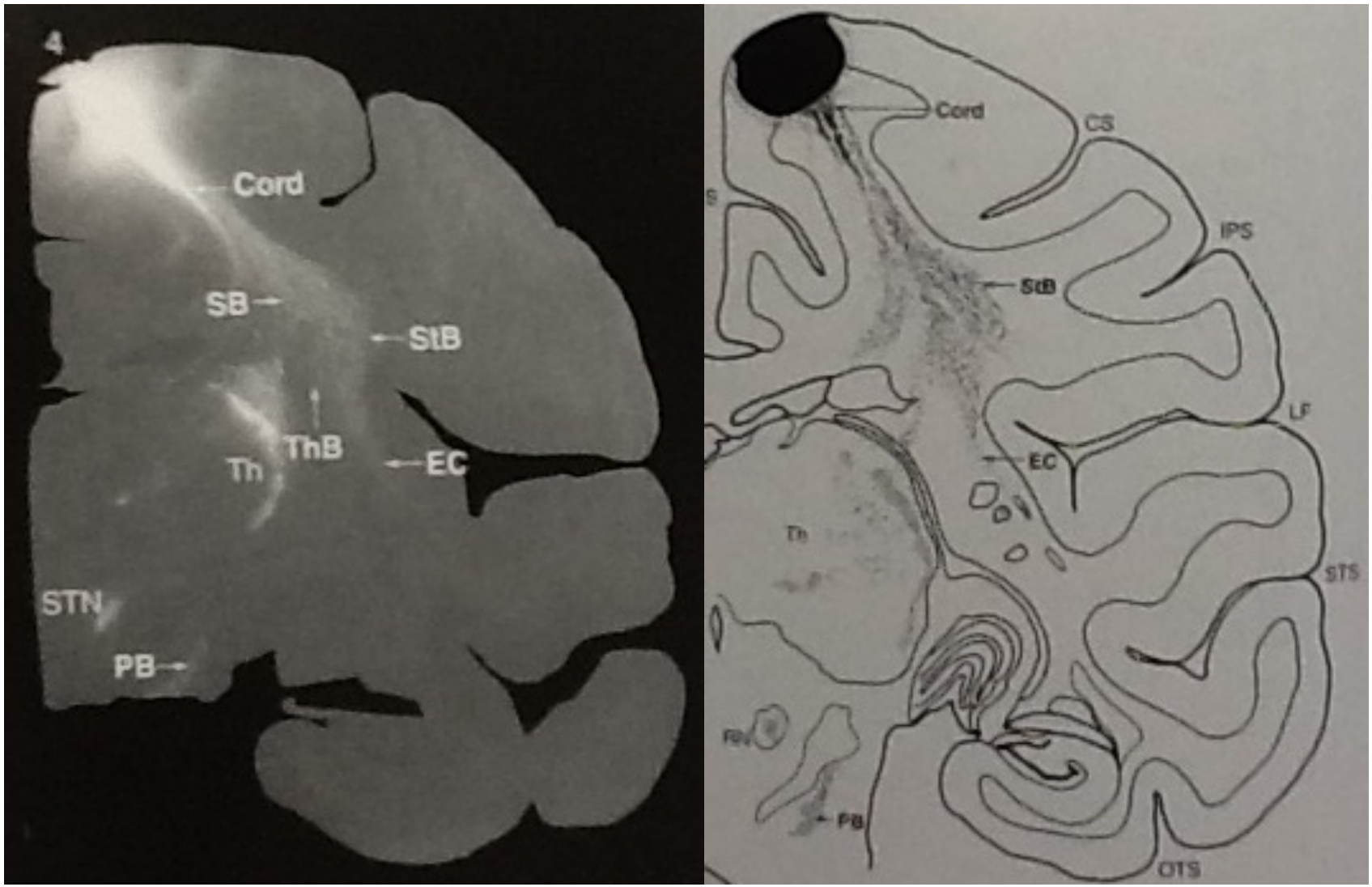

Left: Cord = Paired Cord of fibers that split into callosal fibers and corono radiata fibers;
EC: External Capsule; Th: Thalamus; ThB: Thalamic Bundle; SB: Subcortical Bundle;
StB: Striatal Bundle; PB: Pontine Bundle; STN: Subthalamic Nucleus.
Right: CS: Central Sulcus, IPS: Intraparietal Sulcus; LF: Lateral Fissure; STS: Superior Temporal Sulcus; OTS: Occipitotemporal Sulcus

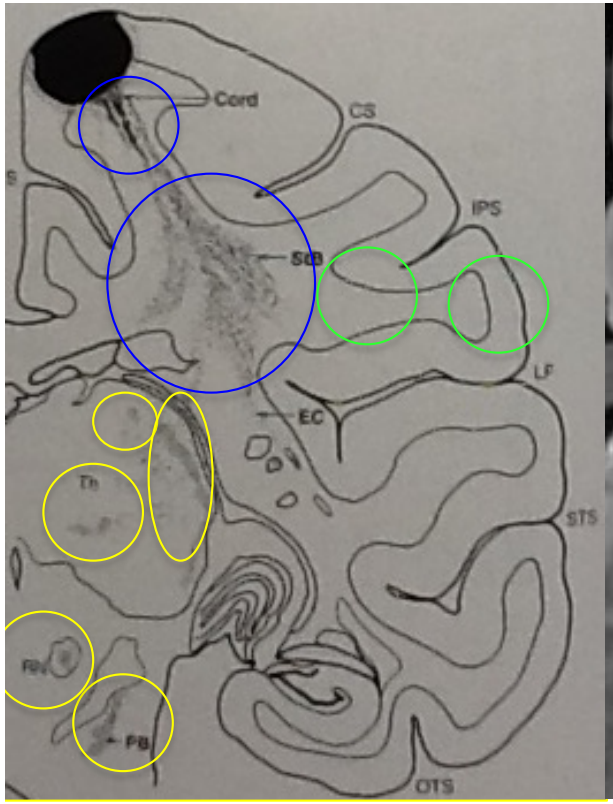

site of the tracer injection (Pre central gyrus)

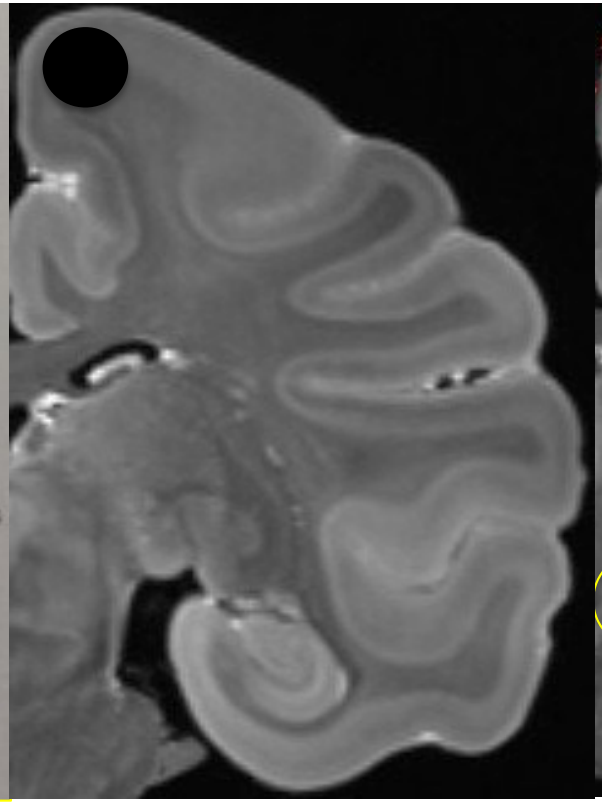

The same region was seeded for tractography in a different monkey

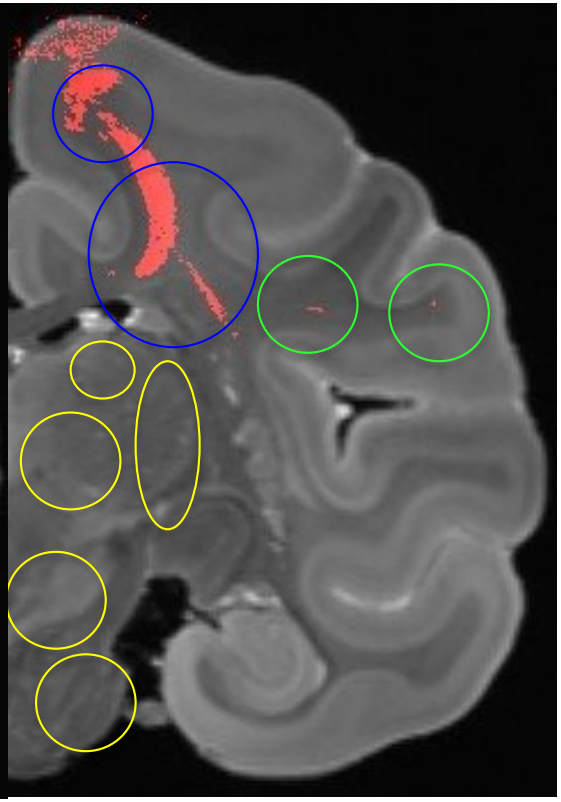

Results of tractography

Blue circles – True positives
Green circles – False Positives
Yellow circles – False Negatives

Note: This slice is 11 slices (2.25 mm) anterior to the seeded coronal slice

The anatomical accuracy of brain connections derived from Diffusion MRI Tractography is inherently limited *Thomas et al.*

PNAS

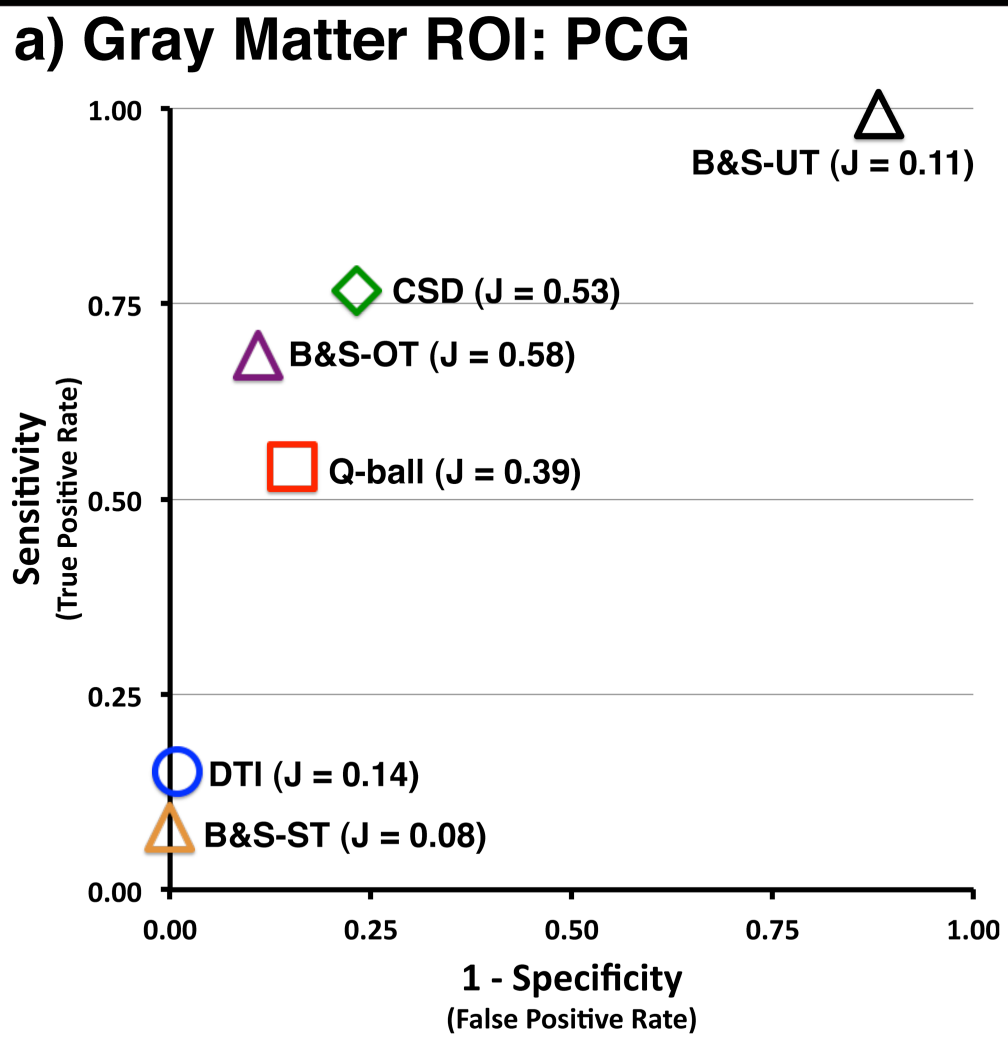

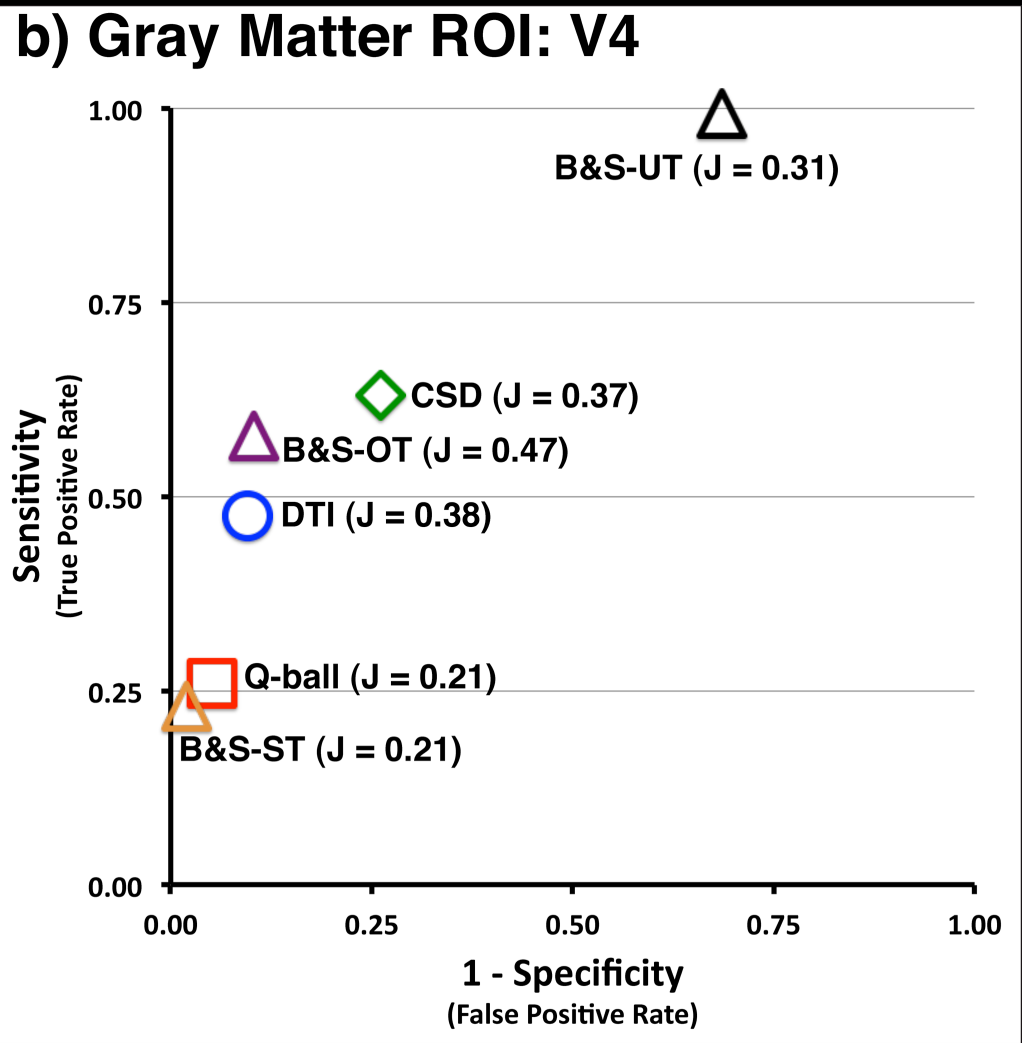

Population-based atlases

Normative databases

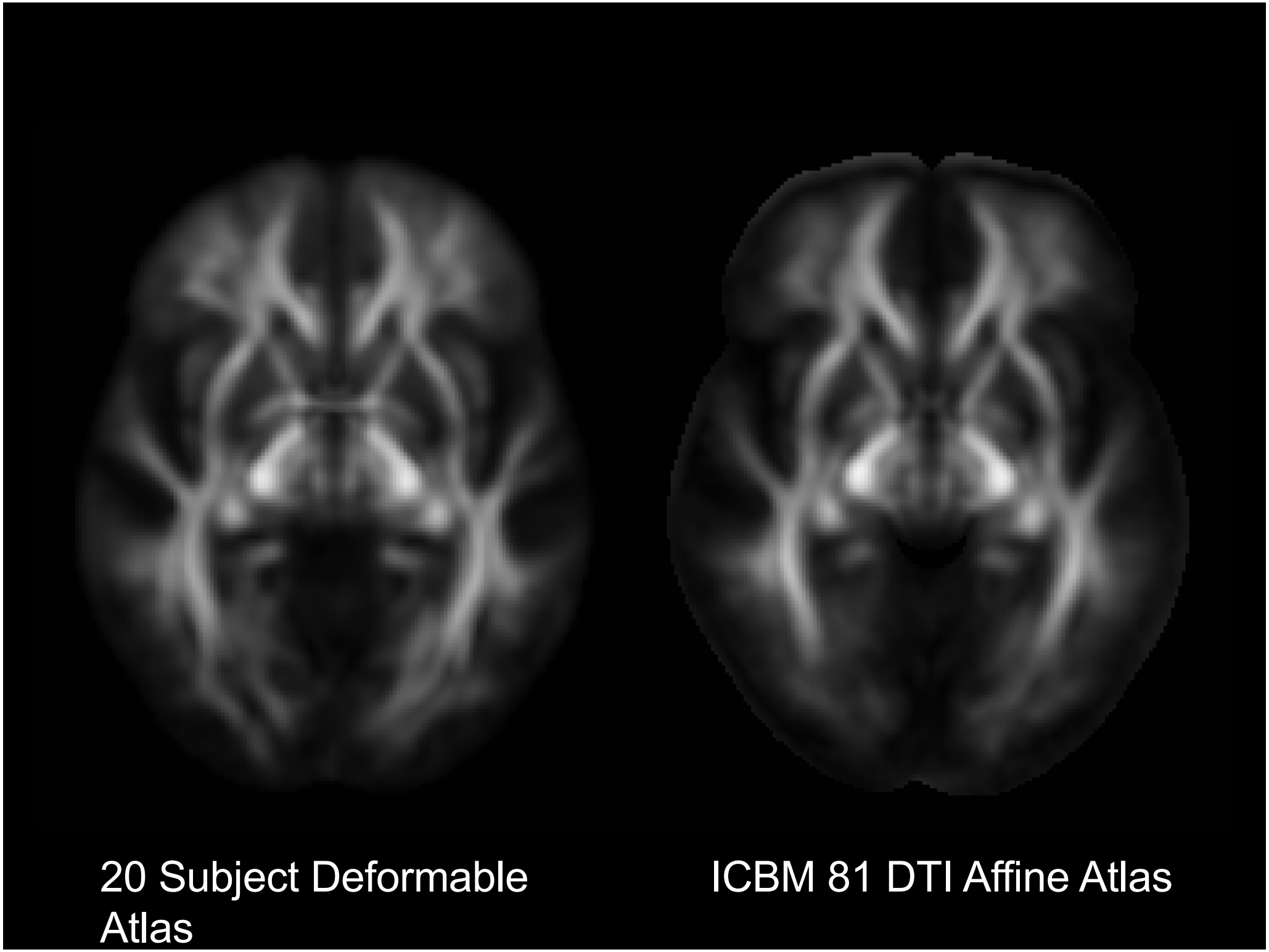
20 Subject Deformable Atlas
ICBM 81 DTI Affine Atlas

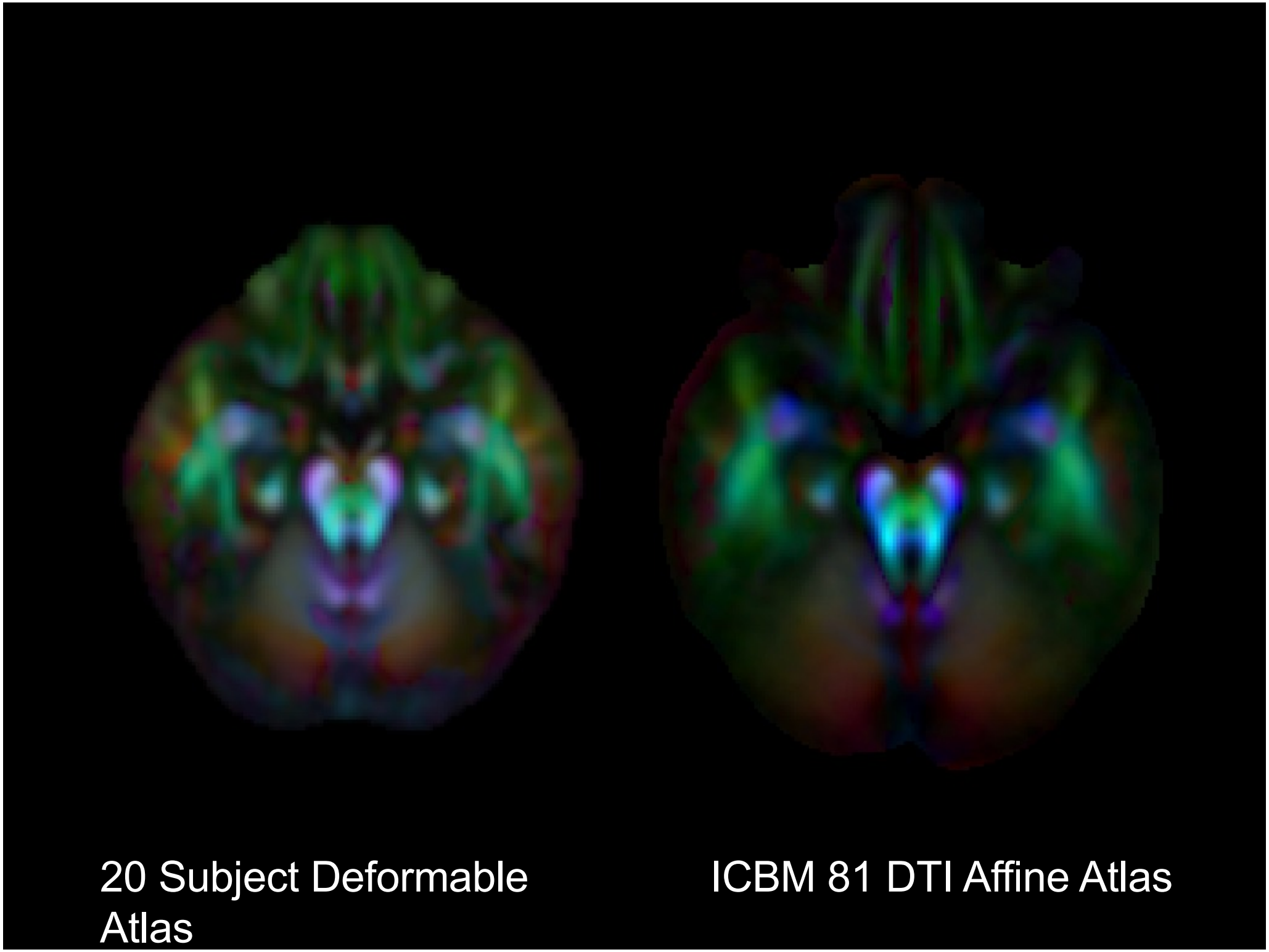
20 Subject Deformable Atlas
ICBM 81 DTI Affine Atlas

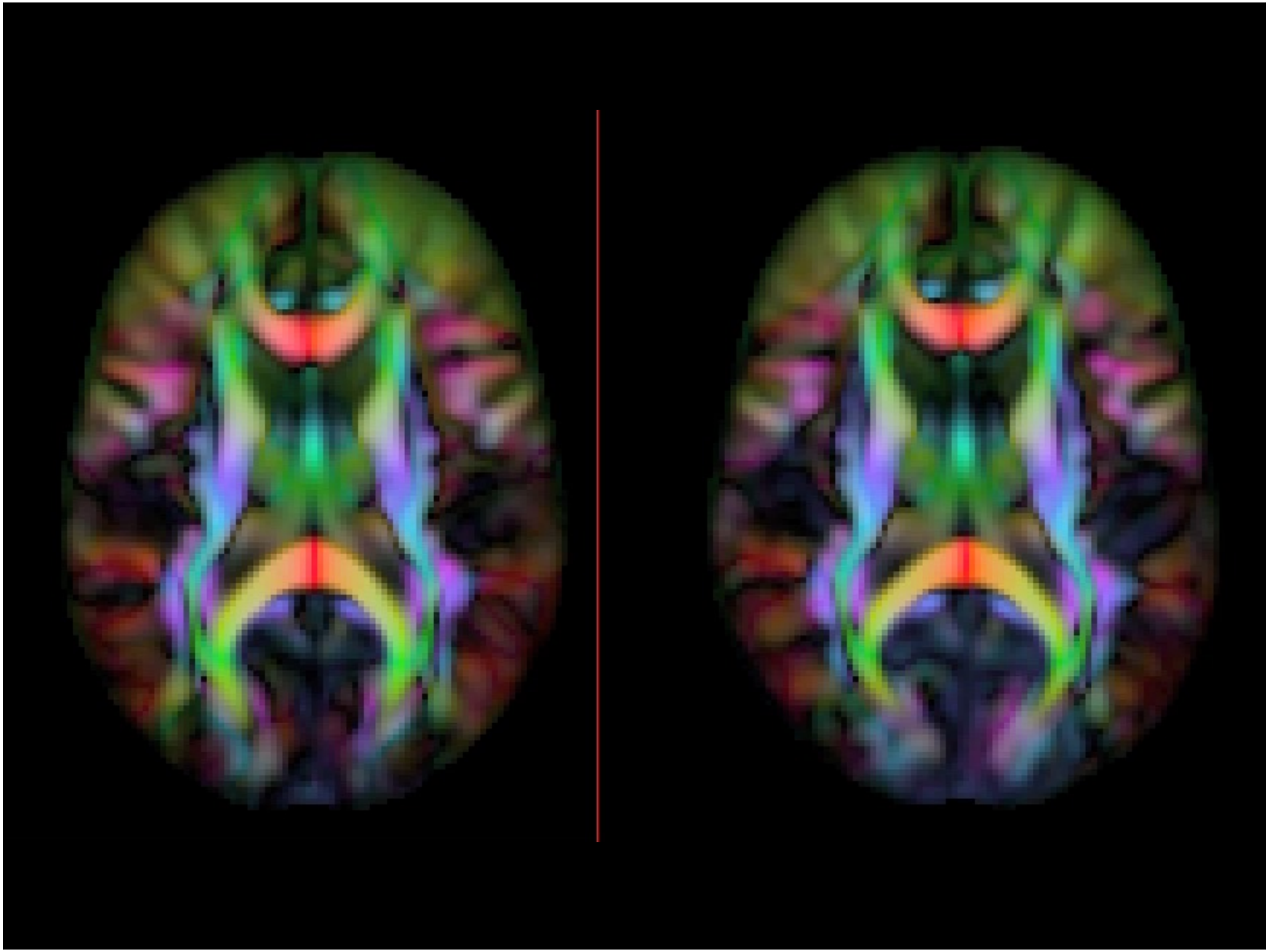

NIH MRI Study of Normal Brain Development

www.NIH-PediatricMRI.org

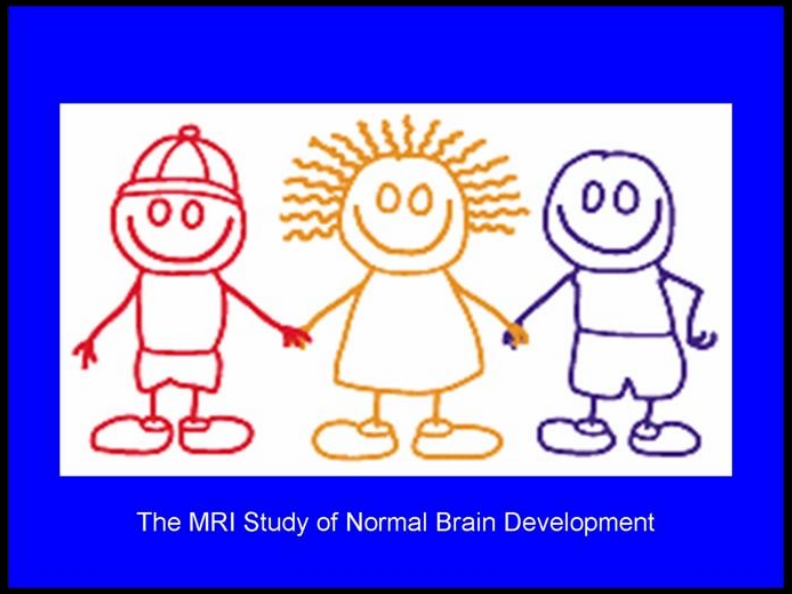

NIH National Institutes of Health | NICHD | NINDS | NIMH National Institute of Mental Health | NIDA National Institute on Drug Abuse | United States Department of Health & Human Services

ARTICLE IN PRESS

YNIMG-12279; No. of pages: 6; 4C: 2, 3

NeuroImage xxx (2015) xxx–xxx

Contents lists available at ScienceDirect

NeuroImage

journal homepage: www.elsevier.com/locate/ynimg

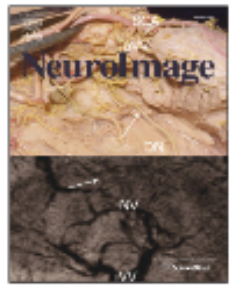

The diffusion tensor imaging (DTI) component of the NIH MRI study of normal brain development (PedsDTI)

Lindsay Walker [a], Lin-Ching Chang [a,1], Amritha Nayak [a], M. Okan Irfanoglu [a], Kelly N. Botteron [b], James McCracken [c], Robert C. McKinstry [d], Michael J. Rivkin [e], Dah-Jyuu Wang [f], Judith Rumsey [g], Carlo Pierpaoli [a,*], the Brain Development Cooperative Group

[a] Program on Pediatric Imaging and Tissue Sciences, NICHD, NIH, Bethesda, MD, USA
[b] Washington University in St. Louis, Department of Psychiatry, Saint Louis, MO, USA
[c] Department of Child Psychiatry, University of California in Los Angeles, Los Angeles, CA, USA
[d] Mallinckrodt Institute of Radiology, Washington University School of Medicine, St. Louis, MO, USA
[e] Departments of Neurology, Psychiatry and Radiology, Boston Children's Hospital, Boston, MA, USA
[f] The Children's Hospital of Philadelphia, Philadelphia, PA, USA
[g] Clinical Neuroscience Research Branch, Division of Translational Research, NIMH, NIH, Bethesda, MD, USA

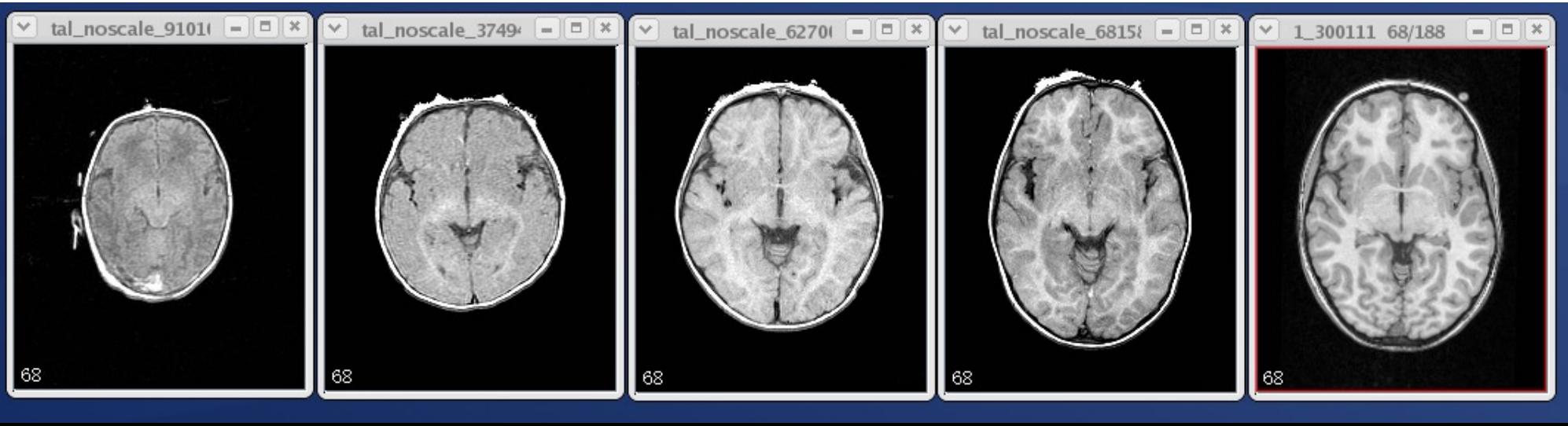
68
68
68
68
68

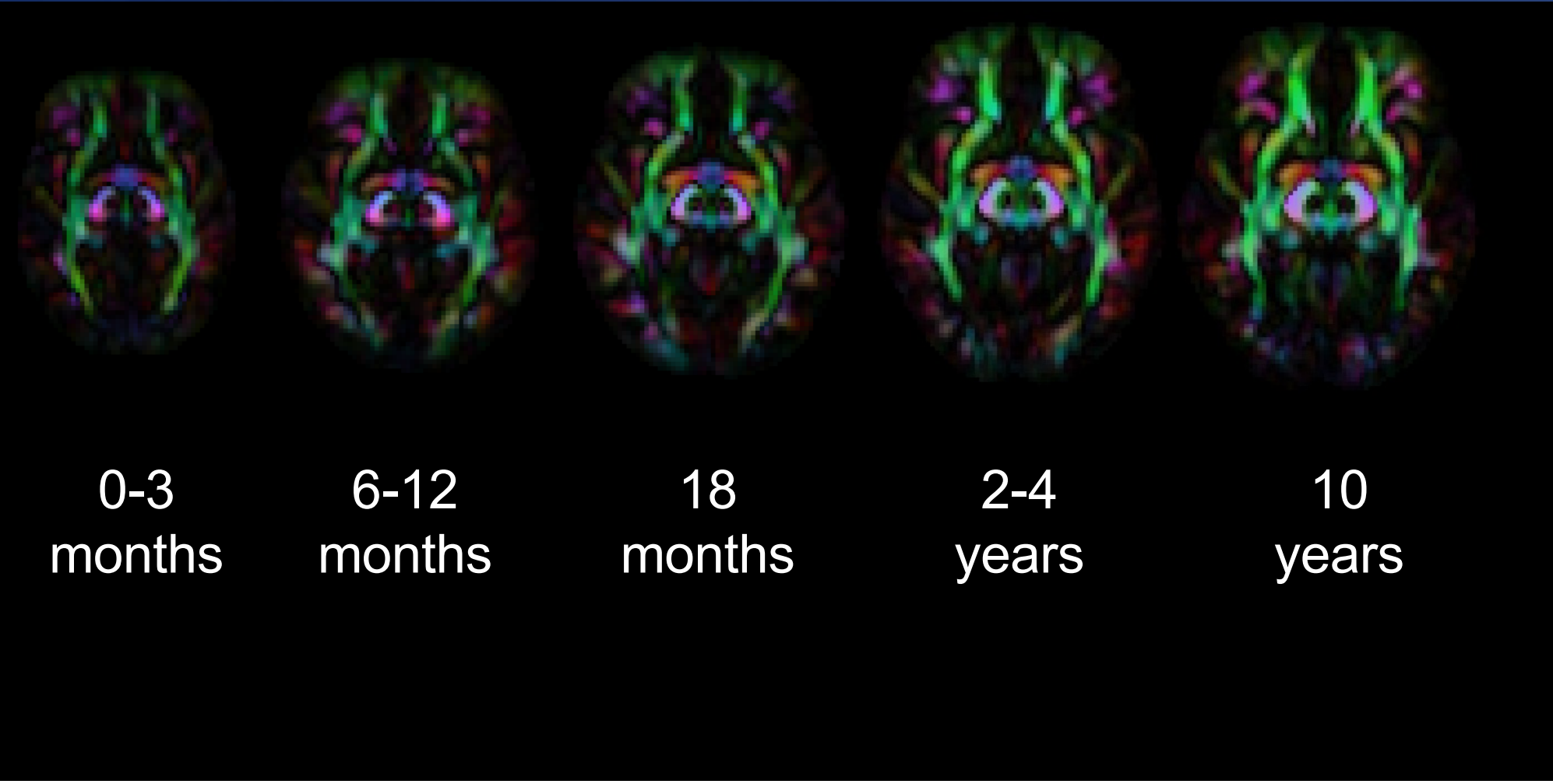
0-3 months
6-12 months
18 months
2-4 years
10 years

Developmental trajectories

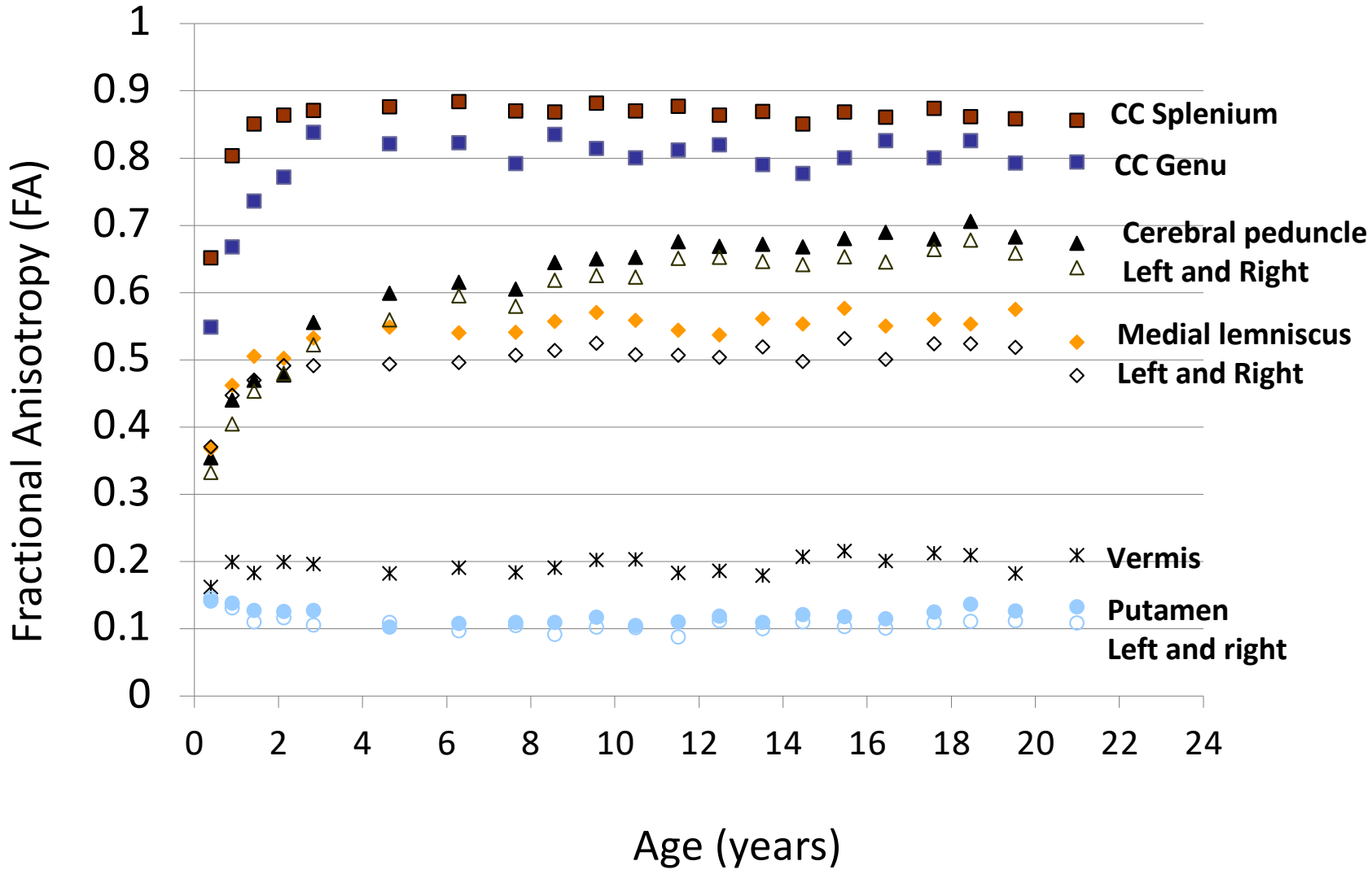

Accuracy and reproducibility
Analysis of confounds
Physiological noise

Image quality issues in clinical Diffusion MRI:

EPI Distortions

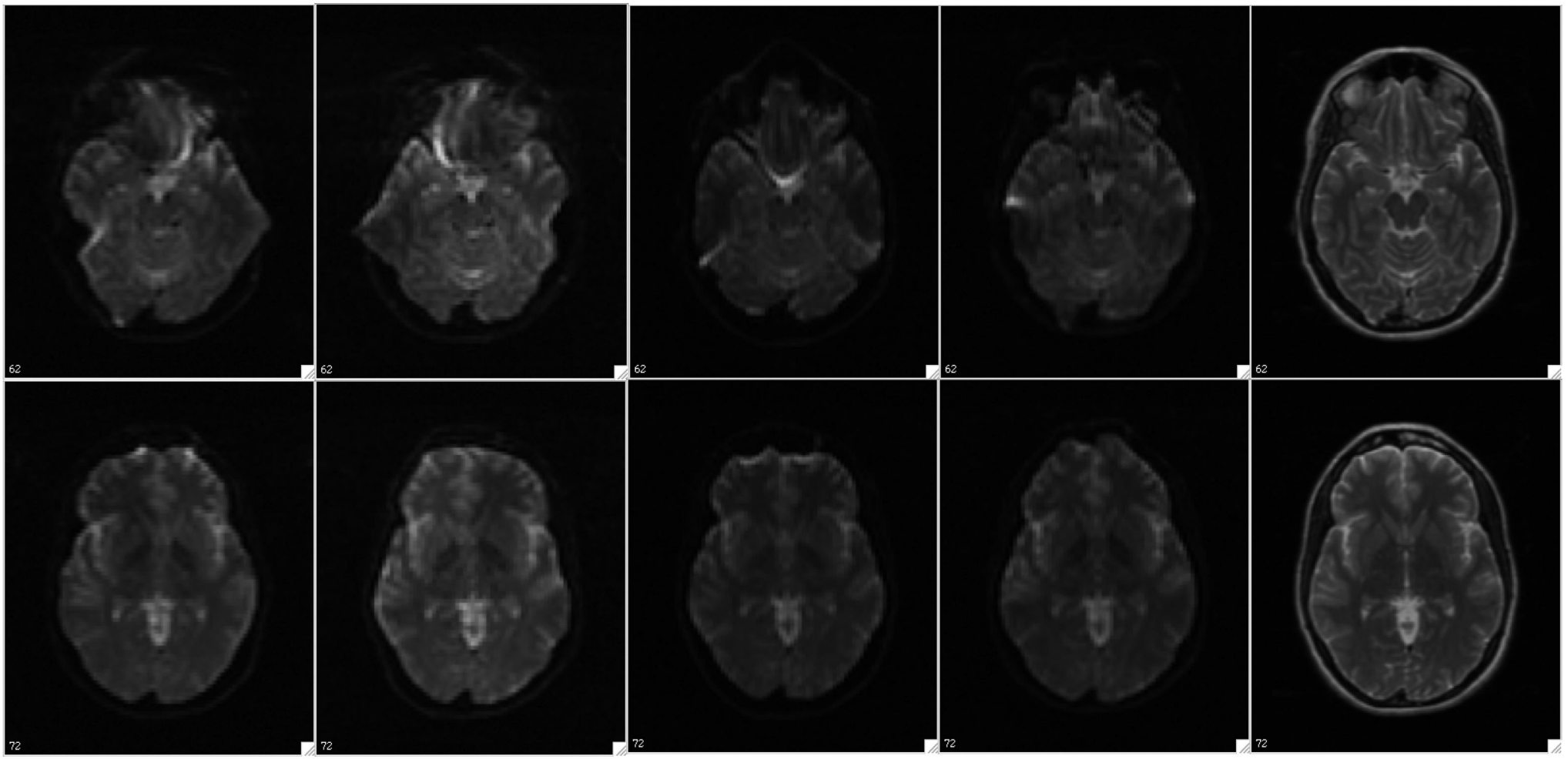

R/L-P R/L-M A/P-P A/P-M T2-FSE

Image quality issues in clinical Diffusion MRI:

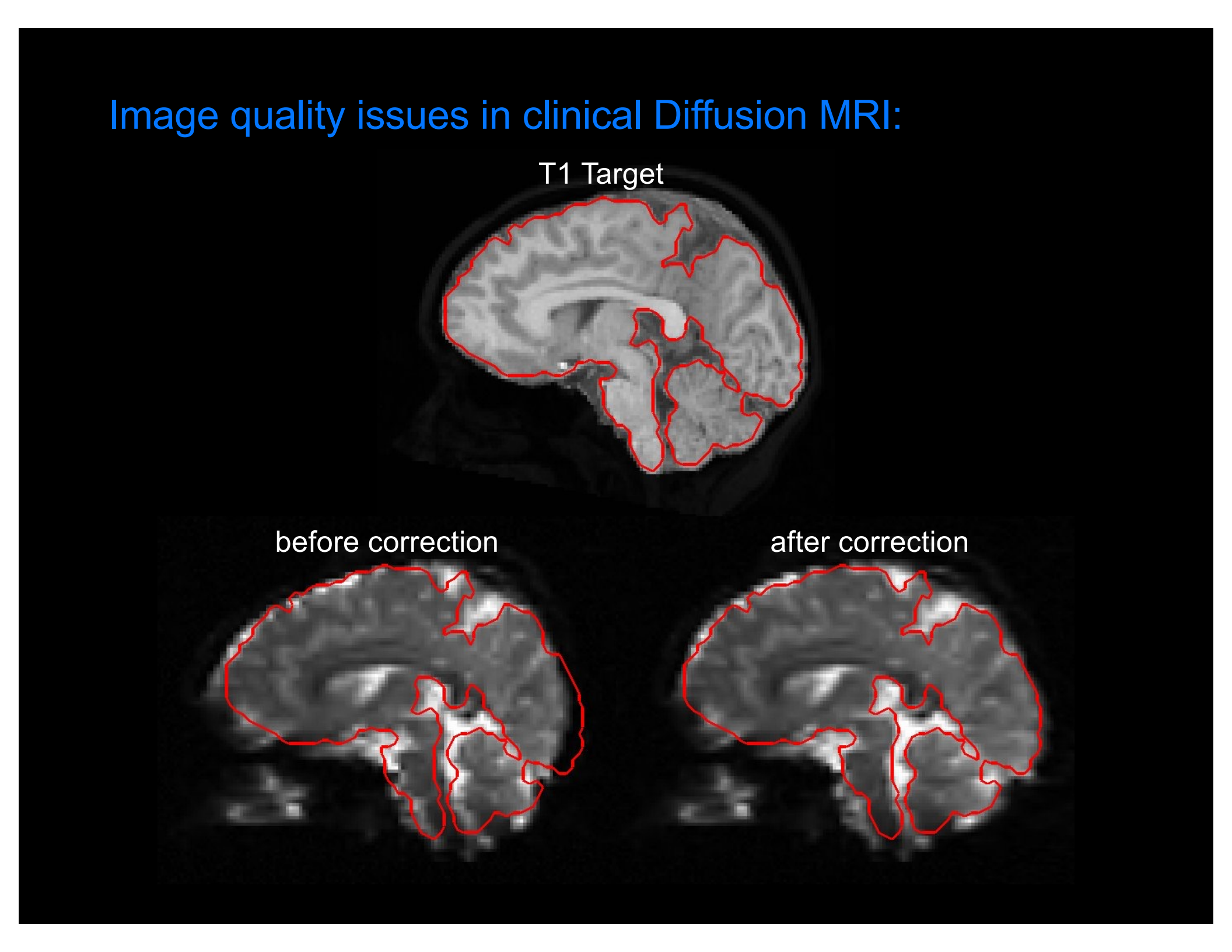

NeuroImage 61 (2012) 275–288

Contents lists available at SciVerse ScienceDirect

NeuroImage

journal homepage: www.elsevier.com/locate/ynimg

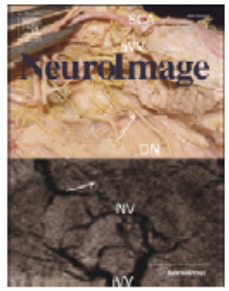

Effects of image distortions originating from susceptibility variations and concomitant fields on diffusion MRI tractography results

M. Okan Irfanoglu [a,b,*], Lindsay Walker [a,b], Joelle Sarlls [c], Stefano Marenco [d], Carlo Pierpaoli [a]

[a] Program on Pediatric Imaging and Tissue Sciences, NICHD, National Institutes of Health, Bethesda, MD, 20892, USA
[b] Center for Neuroscience and Regenerative Medicine, Uniformed Services University of the Health Sciences, Bethesda, MD 20814, USA
[c] National Institute of Neurological Disorders and Stroke, National Institutes of Health, Bethesda, Maryland, USA
[d] Section on Clinical Studies, National Institute of Mental Health, National Institute of Health, Bethesda, MD, 20892, USA

EPI distortions & Tensors

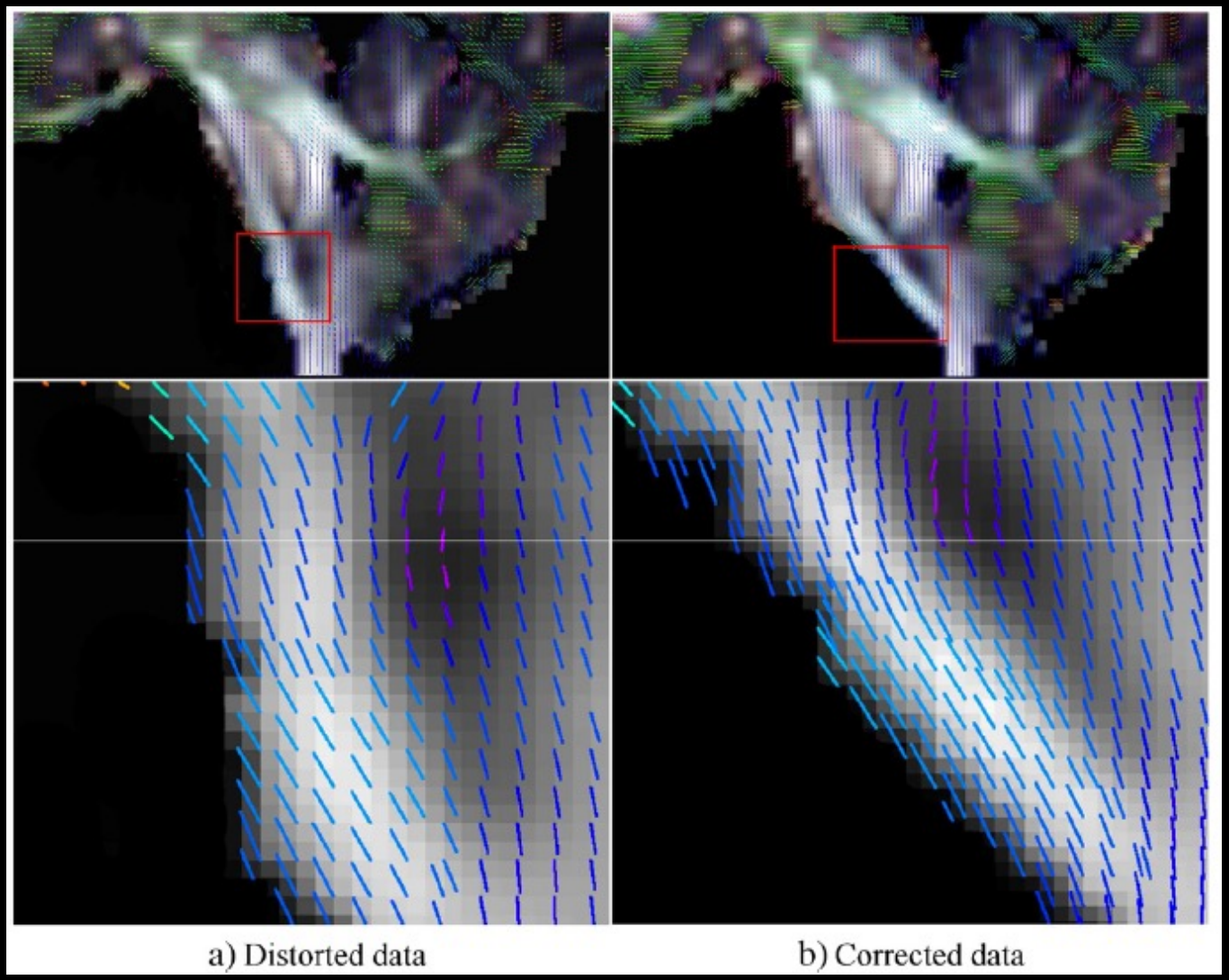

a) Distorted data b) Corrected data

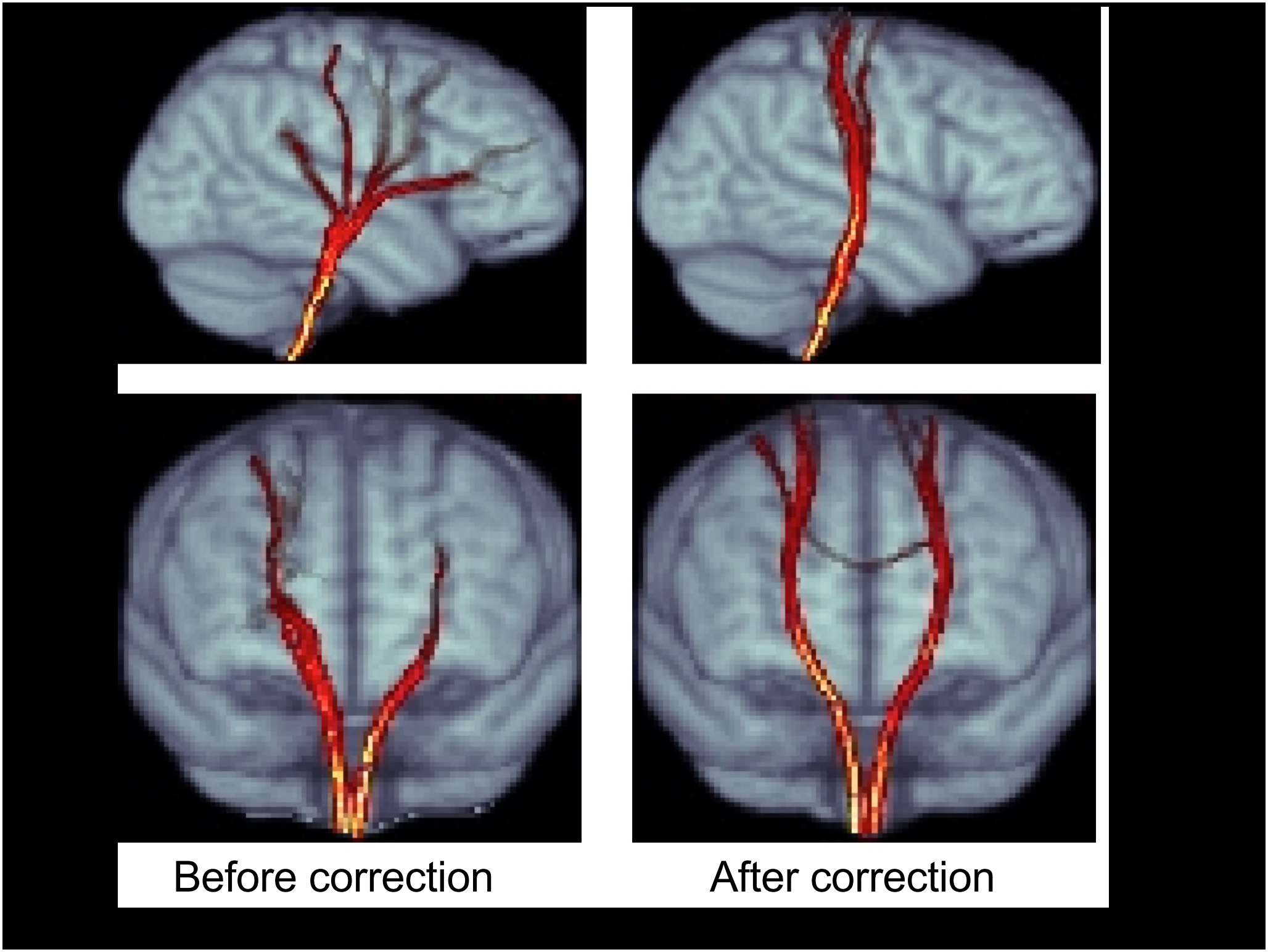
Before correction
After correction

NeuroImage 106 (2015) 284–299

Contents lists available at ScienceDirect

NeuroImage

journal homepage: www.elsevier.com/locate/ynimg

DR-BUDDI (Diffeomorphic Registration for Blip-Up blip-Down Diffusion Imaging) method for correcting echo planar imaging distortions

M. Okan Irfanoglu [a,b,*], Pooja Modi [a], Amritha Nayak [a,b], Elizabeth B. Hutchinson [a,b], Joelle Sarlls [c], Carlo Pierpaoli [a]

[a] Section on Tissue Biophysics and Biomimetics, National Institute of Child Health and Human Development, National Institutes of Health, Bethesda 20892, USA
[b] Center for Neuroscience and Regenerative Medicine, Uniformed Services University of the Health Sciences, Bethesda, MD 20814, USA
[c] NIH MRI Research Facility, National Institute of Neurological Disorders and Stroke, National Institutes of Health, Bethesda, MD 20892, USA

ARTICLE INFO

Article history:
Accepted 19 November 2014
Available online 26 November 2014

Keywords:
Echo planar imaging
Diffusion tensor imaging
Reversed phase encoding
Diffeomorphic image registration

ABSTRACT

We propose an echo planar imaging (EPI) distortion correction method (*DR-BUDDI*), specialized for diffusion MRI, which uses data acquired twice with reversed phase encoding directions, often referred to as blip-up blip-down acquisitions. *DR-BUDDI* can incorporate information from an undistorted structural MRI and also use diffusion-weighted images (DWI) to guide the registration, improving the quality of the registration in the presence of large deformations and in white matter regions. *DR-BUDDI* does not require the transformations for correcting blip-up and blip-down images to be the exact inverse of each other. Imposing the theoretical "blip-up blip-down distortion symmetry" may not be appropriate in the presence of common clinical scanning artifacts such as motion, ghosting, Gibbs ringing, vibrations, and low signal-to-noise. The performance of *DR-BUDDI* is evaluated with several data sets and compared to other existing blip-up blip-down correction approaches. The proposed method is robust and generally outperforms existing approaches. The inclusion of the DWIs in the correction process proves to be important to obtain a reliable correction of distortions in the brain stem. Methods that do not use DWIs may produce a visually appealing correction of the non-diffusion weighted images, but the directionally encoded color maps computed from the tensor reveal an abnormal anatomy of the white matter pathways.

Software download: www.tortoisedti.org

TORTOISE

Tolerably Obsessive Registration and Tensor Optimization Indolent Software Ensemble

The current release is TORTOISE V2.1.0, available on the download page

Click here for version update information.

To get started with TORTOISE: Quick Start Guide

Please register to the TORTOISEDTI Google group for questions and help at:

https://groups.google.com/forum/#!forum/tortoisedti

Outlier Rejection Probability Map

Lindsay Walker et al Neuroimage 2011

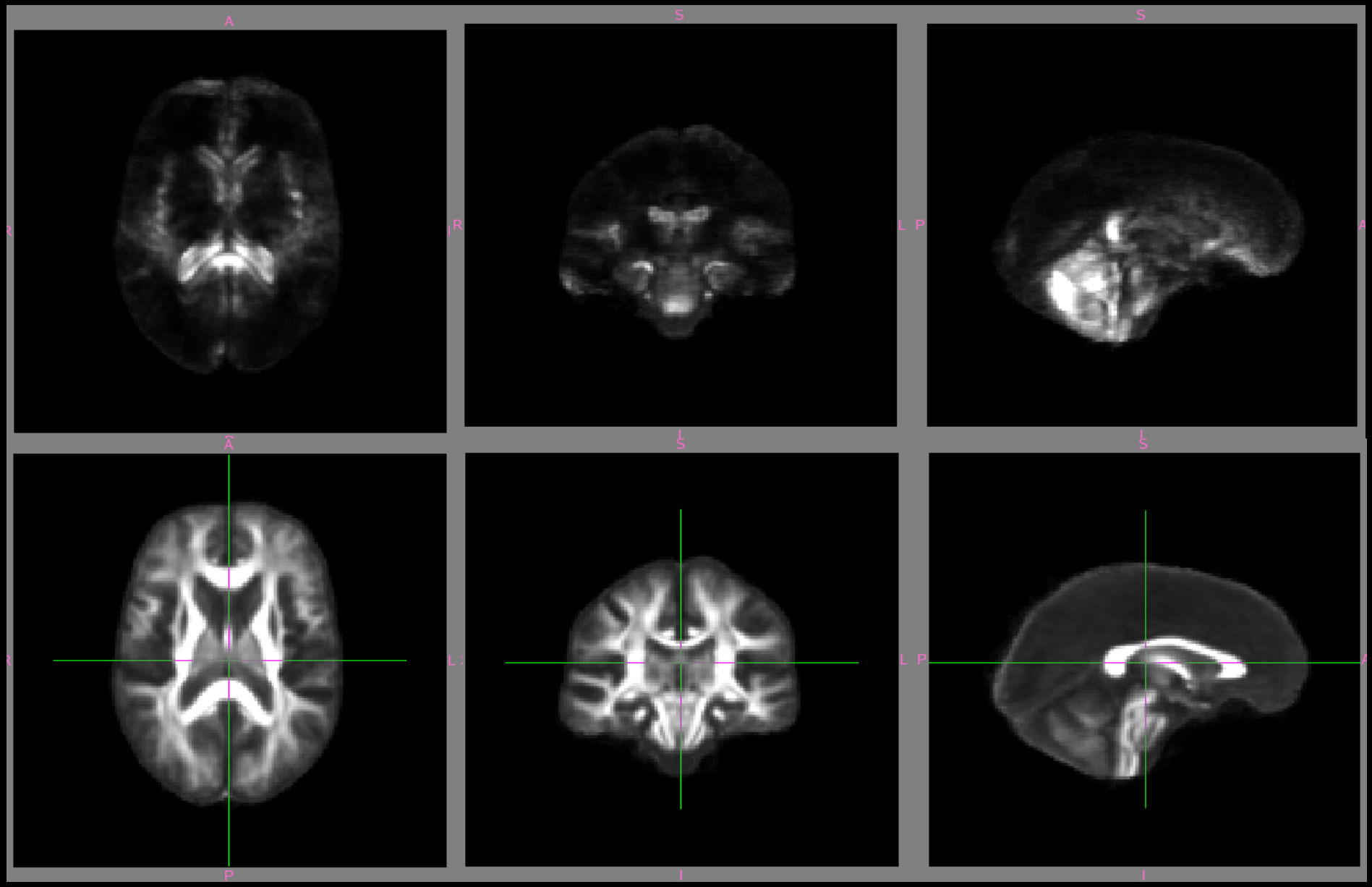

Biological Psychiatry - *2013*

Diffusion Tensor Imaging in Young Children with Autism: Biological Effects and Potential Confounds

Lindsay Walker, Marta Gozzi, Rhoshel Lenroot, Audrey Thurm, Babak Behseta, Susan Swedo, and Carlo Pierpaoli

Background: Diffusion tensor imaging (DTI) has been used over the past decade to study structural differences in the brains of children with autism compared with typically developing children. These studies generally find reduced fractional anisotropy (FA) and increased mean diffusivity (MD) in children with autism; however, the regional pattern of findings varies greatly.

Methods: We used DTI to investigate the brains of sedated children with autism ($n = 39$) and naturally asleep typically developing children ($n = 39$) between 2 and 8 years of age. Tract based spatial statistics and whole brain voxel-wise analysis were performed to investigate the regional distribution of differences between groups.

Results: In children with autism, we found significantly reduced FA in widespread regions and increased MD only in posterior brain regions. Significant age × group interaction was found, indicating a difference in developmental trends of FA and MD between children with autism and typically developing children. The magnitude of the measured differences between groups was small, on the order of approximately 1%–2%. Subjects and control subjects showed distinct regional differences in imaging artifacts that can affect DTI measures.

Conclusions: We found statistically significant differences in DTI metrics between children with autism and typically developing children, including different developmental trends of these metrics. However, this study indicates that between-group differences in DTI studies of autism should be interpreted with caution, because their small magnitude make these measurements particularly vulnerable to the effects of artifacts and confounds, which might lead to false positive and/or false negative biological inferences.

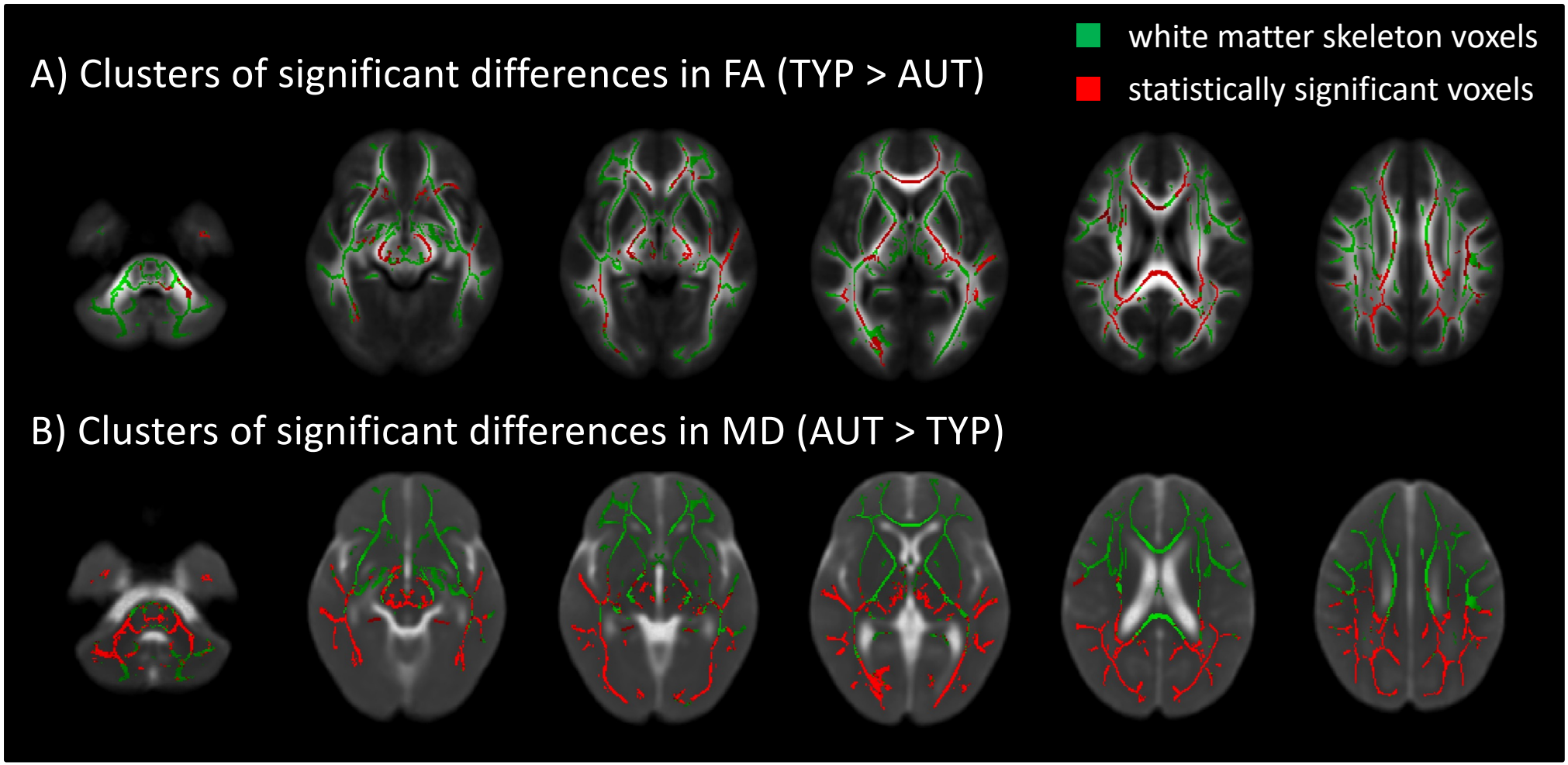
white matter skeleton voxels
statistically significant voxels
A) Clusters of significant differences in FA (TYP > AUT)
B) Clusters of significant differences in MD (AUT > TYP)

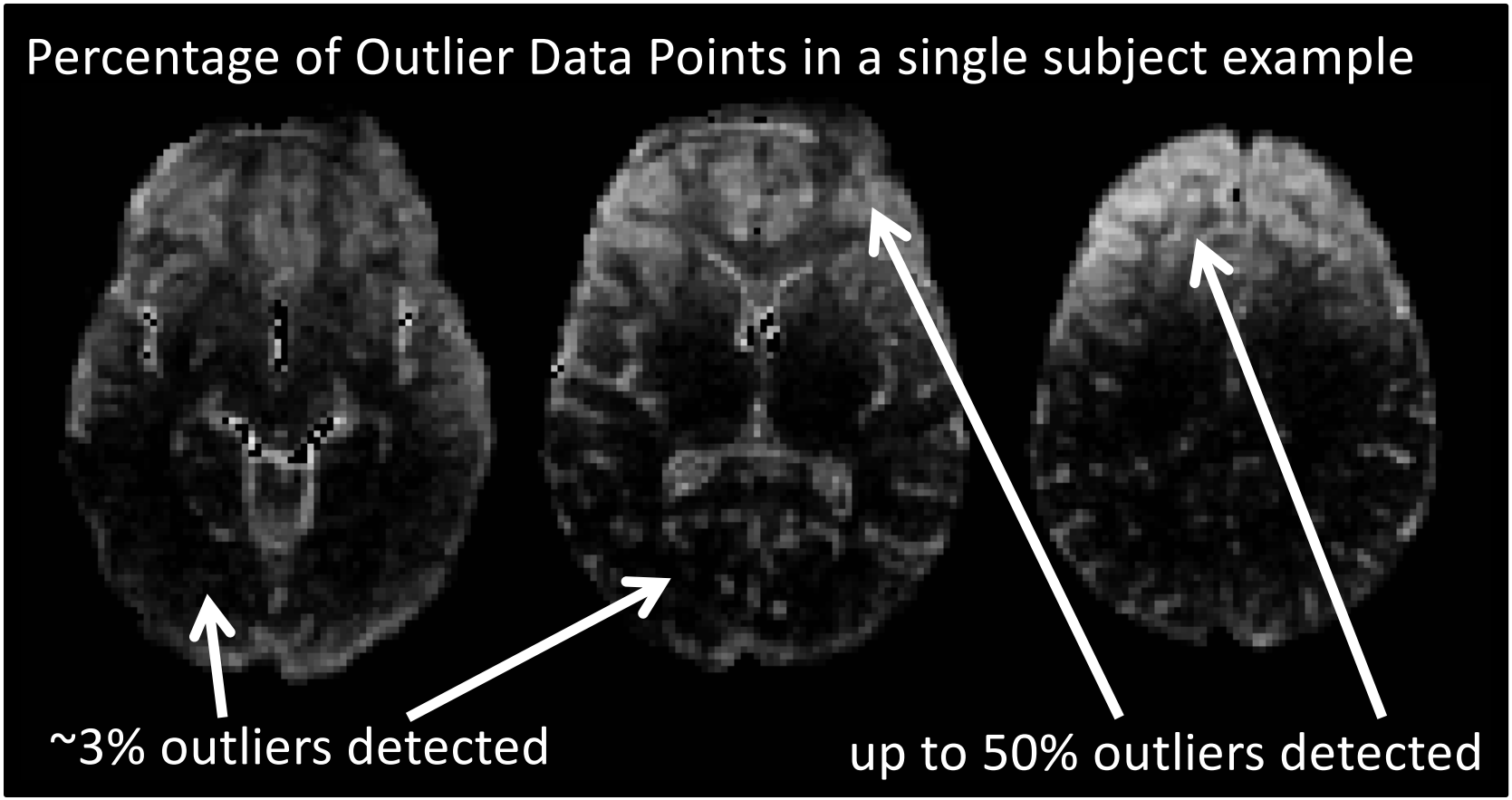
Percentage of Outlier Data Points in a single subject example
~3% outliers detected
up to 50% outliers detected

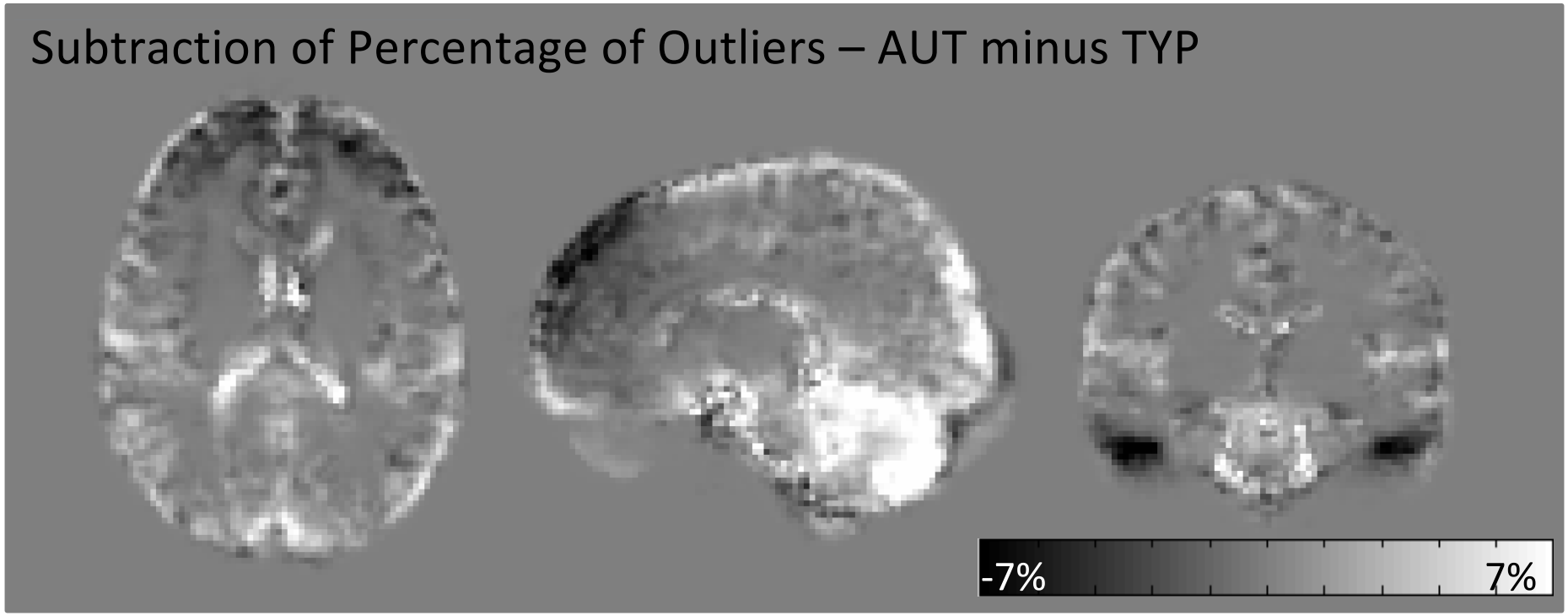
Subtraction of Percentage of Outliers – AUT minus TYP
-7%
7%

“Interpretation” Artifacts

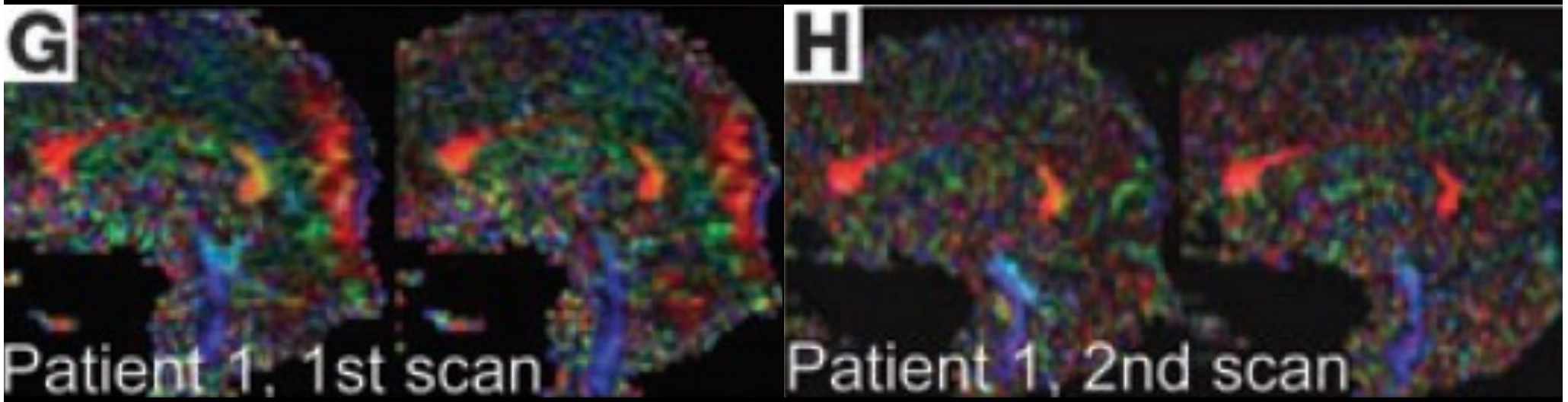

Possible axonal regrowth in late recovery from minimally conscious state
Voss HU, et al. (2006) Journal of Clinical Investigation

One final consideration about HARDI data

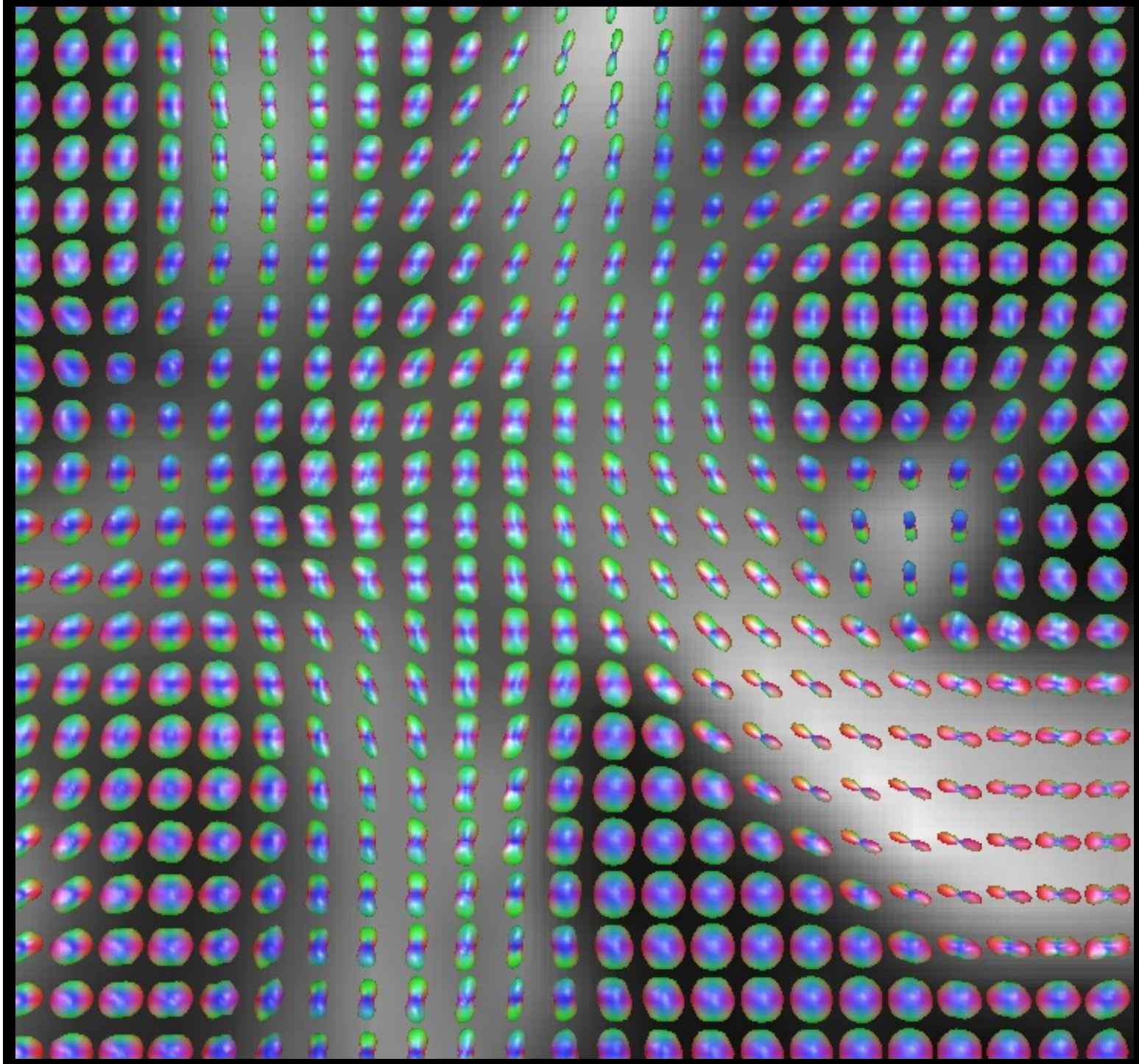

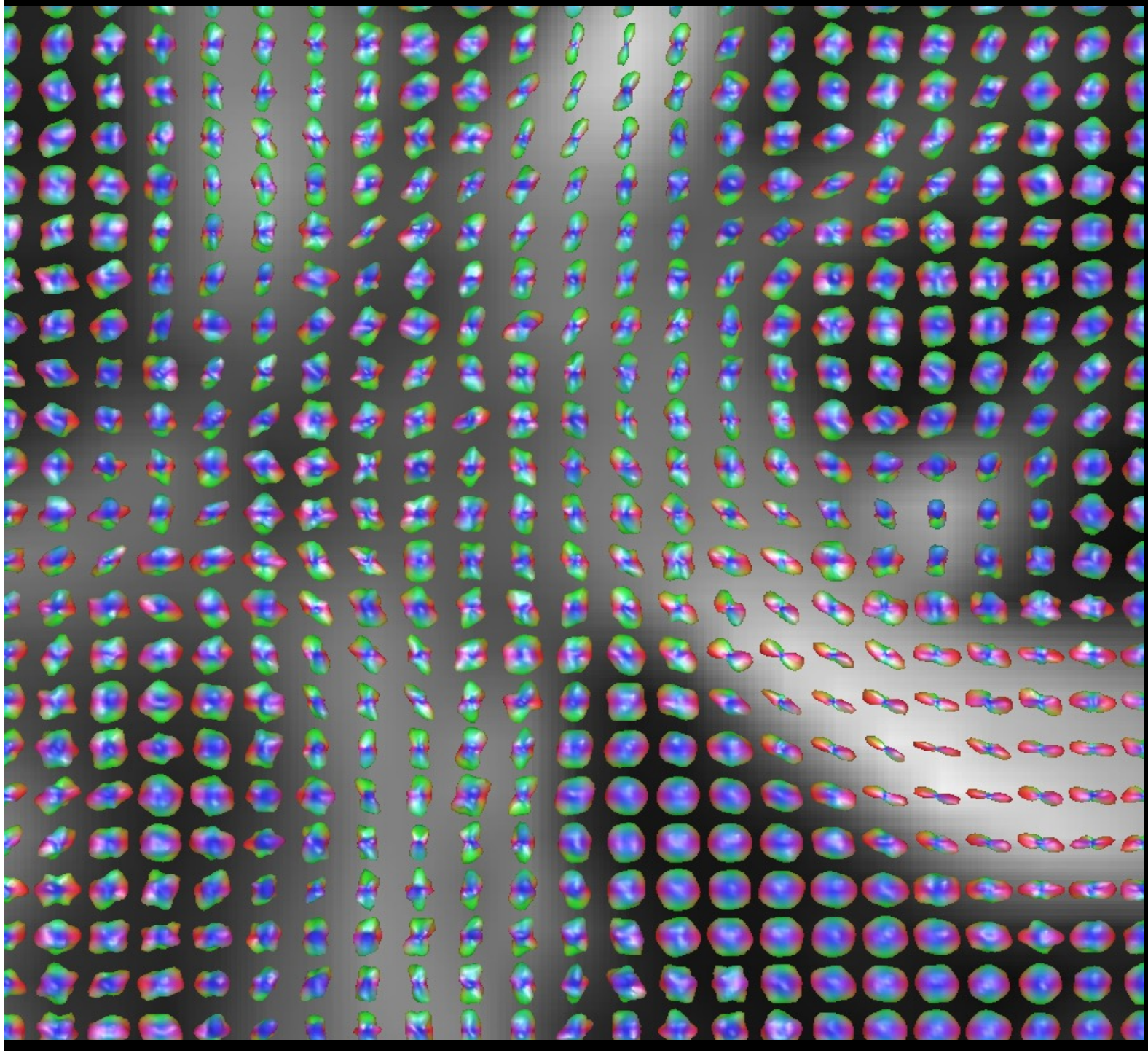

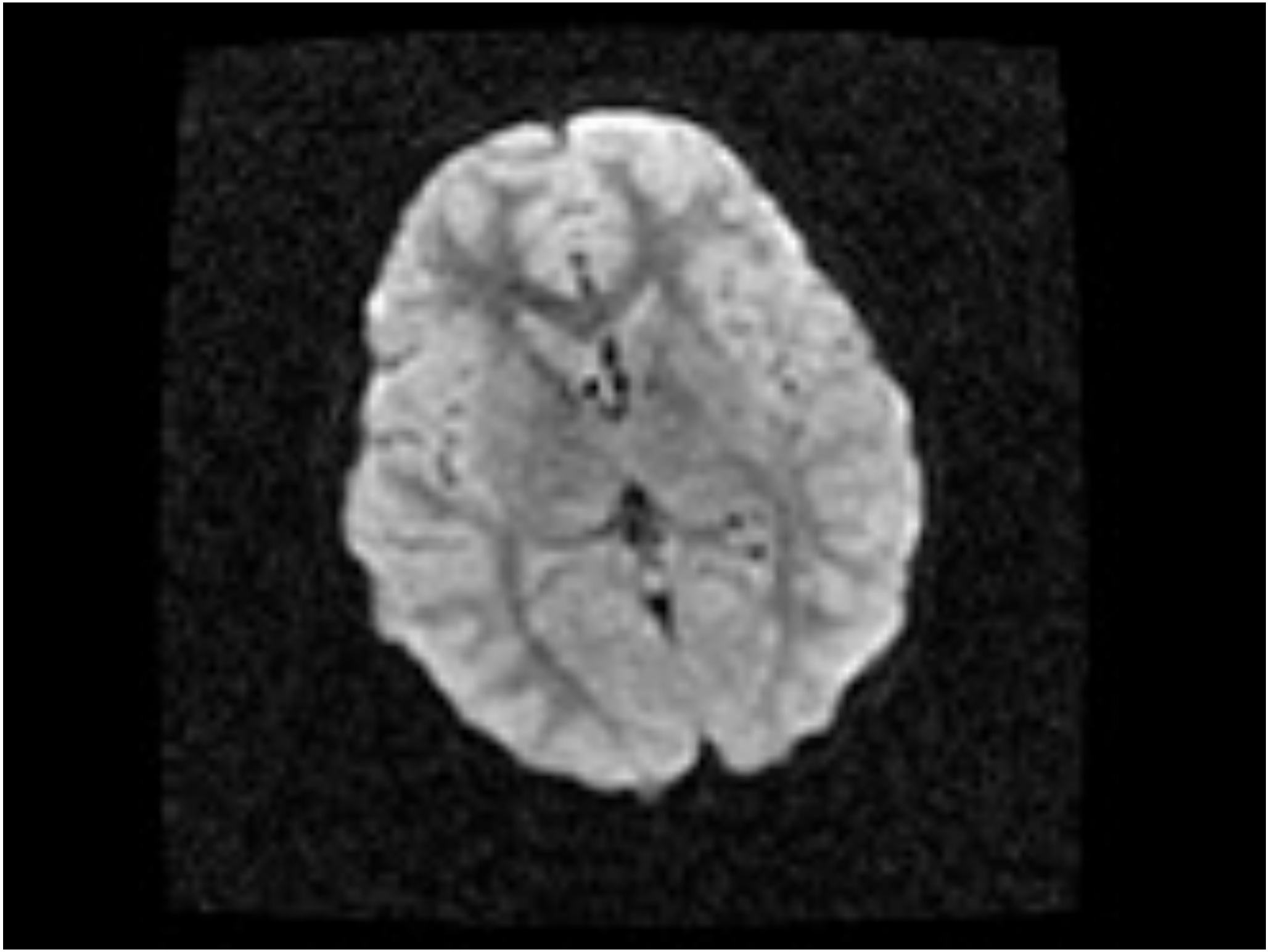

Conclusions

Diffusion MRI provides unique information about tissue structure and architecture.

Clinical use of diffusion MRI requires the development of reliable (accurate and reproducible), specific, fast to acquire, and simple to interpret metrics.

HARDI acquisitions may help improving biological specificity, but are more prone to artifacts and lengthy than DTI.

Suggested reading:

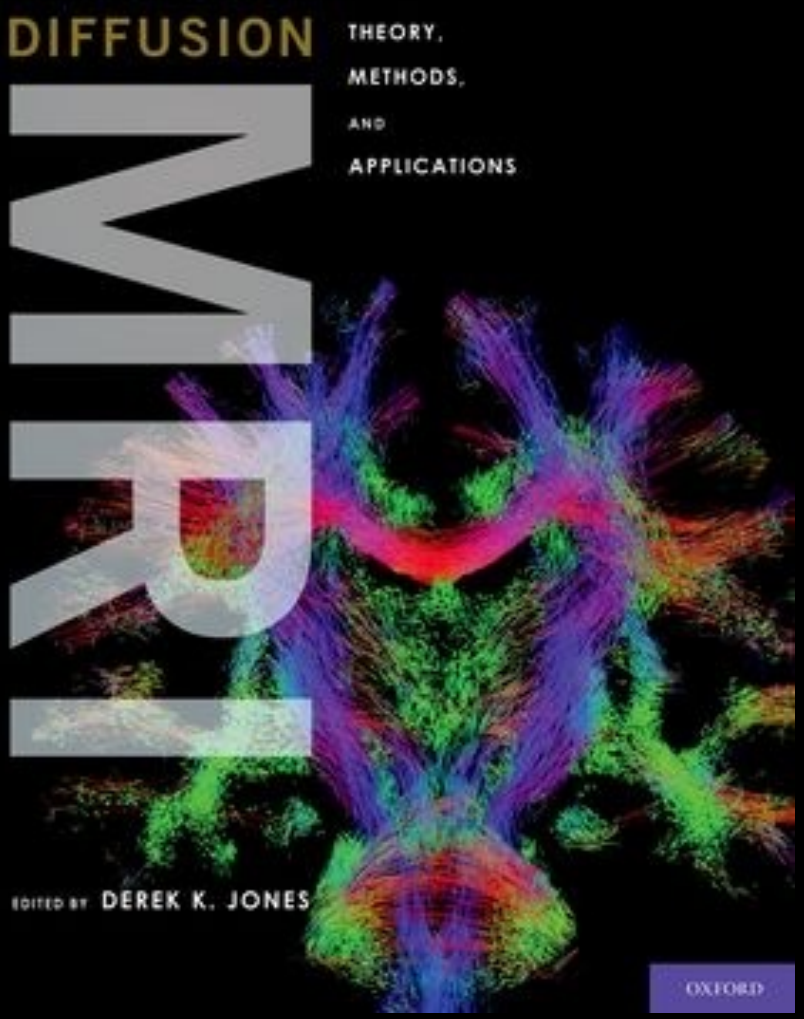

Diffusion MRI: Theory, Methods, and Applications
By Derek K. Jones - Oxford University Press (2010) - 624 pages - ISBN 0195369777